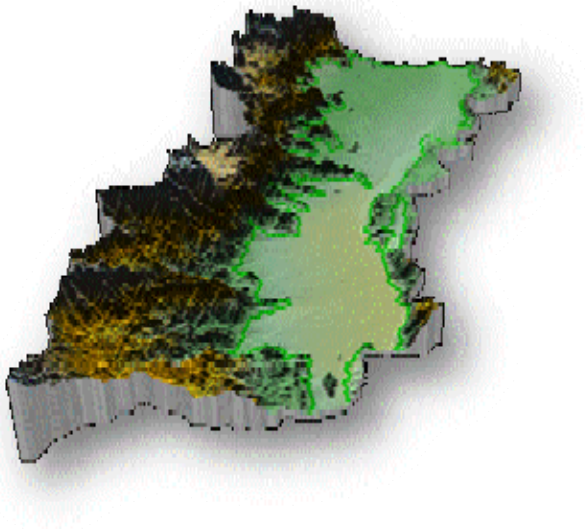
ADDIS ABABA UNIVERSITY

SCHOOL OF GRADUATE STUDIES

DEPARTMENT OF EARTH SCIENCES

AQUIFER CHARACTERIZATION OF THE RAYA VALLEY BASED ON PUMPING TEST AND GEOPHYSICAL DATA ANALYSIS



A Thesis Submitted to the School of Graduate Studies of Addis Ababa University

In Partial Fulfillment of the Requirements for the Degree of Master of Science

in

Hydrogeology

By

AFEWORK HAILU GEBREEZGI

JUNE, 2010

ADDIS ABABA

ADDIS ABABA UNIVERSITY

SCHOOL OF GRADUATE STUDIES

DEPARTMENT OF EARTH SCIENCES

AQUIFER CHARACTERIZATION OF THE RAYA VALLEY BASED ON PUMPING TEST AND GEOPHYSICAL DATA ANALYSIS

A Thesis Submitted to the School of Graduate Studies of Addis Ababa University

In Partial Fulfillment of the Requirements for the Degree of Master of Science in

Hydrogeology

By

AFEWORK HAILU GEBREEZGI

Advisor

Prof. Tenalem Ayenew

June, 2010

Addis Ababa

ADDIS ABABA UNIVERSITY

SCHOOL OF GRADUATE STUDIES

DEPARTMENT OF EARTH SCIENCES

AQUIFER CHARACTERIZATION OF THE RAYA VALLEY BASED ON PUMPING TEST & GEOPHYSICAL DATA ANALYSIS

NORTHERN ETHIOPIA

BY

AFEWORK HAILU

A Thesis Submitted to the School of Graduate Studies of Addis Ababa University In Partial Fulfillment of the Requirements for the Award of the Degree of Master of Science in Hydrogeology

Approved by the Board of Examiners

Dr. Balemwal Atenafu

(Chairman) _____

Prof. Tenalem Ayenew

(Advisor) _____

Ato Paulos Masresha

(External Examiner) _____

Ato Sileshi Mamo

(External Examiner) _____

This work is dedicated to my wife and my family

ACKNOWLEDGEMENT

I would first like to thank my advisor and instructor Prof. Tenalem Ayenew, for all his help, encouragement and guidance and to all staff members of Earth Science department for all their help in every aspect of my work.

I am grateful to my organization Tigray Regional State Water Resources Mines and Energy Bureau for giving me the chance to join my post graduate study and facilitating the necessary logistics during my field work.

I am also thankful to the water works design and supervision enterprise for all their help, especially providing all the necessary and relevant data. I would like to thank Mr. Engda, Mr. Rashid and Mr. Seife for their overall support and updating me with additional data. This project would not have been possible without them!

I can't say enough thanks to Daniel Teka, who provides me the important data for my research work. I would like to thank ALL the people who took time out of their busy schedules to help me with important aspects of my research.

I would like to thank my friends: Gebrerufael, Ephrem, Mahammed sultan, Hiwot, and Getachew for providing me additional data and materials relevant to my work. Also, thank you to Luel for his advice and moral support.

I would also like to thank the Ministry of Water Resources for providing me with the necessary materials.

I would also like to thank the water works drilling and construction enterprise of Tigray region and Tekeze water well drilling company for providing me with relevant data. I would really like to thank the good friends I have made in Addis over the last two years for all their support and friendship. I would also like to thank my wife, Frehiwot, and my Sisters Tsega and Mulu my Brothers Zemenfes and Girmanigus my father and my mother for all their love and support. Thank you to everyone for always being there for me.

ABSTRACT

This work has focused on the quantitative characterization of aquifer hydraulic parameters of the raya valley by establishing a relationship between aquifer properties (specific capacity and BH yield data with transmissivity and between aquifer hydraulic parameters and aquifer electrical properties i.e. Transmissivity and transverse resistance aiming to extrapolate measured aquifer hydraulic parameters to an area with no pumping test data using the established relationships between T and Sc, T and BH yield and between T and R. Before establishing relationships between aquifer hydraulic parameters and aquifer hydraulic and electric properties a huge volume of raw data set are analyzed using different softwares. 135 raw pumping test data are analyzed to determine T & K from constant and recovery. 49 wells tapping unconfined aquifers are corrected for decreasing saturated thickness using Jacob correction method and 64 wells whose pumping rate exceeding 36 l/sec are corrected for well loss using step drawdown test data by employing the Hantush- Bierschenk well loss solution method. Three methods are applied to determine a relationship between T and Sc and one method between aquifer hydraulic and electric properties. By using the three approaches of estimating T from Sc i.e. analytical, empirical and geostatistical a regressed relationship between the parameters (T & Sc) for each approach is established with R^2 value >0.95 and interpolated map of transmissivity and hydraulic conductivity are created through geostatistical approach by using cokriging and kriging techniques for T from Sc and K from K respectively. The results of analytical and empirical techniques are compared based on their mean error and mean absolute error and it is found that the mean absolute error and mean error for transmissivity estimated using the analytic approach are 0.21 and -0.21 respectively. A mean absolute error of 0.21 means on average, the estimated value of T is within a factor of 1.6 of the measured value. The mean absolute error and mean error for T estimated using the empirical approach are 0.073 and 0.00021 respectively. A mean absolute error of 0.073 indicates that, on average, the estimated value of T is within a factor of 1.18 of the measured value. The established relationship between T and BH yield data also shows BH yield can also be a fair estimator of T in areas with only BH yield data. This has a goodness of fit above 0.8. The T and R of the aquifer are also linearly related with R^2>0.95 using an empirical relation and this can be used to extrapolate PT data to an area.

Table of Contents

1.0 INTRODUCTION 1
1.1 BACK GROUNDS 1
1.2 PROBLEM IDENTIFICATION AND STATEMENT 3
1.3 OBJECTIVES OF THE STUDY 4
1.3.1 GENERAL OBJECTIVES 4
1.3.2 SPECIFIC OBJECTIVES 4
1.4 METHODOLOGY, TECHNIQUES AND TOOLS USED 5
1.4.1 METHODOLOGY 5
1.4.2 TECHNIQUES AND TOOLS USED 7
2.0 LITRATURE REVIEW 8
2.1 LITRATURE REVIEW OF PREVIOUS STUDIES 8
2.2 AQUIFER PROPERTIES 9
2.2.1 INTEGRATION OF AQUIFER PROPERTIES 9
2.3 AQUIFER ELECTRIC PROPERTIES 13
2.3.1 INTEGRATION OF AQUIFER HYDRAULIC AND ELECTRIC PARAMETERS . 13
4.0 GEOMORPHOLOGY, DRAINAGE AND CLIMATE 18
4.1 GEOMORPHOLOGY 18
4.2 DRAINAGE 18
4.3 CLIMATE 22
5.0 GEOLOGY 24
5.1 REGIONAL GEOLOGY 24
5.1.1 Precambrian Rocks 24
5.1.2 Paleozoic Rocks 24
5.1.3 Mesozoic Rocks 24
5.1.4 Tertiary and Quaternary Volcanics 25
5.1.5 Tertiary and Quaternary Sedimentary Rocks and Sediments 26
5.2 LOCAL GEOLOGY 26
5.2.1 Volcanic Rocks 26
5.2.2 Unconsolidated Sediments 26
5.2.3 Sedimentary rocks 27
5.2.4 Precambrian Igneous Rocks 27

6.0 HYDROGEOLOGY 28
7.0 ANALYSIS, ORGANIZATION & DATA PREPARATION 36
7.1 PUMPING TEST DATA ANALYSIS 36
7.2 RECOVERY DATA ANALYSIS 43
8.0 DATA ORGANIZATION AND PREPARATION 45
8.1 DETERMINATION OF AQUIFER PROPERTIES FROM PUMPING TEST 48
8.1.1 SPECIFIC CAPACITY 48
8.1.3 Discharge Q (m^3/Day) 59
9.0 ESIMATING TRANSMISSIVITY FROM SPECIFIC CAPACITY AND BOREHOLE YIELD 60
9.1 ESIMATING TRANSMISSIVITY FROM SPECIFIC CAPACITY 60
9.1.1 ANALYTICAL METHOD 60
9.1.2 THE EMPIRICAL METHOD 67
9.1.3 THE GEOSTATISTICAL METHOD 71
9.2 ESTIMATING TRANSMISSIVITY FROM BOREHOLE YIELD 89
10.0 GEOPHYSICAL DATA ANALYSIS 91
10.1 VERTICAL ELECTRICAL SOUNDING 91
10.2 GEO ELECTRICAL INVESTIGAION 96
10.2.1 Geo-electrical section Waja area along A-A’ (SW-NE) 98
10.2.2 Geo-electrical section Alamata area along B-B’ (W-E) 98
10.2.3 Geo-electrical section Gerjale area along C-C’ (NW-SE) 98
10.2.4 Geo-electrical section Hujura area along D-D’ (WNW-ESE) 99
10.2.5 Geo-electrical section Kara area along E-E’ (NW-SE) 100
10.2.6 Geo-electrical section Kukuftu area along F-F’ (SW-NE) 100
10.2.7 Geo-electrical section Mehoni area along G-G’ (NW-SE) 101
10.3 RESULTS OF THE GEOELECTRICAL INVESTIGATIONS 109
10.4 EMPIRICAL RELATION BETWEEN TRANSMISSIVITY AND TRANSVERSE RESISTANCE 111
10.5 ELECTRICAL CONDUCTIVITY (EC) 112
11.0 CONCLUSION AND RECOMMENDAION 113
11.1 CONCLUSION 113
11.2 RECOMMENDATION 115
REFERNCES 116

APPENDICES 119
APPENDIX 1 Analysis results of pumping test and well information 119
APPENDIX 2 EC data (µS/cm) 124
APPENDIX 3 Results of analysis using Analytic Approach 125
Appendix 4 sample boreholes for confined and unconfined aquifer 129
Appendix 5 Final (calibrated) layer parameters 133

LIST OF FIGURES

Figure 1 Location map 17

Figure 2 Drainage Map 20

Figure 3 Elevation map 21

Figure 4 3-D model of the study area 22

Figure 5 Groundwater level contour map 30

Figure 6 Location map of boreholes used for sections 31

Figure 7 Chart for section A-A' 32

Figure 8 Chart for section B-B' 32

Figure 9 Chart for section C-C' 33

Figure 10 Chart for section D-D' 33

Figure 11 Chart for section E-E' 34

Figure 12 Location map of Borehole points 35

Figure 13 Time-drawdown graph of Friatna BH1 using Theis type curve 40

Figure 14 Time-drawdown graph of Friatna BH1 using Cooper-Jacob method 41

Figure 15 Time-drawdown graph of Wf Abergelle2 using Neuman type curve 42

Figure 16 Time-drawdown graph of Wf Abergelle2 using Jacob correction method 42

Figure 17 Recovery graph of Friatna BH1 43

Figure 18 Time-drawdown plot of Friatna BH1 for pumping and non pumping conditions 44

Figure 19 Transmissivity plots from Constant and Recovery data 44

Figure 20 Production rates used for specific capacity tests in the raya valley aquifer 59

Figure 21 Step drawdown plot for well RPW-074 63

Figure 22 Head loss constant in the formation B and well loss constant, C determined from step test 63

Figure 23 comparison of measured T and estimated T from analytic method 67

Figure 24 Empirical relation between log transformed Transmissivity and log transformed Specific capacity with a 69

Figure 25 Empirical relationship between log transmissivity and log specific capacity with a power relationship 69

Figure 26 Empirical relationship between log transmissivity and log specific capacity with a 2^{nd} order 70

Figure 27 flow chart on the analysis of data sets using geostatistical approach..... 72

Figure 28 Transmissivity map created with default parameters in Arc Gis 73

Figure 29 Histogram for T with Skewed distribution…….74

Figure 30 Histogram for T with log transformed 74

Figure 31 Histogram for Sc with Skewed distribution ……74

Figure 32 Histogram for Sc with log transformed Values and nearly normal distribution.....74

Figure 34 QQ plot for Sc……...75

Figure 35 Normal QQ plot for Sc log transformed..... 75

Figure 36 QQ plot for T…….76

Figure 37 Normal QQ plot for T log transformed 76

Figure 38 Trend surface for both transmissivity and specific capacity points 76

Figure 39 Semivariogram cloud for transmissivity 77

Figure 41 Semivariogram cloud for transmissivity 78

Figure 40 Semivariogram cloud for transmissivity 78

Figure 42 cross variogram between transmissivity and Specific capacity 79

Figure 43 Predicted Transmissivity map of the study area..... 80

Figure 44 cross validation result for transmissivity..... 81

Figure 45 Default hydraulic conductivity map..... 83

Figure 46 Histogram for hydraulic conductivity.……84
Figure 47 Hydraulic conductivity created by 84
Figure 48 Histogram of hydraulic conductivity with normal distribution after log transfor.84
Figure 49 Quantile distribution plots before and after log transformation..... 85
Figure 50 Trend Analysis plot for Hydraulic conductivity with a nearly u shape trend Identified in the E-W direction..... 85
Figure 51 Semivariogram cloud for hydraulic conductivity showing 4 semi variance groups between hydraulic..... 86
Figure 52 Data pairs of hydraulic conductivity related with distant pairs..... 86
Figure 53 Predicted map of Hydraulic conductivity..... 88
Figure 55 Empirical relationship between Transmissivity and discharge rate with linear fit 90
Figure 56 Empirical relationship between Transmissivity and discharge rate with polynomial fit..... 90
Figure 57 VES LV72 for BH RPW-021..... 94
Figure 58 Borehole lithological log of RPW-021..... 95
Figure 59. Location map of boreholes and VES points..... 97
Figure 60 Geo-electric section Waja area along A-A' 102
Figure 61 Geo-electric section Alamata area along B-B'..... 103
Figure 62 Geo-electric section Gerjelle area along C-C' 104
Figure 63 Geo-electric section Hujura area along D-D'..... 105
Figure 64 Geo-electric section Kara area along E-E' 106
Figure 65 Geo-electric section Kukuftu area along F-F'..... 107
Figure 66 Geo-electric section Kukuftu area along F-F'..... 108
Figure 67 EC contours..... 110
Figure 68 Transmissivity versus Transverse resistance plot 111

LIST OF TABLES

Table 1 description of boreholes along section A-A' 32

Table 2 description of boreholes along section B-B' 32

Table 3 description of boreholes along section C-C' 33

Table 4 description of boreholes along section D-D' 33

Table 5 description of boreholes along section E-E' 34

Table 6 description of boreholes along section F-F' 34

Table 7 Analysis results of pumping and recovery tests 48

Table 8 Analysis results of specific capacity before and after drawdown correction 54

Table 9 Corrected drawdown using Jacob correction for wells tapping unconfined aquifers 58

Table 10 Pumping times for constant rate test..... 62

Table 11 Data requirements for estimating Transmissivity from specific capacity using analytic solutions 66

Table 12 Calibration of VES LV72 based on lithological log of BH RPW-021 Waja area. 96

LIST OF ACCRONYMS

BH	Borehole
DEM	Digital Elevation Model
EC	Electric conductivity
GIS	Geographic information system
HTS	Hunting technical services
K	Hydraulic conductivity
KAADP	Kobo Alamata agricultural development project
a.m.s.l	above mean sea level
n	Number of data values
PT	Pumping test
Q	Pumping rate
R	Transverse resistance
RVIP	Raya valley irrigation project
RVADP	Raya valley agricultural development project
REST	Relief society of Tigray
RVDP	Raya valley development project
SWL	Static water level
T	Transmissivity
TDS	Total dissolved solids
VES	Vertical electrical sounding
WWDSE	Water works design and supervision enterprise

1.0 INTRODUCTION

1.1 BACK GROUNDS

The concept of groundwater regions is a very important generalization in the study of hydrogeology. These are geographical areas of similar occurrence of groundwater. If an area is subdivided into several smaller regions, useful comparisons can be made between areas of well known hydrogeology and areas that are geologically similar but have not been as well studied (Fetter, 2001).

One way of the useful approach to the study of the groundwater regions is the use of relationships and comparisons between aquifer properties and between aquifer hydraulic and electric parameters.

Knowledge of Transmissivity and hydraulic conductivity is essential for the determination of natural water flow through an aquifer (F.louis and others)

Transmissivity is one of the most fundamental parameters of an aquifer it allows to estimate water levels in and around pumping wells, to estimate groundwater flow and contaminant transport times, to characterize aquifer heterogeneity, and to parameterize numerical ground water flow models. Because transmissivity in aquifers can range over 13 orders of magnitude assuming a constant formation thickness (Freeze and cherry, 1979, p.29, in E.Mace, 2000)

There are many techniques available to assess the Transmissivity of aquifers using time draw down Aquifer tests and analyzed using type curves (e.g. Theis, 1935) or other graphical (e.g. Cooper and Jacob, 1946). However, because of the expense of conducting standard aquifer tests to obtain transmissivity many researchers have tried to relate transmissivity to specific capacity as the specific capacity data are relatively available (Razack[a] and Huntley[b], 1991). Well specific capacity data is readily available from a single observation of pumping rate and drawdown, to estimate aquifer transmissivity.

There are several different approaches for estimating transmissivity from specific capacity (E.Mace, 2000). These approaches include Analytical, Empirical and Geostatistical approaches.

There are also other techniques which lead to the indirect evaluation of the hydraulic properties of aquifers; these are estimating the hydraulic parameters from geo electrical properties of water bearing horizons.

A pumping test is the standard method used to evaluate the hydraulic parameters of subsurface characteristics of water bearing horizons. However, surface VES measurements can be used to determine the hydraulic parameters of aquifers. In addition to these, early hydrogeologists used VES measurements to qualitatively assess the permeabilities of deposits (Zohdy (1965); Page (1969) and Meidav (1960) in Yang[1] and others (1997)).

Geophysical methods can contribute substantially towards this approach and can greatly reduce the number of necessary pumping tests, which are both, expensive and time consuming (F. Louis and others, 2010)

The research area is found in the Raya valley which is located in the northern part of Ethiopia Southern zone of Tigray Region. It is thought to be as one of the promising potential agricultural areas in the region. Recently this region has been working intensively on groundwater development mainly for irrigation purposes and for water supply. There are around 136 borehole data collected from different governmental, non governmental and private companies.

According to (Anon. 1998) the Hydrogeological report of the Raya Valley Agricultural Development Project RVADP (1998), the Valley is sub-divided into two sub-basins called Alamata sub-basin and Mehoni sub-basin.

From 2003 to 2006 a total of 44 productive wells were drilled by REST (Relief Society of Tigray in Alamata and Mehoni sub-basins out of which 31 borehole with well test conducted on them for less than 72 hrs of pumping time and four aquifer tests in four well fields were conducted with each well field having five observation wells RVPIP Anon. (2008). In addition to these there are 100 newly drilled wells for the Raya valley pressurized irrigation project held by Water Works Design and Supervision Enterprise in association with Concert Engineering and Consulting Enterprise. The duration of the test was 15 days. These wells were drilled by REST.

For the future, with increased development and utilization of the ground water resource,

problems such as over exploitation might lead to environmental damage. Thus, the need for optimal management of this resource is crucial. Accordingly, assessment of the areal distribution of aquifer hydraulic properties with sufficient accuracy is important that management tools such as numerical models might be employed (M. Razack[a] and David Huntley[b], 1991). Mapping the distribution of aquifers and estimating the hydraulic parameters of these aquifers are the most important steps in controlling the amount of groundwater abstraction from wells. Studies incorporating Quantitative characterization of aquifer hydraulic parameters are limited in most part of the country.

1.2 PROBLEM IDENTIFICATION AND STATEMENT

Because of the economic limitations, performing large numbers of aquifer tests for the determination of hydraulic properties is unrealistic. So that it is important to turn to other techniques which lead to the indirect evaluation of these hydraulic properties. One of the most common is the use of well specific capacity, readily available from a single observation of pumping rate and drawdown, to estimate aquifer transmissivity (M. Razack[a] and David Huntley[b], 1991). And the other is the transverse resistance computed from the field sounding data measured nearby the wells to the transmissivities measured within the wells. An empirical relation between the transverse resistance and transmissivity could thus be derived. The hydraulic parameters at the VES locations without any well information could still be predicted from such empirical relationships. Thus, the locations of the most promising sites for future drilling could be determined (Yang[1] c. and others, 1997). It can also be applied to predict the hydraulic parameters in locations without available well information in the alluvium covered parts of the Raya valley. This will have great benefit for the future management of ground water in the study area.

Due to the fact that the costs of performing a well designed aquifer test and the expertise required performing and analyzing the data, most water supply wells, especially private wells have not had time draw down tests performed on them. This leaves most of groundwater investigations with only a few tests to characterize the transmissivity of an aquifer resulting in poorly-defined averages (E. Mace, 2000).

In addition to this, and considering the future groundwater management practices the approaches mentioned above could yield valuable information for input to numerical models and for evaluating water resources potential.

1.3 OBJECTIVES OF THE STUDY

1.3.1 GENERAL OBJECTIVES

The main objective of the research is to quantitatively characterize the aquifer hydraulic parameters of the Raya valley by developing:

- Correlation between specific capacity and transmissivity. Because of the expense of conducting standard aquifer tests to obtain transmissivity and the relative availability of specific capacity data transmissivity can be estimated from specific capacity in areas where there is no pumping test data.
- Correlation between transmissivity and borehole yield data, although the quality of the yield data is lower overall than that of the specific capacity or transmissivity data it may help in the estimation of transmissivity thereby predict the productivity of the aquifers.
- To establish empirical relationships between geo-electrical parameters and aquifer hydraulic parameters. This is done by empirically relating the transverse resistance computed from the field sounding data to transmissivity data directly measured within the wells, so that VES data can be used to extrapolate aquifer hydraulic parameters to an area without available well information.

1.3.2 SPECIFIC OBJECTIVES

The specific objectives of the research work are as follows:-

- To increase the number of transmissivity estimates of the Raya valley aquifer. Transmissivity estimated from specific capacity data, borehole yield data and surface geophysical data.
- To parameterize the aquifer hydraulic properties for input to numerical models
- To prepare hydrolithologic cross-sections based on borehole lithologic records to understand the zones of potential horizons for ground water occurrence.
- To observe the grain size distribution of the alluvial materials along and across the valley and to have an idea about the subsurface morphology of the aquifer system.

- Construction of geoelectric- sections using VES data to understand the electric properties of hydrolithologic units vertically and horizontally.
- Preparation of Interpolated Transmissivity map of the project area.
- To compare with previously prepared aquifer productivity maps if any.
- To check the productivity of the aquifers with depth, i.e. qualitatively determine if aquifer productivity increases with depth. This is done by first calculating the specific capacity index for each well.
- To check the variation on the groundwater potential of the aquifer system with grain size distribution.

1.4 METHODOLOGY, TECHNIQUES AND TOOLS USED

1.4.1 METHODOLOGY

The methodology followed for the research work encompasses three main phases to come up with the results; these are pre field work, field work and post field work

1.4.1.1 PRE FIELD WORK

In this phase different works are executed

- Literature reviews of previous works
- Extraction of the surface water divide and preparation of drainage map of the study area from DEM using Arc GIS 9.3 software
- Around 150 pumping test, more than 200 VES raw data, 150 bore hole lithological data and around 80 water quality raw data are collected from different governmental, non governmental and private companies and preliminarily analyzed using Aquitest 3.5, IPI2win 3.0.1, Strater and (Aquachem and XL stat 9.1) softwares respectively.

1.4.1.2 FIELD WORK

- The field work includes rough assessment of the study area and site visit to some borehole sites. It is conducted in order to check up the well locations and collection of other pertinent data.

1.4.1.3 POST FIELD WORK

This is the main phase of the research work and it includes

- Data organization, processing, analysis and interpretations of pumping test, geophysical and borehole lithological data using different softwares.
- The analysis and interpretation is supported by different Softwares for image analysis and processing.

The preliminary analysis results of the pumping test and VES raw data are aquifer hydraulic and electric parameters. These are organized and refined for further analysis as follows The transmissivity data obtained from the analysis of constant rate test, the final drawdown noted and the pumping rate used for the test for each well are grouped in order to establish a relationship between transmissivity and specific capacity. Three main approaches are used for estimating transmissivity from specific capacity data. These are analytical techniques, empirical techniques and Geostatistical techniques. The results of the three techniques are compared

The most commonly used analytical approach is an equation derived from the Theis nonequilibrium formula which requires specific capacity, well radius, production time, and an estimate of storativity for estimating transmissivity. When using the analytical approach, it is appropriate to correct for well loss, vertical flow due to partial penetration. Well loss does not become important in most wells until the production rate exceeds 36 l/s. (E. Mace, 2000)

The empirical approach involves empirically relating transmissivity to specific capacity measured in the same well. This approach is advantageous because specific-capacity data do not have to be corrected for turbulent well loss or vertical components of partial penetration. (E. Mace, 2000)

Geostatistical techniques are applied for estimating transmissivity from specific capacity data. Using this approach interpolated maps of transmissivity are developed and the uncertainty of the estimates are quantified. Two Geostatistical techniques are commonly used: kriging with linear regression or cokriging. The choice of technique depends on the

number of transmissivity and specific-capacity data pairs, and, ultimately, how each performs in estimating transmissivity. If there are greater than 50 transmissivity and specific capacity pairs, cokriging may offer better results than kriging with linear regression. (E. Mace, 2000)

The transmissivity is also estimated from the empirical relationship between transmissivity and borehole yield data and borehole yield data with specific capacity data. Although the quality of yield data are relatively lower than specific capacity and transmissivity data due to different reasons, they can be helpful to be a fair indicator of aquifer productivity in the absence of transmissivity and specific capacity (Graham et.al, 2009)

Transmissivity is also estimated from the relationship between aquifer hydraulic and electrical properties quantitatively by an empirical approach. Therefore in the absence of pumping test data VES data can be used to predict and extrapolate the aquifer hydraulic properties to an area, William E. Kelly[a] (1977).

The data used for the characterization of aquifer hydraulic and electric properties are pumping test and geophysical data. These are Transmissivity, specific capacity and yield data determined from a single borehole and the transverse resistance (ρ*b) computed from surface geophysical (VES) data conducted nearby a well.

In the analysis relevant information is taken from the review of previous works in the area and literature review from similar geologic settings abroad.

1.4.2 TECHNIQUES AND TOOLS USED

After preliminary analysis of the pumping test, geophysical, and borehole lithological data by relevant softwares they are statistically treated for final analysis. Different softwares are employed for the preliminary, image processing and final analysis these are AquiferTest v3.5, Arc GIS 9.3, Global Mapper 1, Surfer 8.1, IPI2win v3.0.1, Aquachem 4.0, Strater, XL stat 9.1 and Microsoft office Excel 2003 and 2007. For geo referencing of some places and borehole locations Garmin GPS 60 is used.

2.0 LITRATURE REVIEW

2.1 LITRATURE REVIEW OF PREVIOUS STUDIES

A number of studies were conducted in the Raya valley; most of them have focused in the assessment and evaluation of the groundwater resources and management aspects.

(D. Nedaw, 2003) studied to characterise the ground water from geological, hydrological and chemical point of view. In his work the mean annual rain fall and mean actual evapotranspiration of the valley are found to be 779 mm and 695 mm respectively. The surface water outflow of the Raya Valley was estimated to be 60 Mm^3 annually from the basin. The annual recharge to the whole Raya valley was computed to be 129.3 Mm^3. Based on calculated transmissivity values potentiality of the aquifers of the valley are classified from high (> 500 m^2/day) to weak (< 0.5 – 5 m^2/day).

Amare (2007) tried to numerically simulate characteristics of groundwater flow system of the Mehoni sub basin under steady state condition.

Hagos (2005) has studied Hydrogeology of Mehoni sub-basin and Lake Ashenge catchment, in his work the mean annual precipitation and mean actual evapotranspiration of the Mehoni sub-basin was estimated to be 723.57mm and 687.24mm respectively. The annual recharge of the sub-basin was computed to be 66.5Mm3

Hunting Technical Services (HTS) has conducted a study in the Mehoni area in the Tigray Rural Development Study conducted during 1974 and 1975 (Hunting, 1976). According to RVDP (Raya Valley Development Project), the HTS report has a lower estimation for the magnitude of surface water flow in Mehoni area. German Consult in 1977 has prepared hydrogeology of the southern part of raya valley at a reconnaissance level under the Kobo - Alamata Agricultural Development Project (KAADP). The study has resulted a conceptual ground water balance and was analysed by the RVDP project. It was found to be less realistic on the conclusion of the amount of ground water inflow to the valley on the western escarpment to be equal to the amount leaving the valley fill on the east owing to the fact that the geological and tectonical condition of the two escarpments being different.

Under the project entitled as Raya Valley Development Project (RVDP) from 1996 to 1998. The Hydrogeological work was mainly conducted to determine the ground water resource potential; the geological work was done in order to give background information for Hydrogeological and dam studies. The hydrological studies were mainly directed with assessment of surface water resources. From this study the ground water flow direction was determined summarised to be West - East and North - South, but in this study it has been found two separate ground water flow system (Mehoni sub basin and Alamata sub basin) on southern part and northern part both having flow towards the centre (RVDP, 1998).

Luel (2010) has conducted a study on the correlation of aquifer resistivity and hydraulic parameters in a locality named Gerjale found in the central part of the Raya valley. In his work he correlated transverse resistance calculated from VES data conducted near calibration boreholes and transmissivity obtained from pumping test conducted at the same boreholes and obtained a non linear regression equation of $T=21.397*(T_R)^{0.5336}$ with $R^2=0.96$, n = 10. Based on this relation he prepared map of transmissivity of Gerjale area. He concluded that this correlation can be applied for estimating transmissivity values in places where pumping test data are not available and he also added that with similar methodology of the research the correlation of resistivity and hydraulic parameters could also be applied in similar Hydrogeological settings, where data on hydraulic parameters are inadequate.

2.2 AQUIFER PROPERTIES

2.2.1 INTEGRATION OF AQUIFER PROPERTIES

Traditionally standard pumping test was the only method for the determination of aquifer hydraulic parameters such as transmissivity and hydraulic conductivity. But, nowadays several researchers have tried to build a relationship between aquifer properties so that one can estimate the aquifer hydraulic parameters in the absence of pumping test data (e.g. E. Mace, 2000; M. Razack[a] and David Huntley [b], 1991; Graham, 2009; Verbovsek, 2008; E. Mace and others,1999;)

E. Mace, 2000 has categorized and summarized the different available techniques for establishing a relationship between transmissivity and specific capacity and has presented three main available approaches for estimating transmissivity from specific capacity: these

are Analytical, Empirical and Geostatistical. He categorized the techniques based on their method of analysis, their importance one over the other and data availability. He also stated that the analytical methods to be advantageous because they are exact but need corrections for non ideal conditions. According to Mace; Thomasson and others (1960) were the first to analytically relate transmissivity to specific capacity using Dupuit- Thiem equation,

$$S_w = (Q/_{2\pi T}) \ln (\frac{R}{r_w})$$

Theis and others, 1963 related specific capacity to transmissivity based on Theis non equilibrium equation, $S_c = 4\pi T/(ln[2.25Tt/r_w^2 S)$

E. Mace, 2000 also noted that the Empirical Methods to be advantageous because the uncertainty in the estimate can be estimated. This method involves statistically relating transmissivity to specific capacity using paired values of both parameters measured in the same well and that the method works good for at least 25 data paires.

E.Mace, 2000 emphasized to use the Geostatistical method if the purpose is to produce an interpolated map of transmissivity from the established relationship of transmissivity and specific capacity and he recommends to use cokriging if the data pairs are more than 50 and kriging with regression if the data pairs are more than 25.

He also noted these techniques have been successfully applied in many aquifers in Texas and elsewhere to provide valuable information for input to numerical models.

Mace and others, 1999 have compiled and analyzed transmissivity, hydraulic conductivity and storativity data for the entire Carrizo-Wilcox aquifer in Texas resulting in a database of 7,402 estimates of hydraulic properties in 4,456 wells for the purpose of regional ground-water management issues by establishing a database readily available for analysis; because developing regional water plans require permeability and storativity data to make accurate predictions of ground-water availability and potential water-level declines.

They also related aquifer and specific-capacity data for the entire Carrizo-Wilcox aquifer and investigated the spatial continuity of transmissivity and hydraulic conductivity in the aquifer through the use of Geostatistical approach. They used empirical and analytical approach to estimate transmissivity from specific capacity based on 217 datasets which have

complete time drawdown and other relevant informations necessary to calculate T using standard PT analysis techniques and estimated transmissivity from specific capacity data. They developed an empirical relationship by linearly relating log-transformed transmissivity to log-transformed specific capacity calculated for the same well and found the best-fit line through the data to be

$T = 1.99 Sc^{0.84}$ with the correlation coefficient, $R^2 = 0.91$ and using the analytical relationship by Theis and others (1963) using the Theis (1935) nonequilibrium equation:

$S_c = 4\pi T/(ln[2.25Tt/r_w^2 S)$ Solved it iteratively in a spreadsheet and evaluated the relative accuracy of transmissivity estimated using the empirical relationship against transmissivity estimated using the analytical relationship. They also determined the mean absolute error and mean error between calculated transmissivity (using time-drawdown data) and transmissivity estimated using the two specific capacity methods and found that the analytical approach provides slightly more accurate estimates of transmissivity than does the empirical approach.

They have presented the analysis results using semivariograms and indicated that the Carrizo Sand and undivided Wilcox Group are spatially correlated over about 17 and 25 mi, respectively. They developed Kriged maps of transmissivity and hydraulic conductivity and showed areas with greatest values of the hydraulic parameters. They concluded that study quantifies the variability and spatial distribution of transmissivity, hydraulic conductivity, and storativity and indicated that the results of their study will be useful for developing local and regional water plans and to develop numerical ground-water-flow models to predict the future availability of the water resource. Transmissivity and hydraulic conductivity vary vertically among formations and laterally within formations and lateral variations of transmissivity and hydraulic conductivity have spatial continuity.

Graham and others, 2009 have tried to integrate aquifer properties of the Scottish aquifer by collecting data from more than 3000 groundwater sources aiming to better understand Scotland's aquifers through the collation of a comprehensive set of quantitative data. They analyzed 157 transmissivity values, 307 specific capacity values and 1638 borehole yield values and categorized the Scottish aquifers based on their productivity. After working with some data quality issues they established an empirical relationship between transmissivity and specific capacity and transmissivity and borehole yield data and found that a strong

correlation between specific capacity and transmissivity $T= 1.6(Q/S)^{0.93}$ with ($r^2 = 0.8$, n=116) and indicated that SC can be a reliable indicator of aquifer productivity where no transmissivity data are available and $T=0.13Q^{1.03}$ with ($r^2 = 0.57$ and n= 131) for the correlation between transmissivity and borehole yield data although the quality of the yield data is lower overall than that of the specific capacity or transmissivity data. The relationship they obtained for SC and borehole yield is reasonable with best fit line of $Q/S = 0.13Q^{0.99}$, $r^2 = 0.62$ and n = 302 and they stated that although this shows a significantly weaker correlation than was found between specific capacity and transmissivity. Borehole yield may, therefore, be a fair indicator of aquifer productivity in the absence of specific capacity or transmissivity values. In their conclusion they stated that there is good agreement between the available data for all three parameters and the categories assigned to the existing bedrock aquifer productivity map of Scotland and this may be a viable alternative to use specific capacity data to assess aquifer productivity in Scotland.

Razack[a] and Huntley[b], 1991 have established a relation between aquifer transmissivity and specific capacity in order to estimate transmissivity in Haouz Basin a large and strongly heterogeneous aquifer in the region of Marrakech city (Morocco) based on a large (215 pairs) data set from a heterogeneous aquifer taking in to consideration the expense of conducting standard aquifer tests to obtain transmissivity and the relative availability of specific capacity data. They analyzed the data sets using analytic expressions derived by Thomasson and others (1960) and Theis (1963) to relate specific capacity to transmissivity. They found that the analytic solutions predicting transmissivity from specific capacity do not agree well with the measured transmissivities, apparently due to turbulent well loss within the production wells, which is not taken into account by any of the analytic solutions. Empirical relations are better than the theoretical relations. Log-log functions have greater correlation coefficients than linear functions. The best relation they found for the data set chosen for this study has a correlation coefficient of 0.63 and they suggested that correlations based on data sets of 10 points or less are of limited value. They concluded that use of analytical approach for the estimation of transmissivity from specific capacity does not agree well with the measured values of transmissivity for valley-fill sediments from the Haouz Plain. The analytic solutions generally under predict the transmissivity based on measured specific capacity. This error appears to be due to turbulent well loss, which is not

taken into account by any of the analytic approaches. Empirical relations between transmissivity and specific capacity produce less error than analytic solutions and they found that the correlation coefficient of the log-log relation (0.63) was better than the correlation coefficient of the linear relation (0.40) and the best-fit regression line for the Haouz Plain data set is $T = 0.36 (Q/S)^{0.67}$ for transmissivity and specific capacity both in units of sq meter/second.

2.3 AQUIFER ELECTRIC PROPERTIES

2.3.1 INTEGRATION OF AQUIFER HYDRAULIC AND ELECTRIC PARAMETERS

Relationships between aquifer characteristics and electrical parameters of the geolelectrical layers have been studied and reviewed by many authors (Kelly, 1977; Niwas and Singhal, 1981; Onuoha and Mbazi, 1988; Mazac et al., 1985; Mbonu et al., 1991; Huntley, 1986). Some researchers assume that the geology and ground water quality remains fairly constant within the area of interest and the relationships between aquifer and geophysical parameters deduced, are based on this assumption (Niwas and Singhal, 1981; Mbonu et al., 1991).

Louis and others, 2010 have conducted a study on the determination of aquifer hydraulic parameters using resistivity investigations in Mornos River Valley at central Greece which have an area of $25km^2$. They attempted to determine the aquifer transmissivity on the basis of monitoring the variations of the ground water resistivity within the area of investigation and aquifer depths resulting from multilayer resistivity models were also used in the determination of aquifer characteristics within the alluvial plain area of Mornos river valley. They conducted 34 VES and 13 of them nearby calibration wells and around 47 measurements of groundwater resistivity in the same number of wells. Based on the fact that the resistivity of the saturated rock, ρws is directly proportional to the resistivity of the water, ρw filling the pores (Archie, 1942):

$\rho_{ws} = F^* \rho_w$ they calculated the formation factor F from the measured water resistivity and the resistivity of the saturated formations determined from the interpretation of surface resistivity data and established an empirical relationship between the formation factor and hydraulic conductivity determined from the pumping test analysis of the calibration boreholes and got K= 2.12F-1.59 (R=0.958) by using linear regression. they calculated transmissivity from the relationship T = Kb; where k is the hydraulic conductivity obtained

from the empirical relationship and b is the thickness obtained from geoelectric analysis and also they developed an empirical relation between transmissivity and transverse resistance T= 0.22TR-287.61 (R = 0.95) by linear regression from Calibration resistivity soundings performed at wells where pumping tests were carried out. Finally they concluded that the application of the resistivity exploration technique permitted the extrapolation of the data obtained by drilling tests within the study area.

Salem, 1999 also conducted a research on the determination of aquifer fluid transmissivity and electric transverse resistance for shallow aquifers in (Schleswig-Holstein, northern Germany) and deep reservoirs (Jeanne d'Arc Basin, offshore of eastern Canada) with geology of Sand and gravel underlain by Clay and shaly Sandstone respectively, utilizing surface and well-log electric measurements. He calculated the transmissivity and transverse resistance of the aquifers and reservoirs from the surface and borehole electric measurements. As T = k*b; he determined k for each layer from an empirical relationship with respect to formation factor F; the F was obtained as R_b/ Rw (bulk resistivity divided by pore-water resistivity). The R_b (Ω.m) was obtained from VES, and R_w (in Ω.m) was obtained from chemical analysis of the pore water and b from the analysis of VES data. Determination of these parameters provides a good knowledge of the potential of porous media, because they relate fluid flow to electric-current conduction, in terms of layer thickness, permeability and resistivity. He obtained Direct relationships between both parameters $T=62.296*T_R^{0.70203}$, with coefficients of correlation of 0.99 in Germany and $T=112.41*T_R^{0.2189}$ with R^2 of 0.94 in Canada the relationships suggest that an increase in both parameters indicate presence of zones of high fluid potential within the aquifers.

Yang[1] and others, 1997 conducted a research on the relationship of aquifer hydraulic parameters and geolelectrical behavior in the Pachang-chi and Tsengwen-chi, southern Taiwan, which is characterized by a recent alluvial cover. They conducted 102 VES data of the schlumberger array to map the paleo depo- and hydro-environment of the area based on the vertical and horizontal distribution of the resistivity and to evaluate the physical parameters of the aquifer i.e. hydraulic and electric parameters.

The interpretation method they followed for the resistivity data analysis was qualitative and quantitative approach. Qualitatively by using contours of apparent resistivity with different

half electrode spacings (namely, 10m, 25m, 50m, 100m, …300m). The contour maps reflect variation of regional apparent resistivity with depth and they tried to predict the paelo-depositional environment. They also added that the deposition/transportation direction can be deduced from the trend of apparent resistivity distribution. Quantitatively they related the final layer parameters obtained from VES data using computer program automatic iteration to nearby borehole lithology, logs of sea level change and ^{14}C age obtained from a well. Finally from the map of resistivity distribution they concluded that the source of deposition was the northeastern hill based on the trend of decreasing values from northeast to south west. They also confirmed the decrease in grain size of the deposition medium from northeast to southwest.

Regarding the evaluation of the physical parameters of the aquifers they used the analytical relationship between hydraulic and electric parameters developed by Sri Niwas and Singhal (1981); $T = K*\sigma*R$

Assuming the product $K*\sigma$ to be a constant of a locality they established a local empirical equation using $T = K*\sigma*R$ after dividing the region in to localities. They estimated the local transmissivity from the parameters obtained from pumping test analysis and the resistivity data interpretation and compared the computed map of transmissivity with the observed ones and got same features.

3. DESCRIPTION OF THE STUDY AREA

3.1 LOCATION

The Raya valley is located in the southern part of Tigray regional state, northern part of Ethiopia, about 608 kilometers from Addis Ababa. Geographically it is bounded by $12^0$5'-$12^0$58' Latitude N and $39^0$20'- $39^0$53' Longitude E. It has an enclosed surface water shed area of 2579.75km^2 (Fig.1)

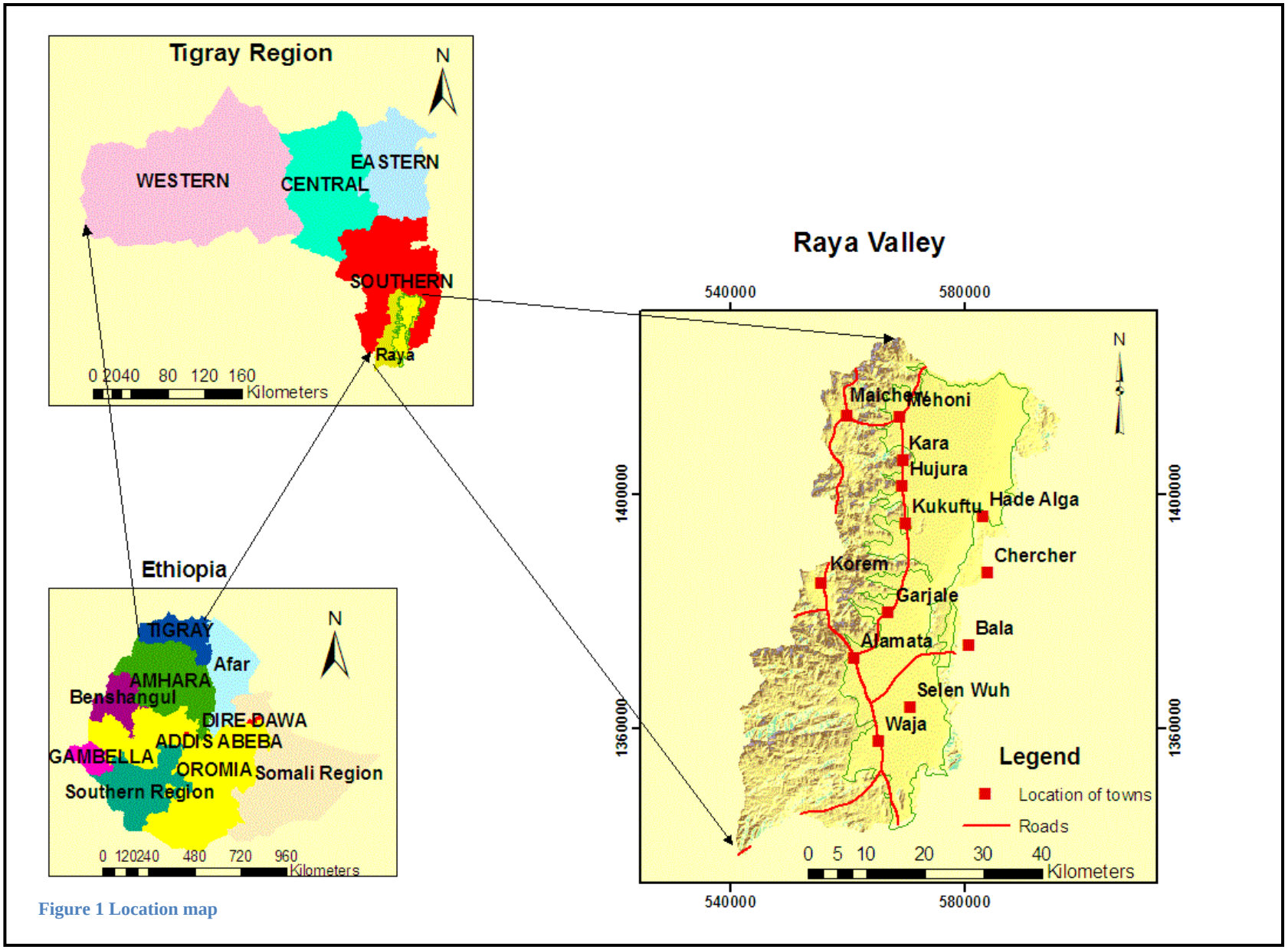


Figure 1 Location map

4.0 GEOMORPHOLOGY, DRAINAGE AND CLIMATE

4.1 GEOMORPHOLOGY

The geomorphologic features of the Raya valley can be seen clearly from the three dimensional view of the digital elevation model and elevation map of the study area prepared by applying Surfer 8.1 and Arc Gis 9.3 softwares respectively (Fig3 and Fig4). As can be clearly seen from the Figures the area is characterized by a nearly N-S aligned valley with graben like structure bordered in the west and east by volcanic ridges. It can be classified in broad sense namely the western mountain chains, the associated sloppy topography, the valley floor and the eastern margin of the valley which is less pronounced than the western margin. The elevation range in the area is between 1424 and 3678 meters a.m.s.l, where the valley floor is characterized from 1700 meters in the north to 1424 meters in the south describing the general surface water flow direction to be nearly N-S where it drains through the outlet in the south eastern part of the valley to Afar depression and from this it can be deduced that the Raya valley is part of the Danakil depression (Fig 4).

The Raya Valley plain is bounded in the west by Korem and Maichew mountain chains in the west and Chercher uplands in the east and Waja town in the south with respect to the valley axis.

It is regarded as part of a series of interconnected valleys of the Ethiopian rift system (RVPIP, 2008).

4.2 DRAINAGE

The Raya valley consists of three major drainage systems emerging dominantly from the western mountain ranges, partly from the eastern margin and the drainage system of Sulula River (Fig 2). The streams which emerge from the western uplands are characterized by a dendritic drainage pattern with separate and nearly parallel flow paths and follow a nearly W-E flow direction up to the central valley where they disappear in the central valley floor with no defined path, how ever the streams from the eastern margin of the valley are connected to Sulula River which is the major drainage system in the area and follows a nearly NNE-SSW flow direction and drains the valley through the only out let in Selembir which is characterized by least elevation (Fig 3). All the streams in the area are intermittent; there was no any perennial flow of surface water during the field visit in April in all parts of

the valley, except the minor seepages from Waja springs which die out with in short distance in the valley. During summer season the run off from the western upland areas may flow as sheet flow when it intersects the valley floor, because there is no any defined stream channel in the central floor of the valley. This situation may have a contribution to the swampy nature of the Gerjale area located in the centre of valley in addition to other additional cases.

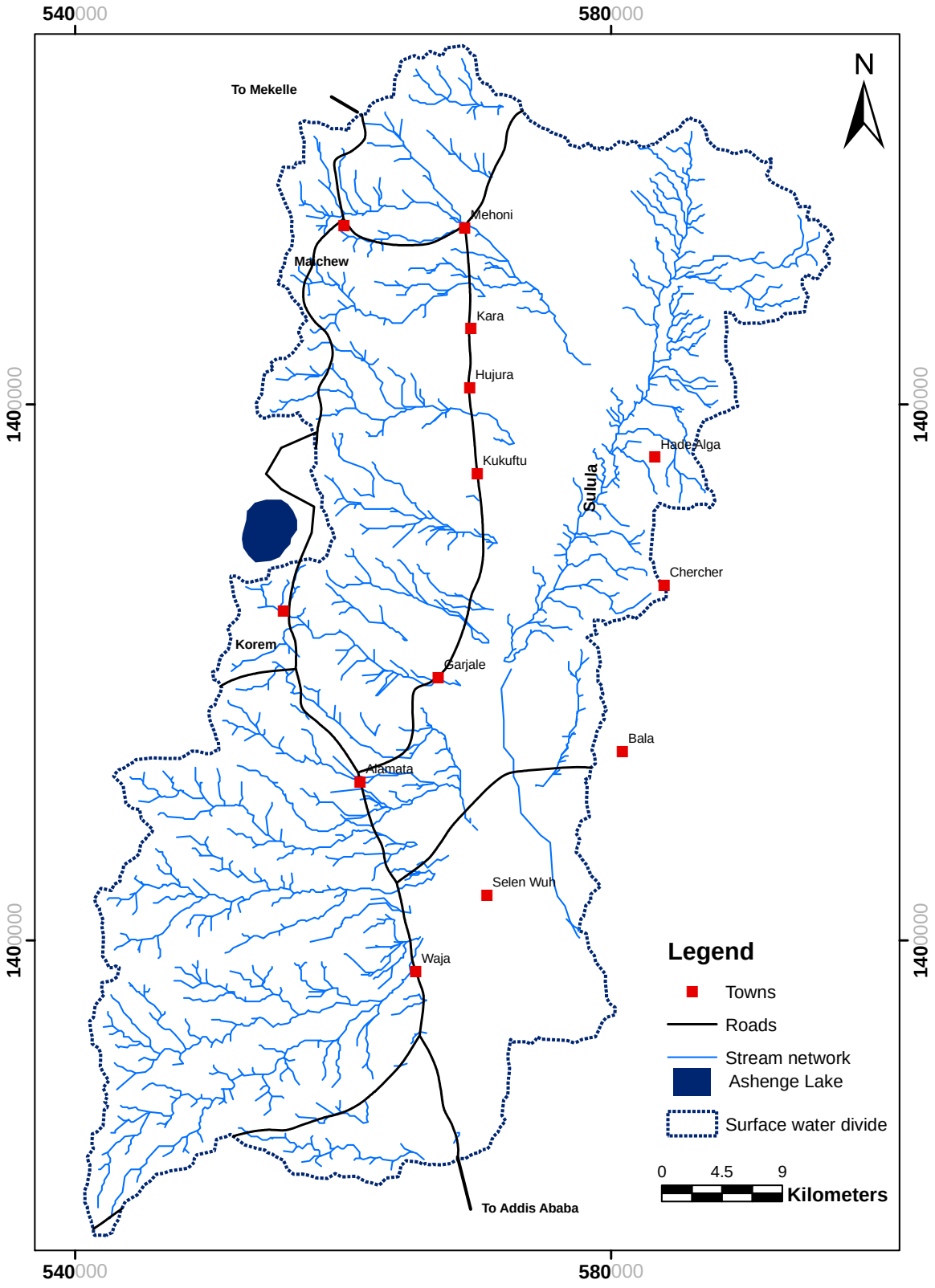


Figure 2 Drainage Map

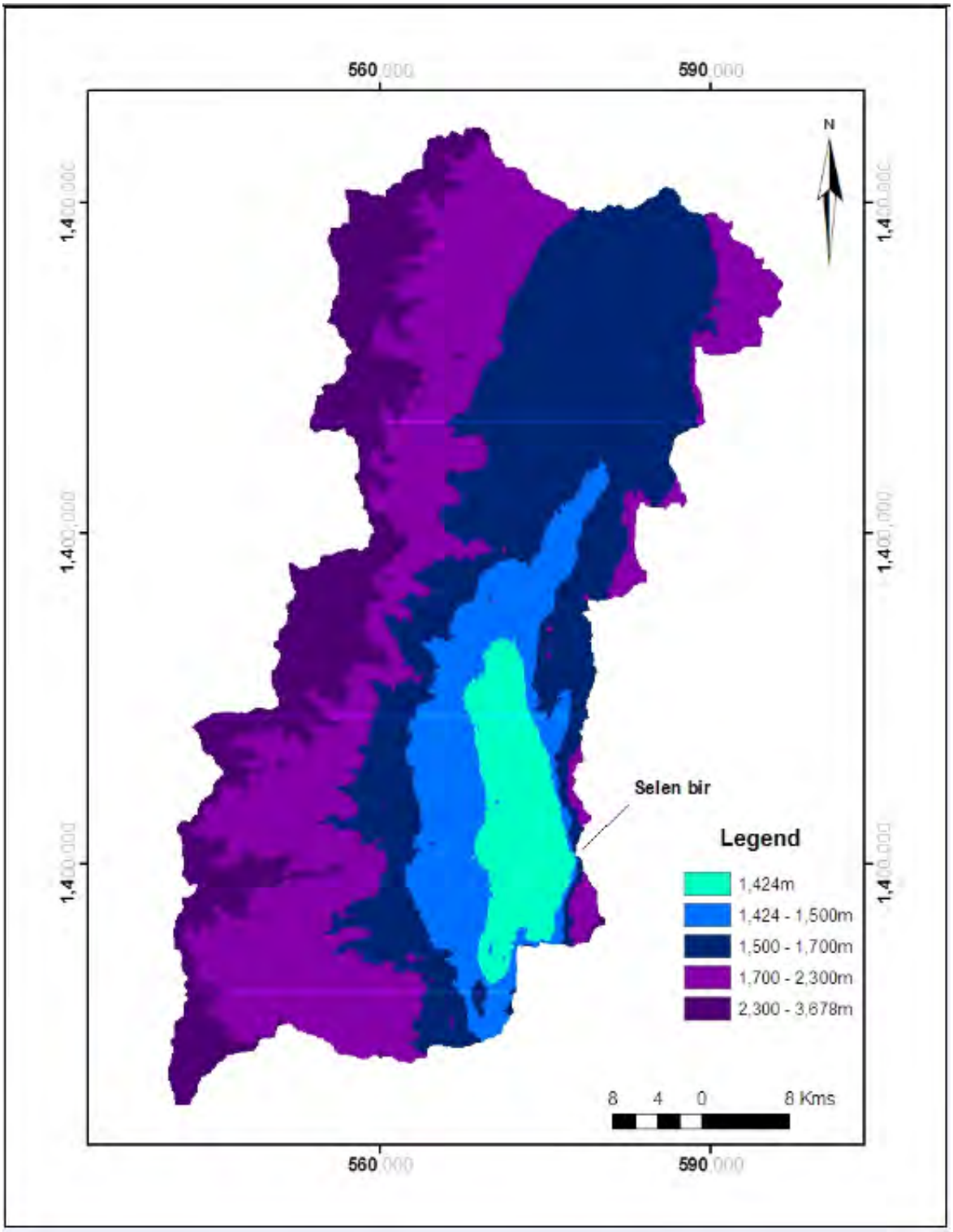


Figure 3 Elevation map

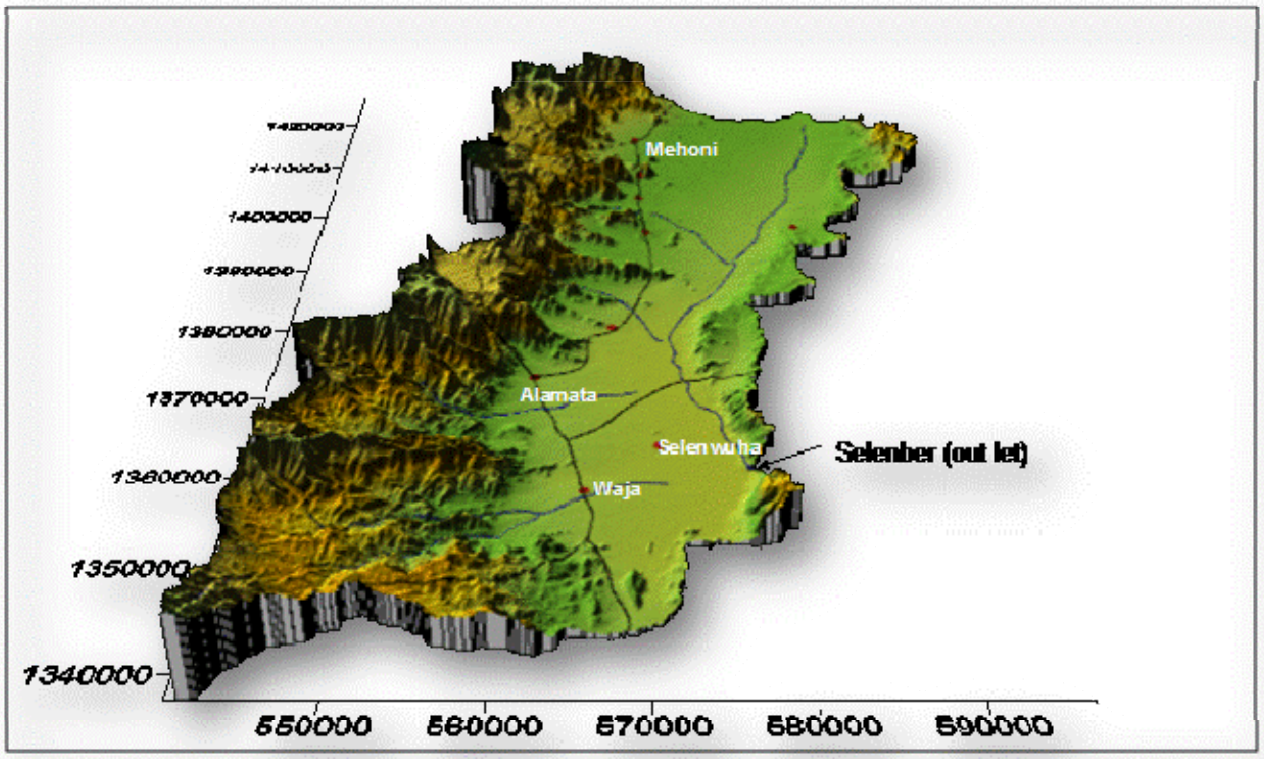


Figure 4 3-D model of the study area

4.3 CLIMATE

According to the classification method of the National Atlas of Ethiopia based on the altitude- climate relationship, the climate of the study area can be grouped in to four main groups. These are tropical (kola), Subtropical (woina dega), temperate (dega) and Alpine (Kur) to areas between 500-1550, 1550-2300, 2300-3300 Denakil depression a.m.s.l respectively. The altitude range of the study area is between 1,424-3,678 m so it can be correlated to the above categories.

The rainfall distribution in the area seems to be correlated with altitude, because the main recharge areas of the valley are the adjacent uplands of the western marigin where there exists high precipitation than the low lying areas of the valley. D. Nadew, 2003 has discussed on the variation of rainfall with altitude i.e. the highest rainfall is related to highest elevation and vice versa based on the analysis of data from rainfall stations located at different altitudes within the Raya watershed boundary.

The study area receives bimodal rainfall "big rains" in summer and "small rains" in spring. The easterly and the south-easterly moist air currents from gulf of Aden - Indian ocean high pressure system, causes the "small rains" in the spring and the Atlantic equatorial westerly brings "Big rains" in summer (Dessie, 2003). The mean annual rainfall of the basin using isohythal method is found to be 779 mm (Dessie, 2003).

5.0 GEOLOGY

5.1 REGIONAL GEOLOGY

The geological units in Ethiopia fall into one of the following three major categories, the Precambrian basement, Late Palaeozoic to early Tertiary sediments and the Cenozoic volcanics and associated sediments. (Mengesha et.al, 1996). According to (Kazmin, 1975; Tefera et al., 1996) these are quantified in terms of areal coverage in the country: Precambrian basements (17%), Paleozoic-Mesozoic sedimentary rocks (22%) and Cenozoic-Quaternary dominantly volcanic rocks and minor sedimentary rocks (60%).

The brief description of the Major categories of the geological units is as follows (the descriptions are adopted from (T. Alemayehu, 2006) and (T. Ayenew & T. Alemayehu, 2001)

5.1.1 Precambrian Rocks

The Basement Complex upon which all younger rock formations were deposited consists of the oldest rocks in the country. The Precambrian are found within the structural discontinuities of various crystalline rocks occurring mainly both in the lower complex (high grade gneiss, migmatites, granulites and metamorphic granitoids), in the upper complex, syn-tectonic and post-tectonic granitoids. Since metamorphic rocks are subjected to several orogenic episodes, they are strongly folded, foliated and fractured.

5.1.2 Paleozoic Rocks

The Paleozoic and Mesozoic rocks are entirely sedimentary. The Paleozoic formations are localized in the Ogaden and Tigray regions. They are essentially constituted of Edagarbi tillites, shales, silts and Enticho Sandstones. The Edaga Arbi Glacials constitute very heterogeneous morenic sediments and strong silty-clayey cement. The Enticho sandstone is a coarse calcareous arenaceous and having in parts a conglomeratic nature.

5.1.3 Mesozoic Rocks

The deposition of Mesozoic sedimentary rocks is attributed to the transgression and regression of the sea. They outcrop in the nortwestern plateau, mainly in Tigray, in the Blue Nile Gorge in sourtheastern Ethiopia, in Harrghe, Bale and southern Sidamo. These sedimentary rocks are Lower Sandstone (Adigrat Sandstone), Abay Beds (Gohatsion

Formation), Antalo Limestone, Agula Shales or Mugher Mudstone and Amba Aradom Formation. In the Ogaden they include Hamanlei Series mainly comprise of limestone, Kabridahar Series, Mustahil Limestone and Belet Wein Limestone.

5.1.4 Tertiary and Quaternary Volcanics

The eruption of voluminous fissural and central type volcanics during the Cenozoic is the fundamental geological event in the Horn of Africa. In Ethiopia the Tertiary and Quaternary volcanic rocks cover very wide area. The volcanites of Tertiary, known as the Trap Series, overlie the Mesozoic sedimentary rocks. They usually form the highlands or the plateaux. They are highly weathered and form thick residual soils.

The simplified stratigraphy, from the oldest to the youngest of the Cenozoic volcanics is given below.

Ashangi Group - consists of basaltic lava flow with interbedded pyroclastics, ignimbrite and rhyolite. The top most part of the group is tuffaceous, contains lacustrine deposits in places including lignite seams and acidic volcanics. The total thickness varies from 200 to 1,200 m. differently oriented dolerite sills; acidic dikes and other intrusions are common.

Shield Group - consists mainly amygdaloidal basalts and rhyolites. They are exposed mainly in Gonder, Gojam and Keffa regions. The most prevalent exposure sites are on the Siemen Mountains. Most of the big mountains of the country belong to this group.

Maqdala Group - They are abundant within the Ethiopian rift and on the adjoining plateaux. The thickness varies from 180 to 4,000 m in northern Ethiopia. It consists of tuffs, ignimbrites, rhyolites and trachytes. They are interbedded with lavas and agglomerates of basaltic composition.

Aden Volcanic Series - They are the youngest Quaternary volcanics. The rocks of this series are obsidian flows, ignimbrite, pumice deposits associated with rhyolitic flows and domes, pyroclastics surge deposits, basaltic lava flows and spatter cones. This series is almost all exposed in parts of the Ethiopian Rift and is intensively affected by tectonism. Few outcrops exist in the Lake Tana basin.

5.1.5 Tertiary and Quaternary Sedimentary Rocks and Sediments

Though not extensive, there are some sandstone outcrops of Cenozoic age in the Afar and eastern Ogaden. These are variegated sandstone (Jessoma Sandstone), biogenic massive limestone (Auradu Series), gypsum, dolomite, cherty limestone and clays (Taleh Series), and fossiliferous limestones with marly and clayey intercalations (Karkar Series) and the Red Bed (Garsat Formation).

5.2 LOCAL GEOLOGY

The major geological formations identified in the Raya valley are based on field observation and lithological logs of boreholes drilled in the area and are dominantly the volcanics and the unconsolidated sediments. However, there are also minor remnants of sedimentary rocks exposed in a few places.

5.2.1 Volcanic Rocks

The volcanic rocks are exposed at the western escarpments and the associated plateau, the eastern margin and sporadically with in the valley as domes and elongated hills.

As many parts of the highlands of Ethiopia are made up of flood basalts, the volcanic rocks in this area could be related to these categories.

The continental flood basalts of Ethiopia are commonly termed as the trap series to distinguish them from the post rift Aden series. The flow is classified into two distinct chrono stratigraphic units: Pre Oligocene stage: Ashange basalt; and Oligocene – Miocene stage: Aiba basalt, Alaji fissural basalts and Rahyolites and Termaber basalts (B. Zenetin et.al, 1980, Berhe et.al, 1987 cited in D. Nadew, 2003).

5.2.2 Unconsolidated Sediments

The unconsolidated sediments are characterized by filling the valley floor. The valley is dominated by thick undifferentiated alluvial and lacustrine sediments bounded in the E and W by Ashenge formation (Mengesha et.al. cited in Abdella, 2010).

The lithological logs of boreholes drilled in the area show that the thickness of unconsolidated sediments ranges from 18 meters to about 310 meters at boreholes RPW-022 and PZ7 respectively.

The sediments are thinner and coarser in the west and get finer and thicker to the centre (RVDP, 1998). The maximum so far penetrated borehole in the valley is at RPW-093 with a total depth of 288 meters and with an alluvial thickness of 276 meters. According to borehole lithological logs of the area the unconsolidated materials are composed of clays, sands, gravels, boulders and mixtures of these.

There are also colluviums (piedmont deposits) dominantly at the foot of western escarpments. These are products of mass wasting of materials from mountainous areas due to the effect of gravity.

5.2.3 Sedimentary rocks

According to D. Nadew, 2003 there are Sandstone and limestone formations exposed near Bala town and Adi Bedera area respectively.

Sandstone: This rock unit is observed within a river near Bala town. It is white in colour, coarse grained and its areal coverage is small.

Limestone: this rock unit is exposed at the north eastern part of the valley near to Adi Bedera. It is light in color, Stratified with average thickness of three to four meters.

5.2.4 Precambrian Igneous Rocks

There are also Precambrian Meta intrusives in the eastern part of the valley. According to (Anon, 2008); in the southeastern part of the Alamata sub sheet intrusive rocks including gabbro, pyroxenite and anorthosite (granite) are distributed on and at foot of Guba Gala ridge and Amede Ager ridge.

6.0 HYDROGEOLOGY

The raya valley consists of thick sand and gravel deposits beneath floodplains and stream terrace deposits. The alluvial valley region is not one of geographic continuity, but rather one of similar geologic origin (Fetter, 2001). Many stream networks mainly from the western upland areas are supposed to deposit the thick sequences of sand and gravel which are highly porous and permeable. The productivity of aquifers in the raya valley depends mainly on the combined effect of thickness, grain size and sorting of the unconsolidated sediments and closeness to the recharge area. Generally wells drilled nearby the western margin of the valley have a higher production rate. The production rates of the wells drilled in the whole valley is variable with minimum, maximum, median, mode and average discharges of 2, 121.06, 35.75, 35 and 40.98 l/s respectively. This indicates heterogeneity of the aquifers related to grain size of sediments, variation in drilling depth, proximity to recharge and a combined effect of many variables.

In order to see the variation of aquifer productivity across the valley i.e. W-E and the influence of grain size on production rates 6 sections are considered covering the study area from the northern to the southern part. Each section contains 3-5 boreholes and referenced from the western margins of the valley (Fig.6) the yield and depth of the boreholes with respect to their distance from the reference point are statistically compared and found that the production rates of the wells closer to the western margin are generally higher than those further away. Even though, the depth of the wells is increasing from west to east direction, their production rates decreases in the same direction (Fig 6,7-12 and Tables 1-6.) This could be attributed to the variation of grain sizes of the sediments i.e. decreasing from west to east and proximity to recharge area. However, the above generalization may not work always due to several factors e.g. drilling depth; complications related to depositional processes of the unconsolidated sediments, hence, in some circumstances wells with higher discharge rates may be obtained in the central and eastern part of the valley.

The thickness of unconsolidated sediments increases from west to east and attains its maximum thickness in the south eastern part i.e. 310 m and generally grain size decreases in the same direction.

Groundwater flow direction as revealed from the groundwater level contour map is generally from west to east and from north to south and seems to follow the surface water flow direction through the only out let in the south eastern direction called Selen Ber (Fig 5.) The presence of more than 136 boreholes in the valley indicates the potentiality of the area (Fig. 13)

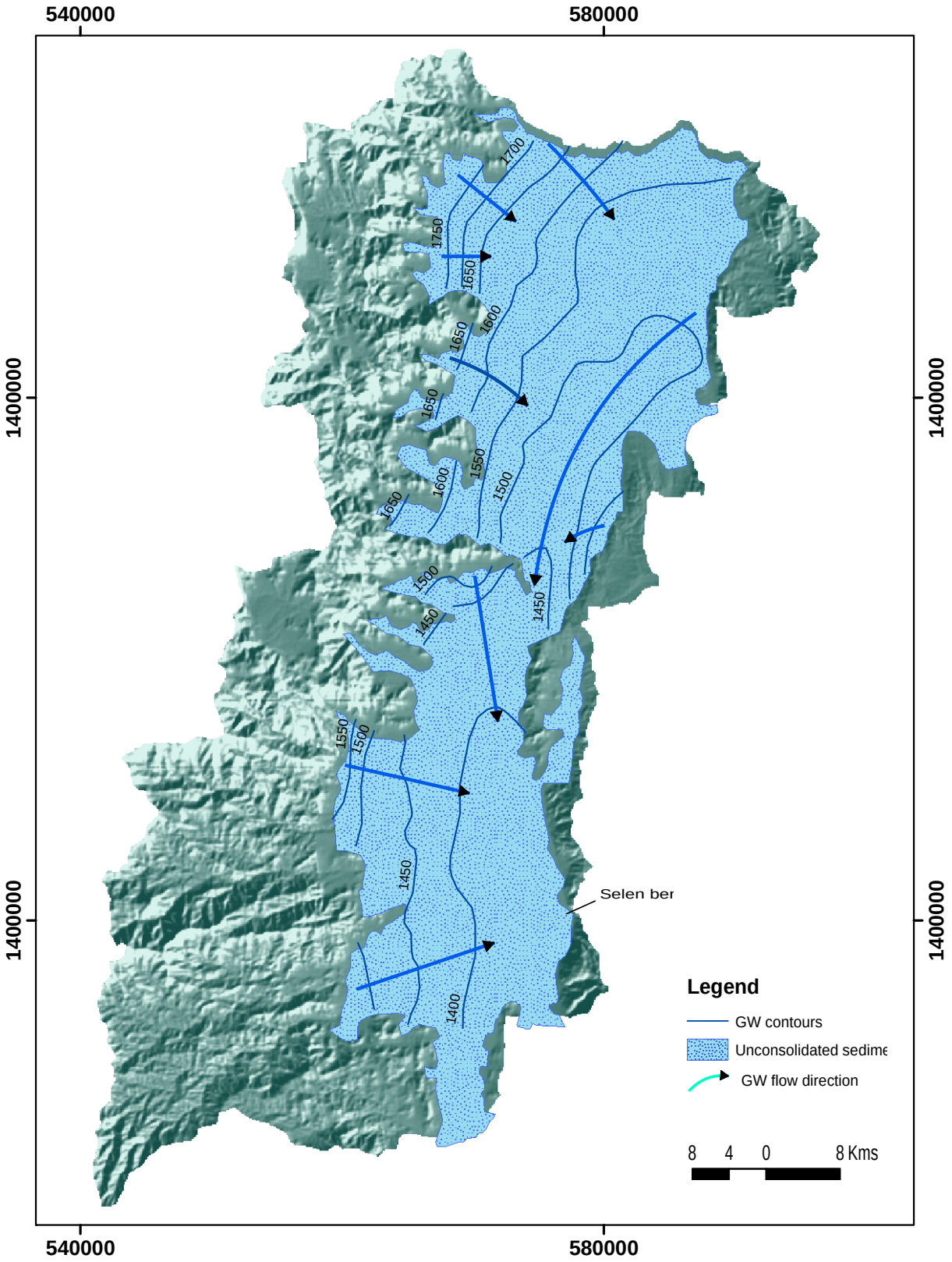


Figure 5 Groundwater level contour map

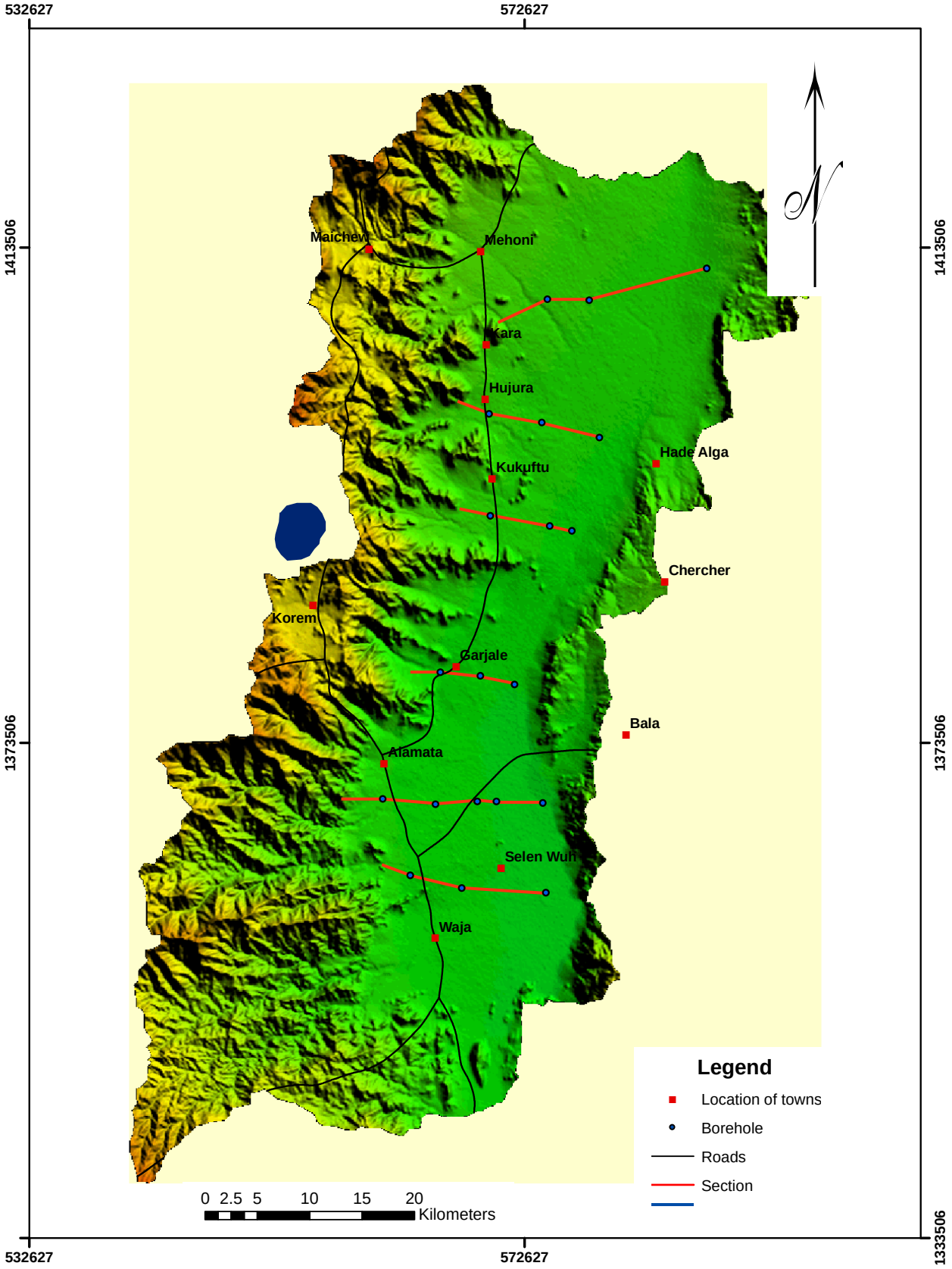


Figure 6 Location map of boreholes used for sections

Well Id.	E	N	Yield (L/sec)	Depth(m)	Distance from Reference(Km)
Wf13/BH1	574502	1409298	34	137.5	4.55
RPW-005	577889	1409202	23.5	128	7.18
PBH3	587384	1411774	5.6	204	17.02

Table 1 description of boreholes along section A-A'

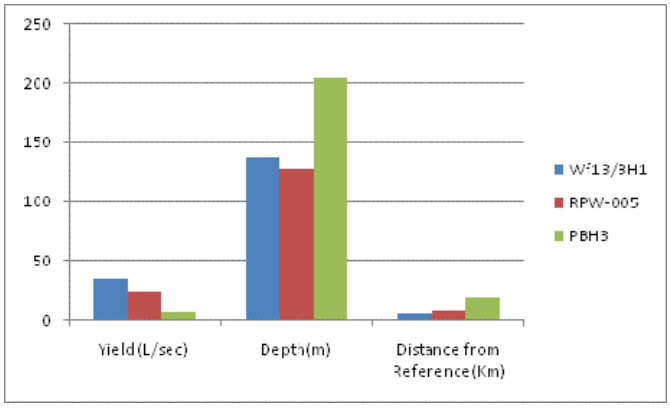


Figure 7 Chart for section A-A'

Well Id.	E	N	Yield (L/sec)	Depth(m)	Distance from Reference(Km)
Wf9BH3	569798	1400023	30	128	2.71
RPW-024	574055	1399330	28	140	7.04
RPW-028	578718	1398109	28	226	11.88

Table 2 description of boreholes along section B-B'

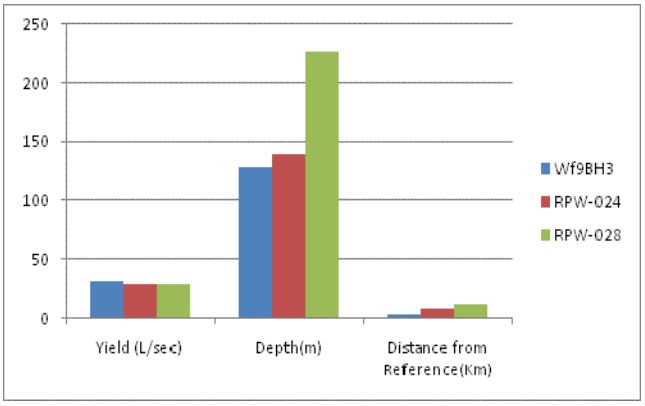


Figure 8 Chart for section B-B'

Well Id.	E	N	Yield (L/sec)	Depth(m)	Distance from Reference(Km)
RPW-040	569910	1391794	31.8	143	2.53
RPW-037	574690	1390976	30	160	7.41
Wf/Savana4	576495	1390581	32	180	9.25

Table 3 description of boreholes along section C-C'

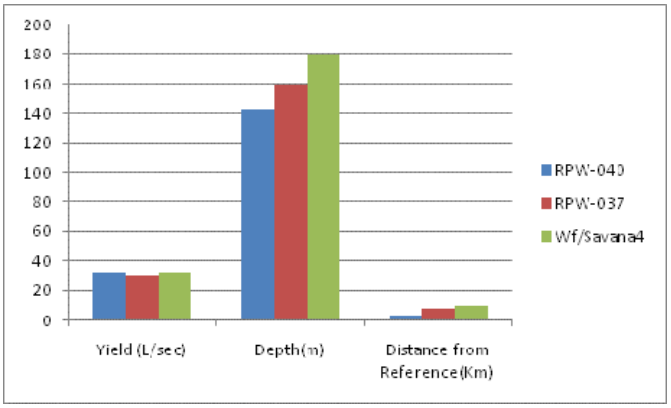


Figure 9 Chart for section C-C'

Well Id.	E	N	Yield (L/sec)	Depth(m)	Distance from Reference(Km)
RPW-086	563445	1362750	93.22	118	2.43
RPW-087	567591	1361714	41.6	170	6.7
PZ-7	574387	1361357	34.8	311	13.5

Table 4 description of boreholes along section D-D'

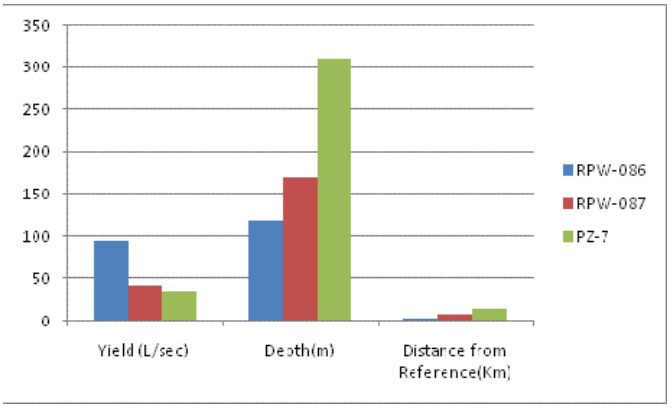


Figure 10 Chart for section D-D'

Well Id.	E	N	Yield (L/sec)	Depth(m)	Distance from Reference(Km)
RPW-059	565861	1379159	58.1	174	3.37
RPW-044	569097	1378878	50.6	209	6.67
RPW-055	571864	1378166	48.3	216	9.5

Table 5 description of boreholes along section E-E'

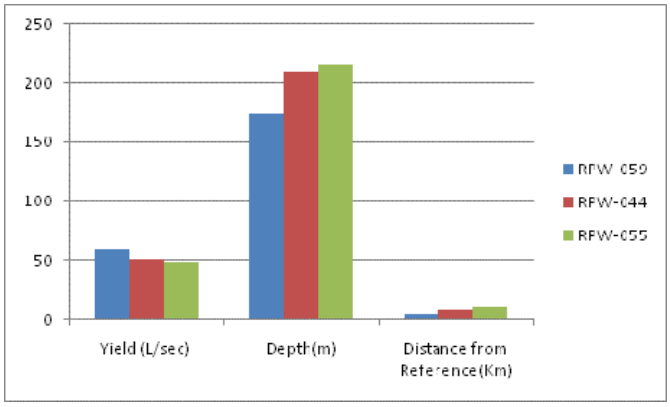


Figure 11 Chart for section E-E'

Well Id.	E	N	Yield (L/sec)	Depth(m)	Distance from Reference(Km)
RPW-075	561215	1368924	48	130	2.15
RPW-077	565483	1368490	41.6	137	6.43
RPW-084	568850	1368728	30.3	146	9.86
RPW-080	570393	1368715	13	138	11.39
RPW-025	574144	1368595	41.3	267	15.11

Table 6 description of boreholes along section F-F'

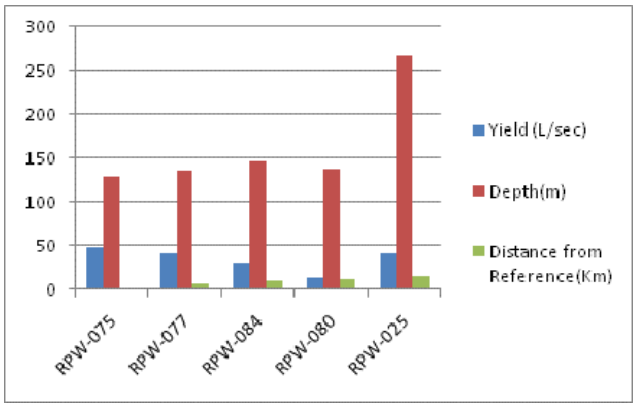


Fig 12 chart for section F-F'

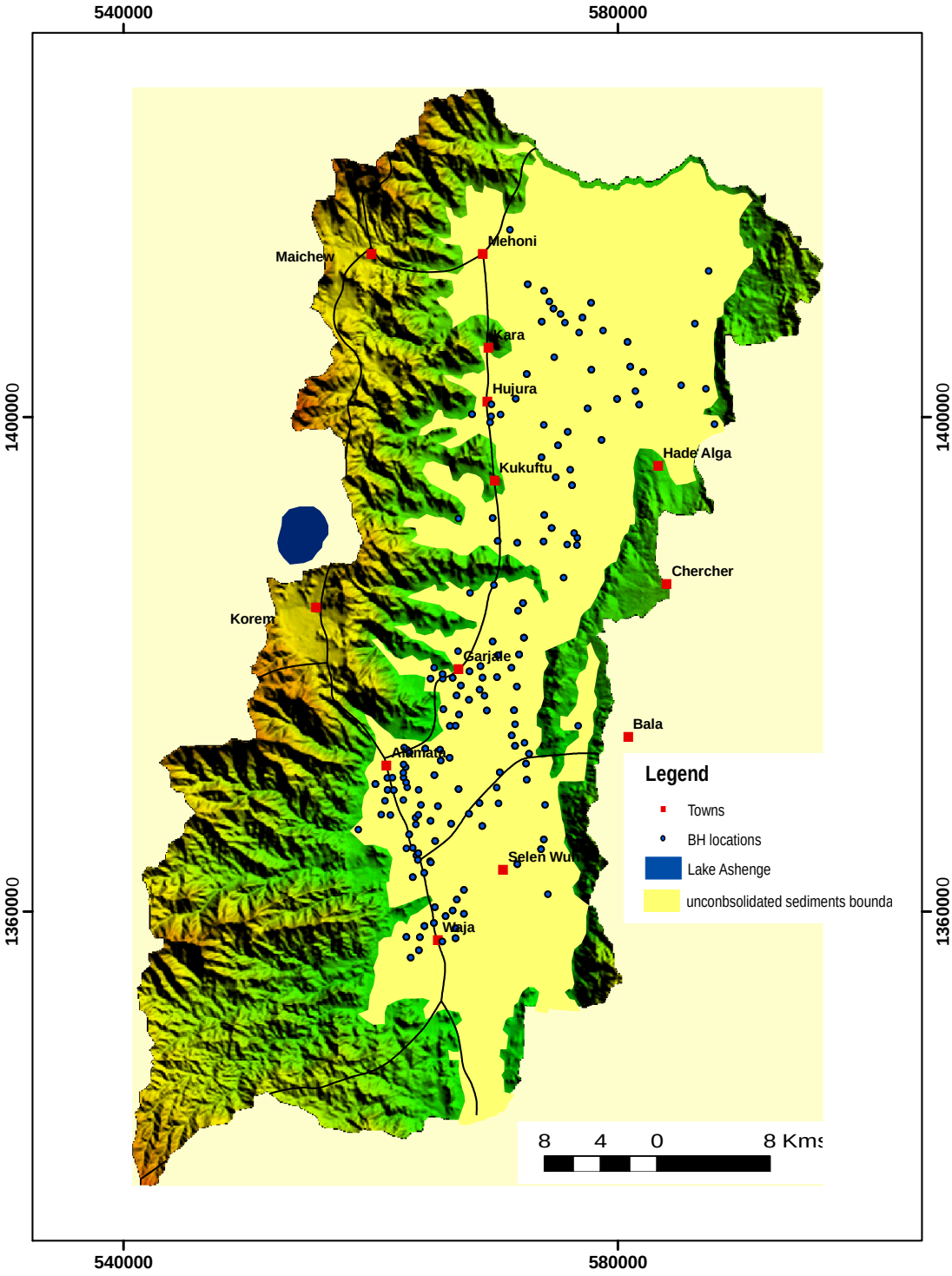


Figure 12 Location map of Borehole points

7.0 ANALYSIS, ORGANIZATION & DATA PREPARATION

7.1 PUMPING TEST DATA ANALYSIS

Pumping test is the basic and commonly used method for the determination of aquifer hydraulic parameters. It is a means of determining the aquifer properties indirectly. In this study 135single well aquifer test raw data are analyzed using AquiferTest v3.5 and the hydraulic parameters are determined through constant rate test and recovery data analysis. The data are categorized based on a preliminary analysis using well log data, curve type of the pumping test raw data and using general information from previous works, accordingly the methods of analysis are selected. One of the important steps before selecting the solution methods is to classify the aquifer type correctly. This can be conducted by integrating the lithological logs and by comparing the field data plotted on log-log paper i.e. drawdown vs. time with typical curves

The analysis methods are governed by the following basic assumptions for steady and unsteady state flows. These are: the aquifer has infinite areal extent and horizontal layering; the aquifer is bounded on the bottom by a confining layer, the aquifer is homogeneous and isotropic, Darcy's law is valid, prior to pumping the hydraulic head is horizontal over the area that will be influenced by the test, the pumped well penetrates the entire thickness of the aquifer and thus receives water by horizontal flow, the aquifer is pumped at a constant discharge rate, the pumped well has an infinitesimal diameter so that the storage in the well is negligible (Tenalem and Tamiru, 2001) and (Fetter, 2001). Some of the basic assumptions listed above are met in the study area e.g. all the wells drilled in the area are fully penetrating and are bounded on the bottom by a confining layer. The hydrolithology of the area is consisted by porous unconsolidated sediments underlain by basaltic bedrock which is partly weathered on top. According to the lithological logs of boreholes drilled in the area the unconsolidated sediments are characterized by inter layering of fine, medium to coarse grained sand, pebbles, gravels and boulders with some clay seams inter fingered. These clay bands could be responsible for the local confining of groundwater in most of the wells. According to the analysis of raw pumping test data from a data set of 135 boreholes the maximum and minimum transmissivity obtained is 2.74E+03m2/day and 5.40E-03m2/day respectively and a median value of 3.23E+02m2/day this indicates the

heterogeneity of the aquifer materials as indicated by their variation in the values of transmissivity.

THEORETICAL BACKGROUND

All the theoretical backgrounds underlying the pumping tests carried out in extensive confined and porous aquifers (unconsolidated sediments) whereby groundwater flow to the pumped well is either in steady state, or unsteady state is as follows.

STEADY STATE FLOW IN A CONFINED AQUIFER

The relationship, which describes steady state flow to the well, can be derived by combining the continuity equation for steady state and the Darcy equation for radial flow (Nonner, 2002). The following additional assumptions are used: the aquifer is characterized by confining layers on top and bottom, the well is pumped at a constant rate and equilibrium has been reached. This problem was solved by G. Thiem (Thiem 1906)

$T = \frac{Q}{2\pi(h_2 - h_1)} \ln\left(\frac{r_2}{r_1}\right)$, Thiem equation for confined aquifers (Fetter, 2001)

Where T is aquifer transmissivity (L^2/T; m^2/d), Q is pumping rate (L^3/T; m^3/d), h_1 is head at distance r_1 from the pumping well (L; m) and h_2 is head at distance r_2 from the pumping well (L; m)

UNSTEADY STATE FLOW IN A CONFINED AQUIFER

Many aquifer tests will never reach steady state i.e. the cone of depression will continue to expand with time.

The relationship, which describes unsteady state flow to the well, is also based on the combination of the continuity equation for unsteady steady state flow and Darcy equation for radial flow (Nonner, 2002). The assumptions are the same as above.

$T = \frac{Q}{4\pi(h_0 - h)} W(u)$, (Theis, 1935) equation

Where $u = \frac{r^2 S_s}{4Tt}$ and $W(u) = -0.5772 - \ln(u) + u - \frac{u^2}{2.2!} + \frac{u^3}{3.3!} - \frac{u^4}{4.4!} + \cdots$

T is aquifer transmissivity (L^2/T; m^2/d), Q is the constant pumping rate (L^3/T; m^3/d), h_0-h is the unsteady drawdown (L; m), r is distance to the center of the pumped well (L; m), t is

time since pumping started (T; days), S_s is dimensionless storage coefficient and W (u) is the well function of u (dimensionless).

THE COOPER- JACOB METHOD

The cooper- Jacob (1946) method is a simplification of the Theis method valid for greater time values and decreasing distance from the pumping well (smaller values of *u*). This method involves truncation of the infinite Taylor series that is used to estimate the well function W (u). Due to this truncation, not all early time measured data is considered to be valid for this analysis method. The resulting equation is:

$$S = (\frac{2.3Q}{4\pi T})log\frac{2.25Tt}{Sr^2}$$

In addition to the above basic assumptions the cooper –Jacob method considers the following additional assumption i.e. the values of *u* are small (rule of thumb $u < 0.01$)

The above equation plots as a straight line on semi-logarithmic paper if the limiting condition is met. Thus, straight-line plots of drawdown versus time can occur after sufficient time has elapsed. Time is plotted along the logarithmic X axis and drawdown is plotted along the linear Y axis.

Transmissivity and storativity are calculated as follows:

$$T = \frac{2.3Q}{4\pi\Delta S'} \qquad S = \frac{2.25Tt_0}{r^2}$$

JACOB CORRECTION FOR UNCONFINED CONDITIONS

The water Table in an unconfined aquifer is equal to the elevation head (potential). Transmissivity is no longer constant, and it will decrease with increasing drawdown. This means that there is not only horizontal flow to the well, but there is also a vertical component, which will increase the closer you get to the well.

Since transmissivity in unconfined aquifers is not constant, there is no closed solution for this aquifer type. That is why the measured drawdown is corrected, and the pumping test is interpreted as being in a confined aquifer. It is neither an empirical procedure nor an approximated solution.

Jacob (1944) proposed the following correction to drawdown, to approximate confined conditions

$Scor = s - (s^2/2D)$

Where:

Scor = the corrected drawdown

s = measured drawdown

D = original saturated aquifer thickness

The correction lets to use the Theis, Cooper-Jacob, Theis Recovery, and Theis Step test Solutions for the analysis of pumping test data recorded for an unconfined aquifer.

$u_A = r^2S / 4Tt$ (Type A curve for early time)

$u_B = r^2S_y / 4Tt$ (Type B curve for later time)

$\beta = r^2K_v / D^2K_h$

Two sets of curves are used. Type-A curves are good for early drawdown data when water is released from elastic storage. Type-B curves are good for later drawdown data when the effects of gravity drainage become more significant.

The Neuman Solution assumes the following: The aquifer is unconfined and has an "apparent" infinite extent, the aquifer is homogeneous, isotropic, and of uniform thickness over the area influenced by pumping (assumes drawdown is small compared to saturated thickness), the piezometric surface was horizontal prior to pumping, the well is pumped at a constant rate flow is unsteady, the well diameter is small, so well storage is negligible and the well penetrates the entire aquifer.

CONFINED AQUIFERS

Out of the collected 135 pumping test raw data 95 of them are treated to be confined aquifers because most of them have showed a best fit either with Theis type curve or Cooper- Jacob graph and the lithological logs of these wells is dominated with inter layered clay beds between sand, gravel, pebble, cobble, boulder and mixture of these; and all the

confined aquifer raw data are fitted with either Theis type curve and graphical methods like cooper-Jacob and the aquifer hydraulic parameters determined Table 7. The time-drawdown curve of Friatna BH1 is presented in Figure 14 with Theis type curve and in Fig 15 with Cooper-Jacob Graph. From these Figures it can be observed that within two days of continuous pumping, the total observed drawdown was 10.98 meters. The time-drawdown plots of both graphs show best fit with these confined aquifer models and the hydraulic parameters obtained using both methods are in good agreement even with the analysis results from recovery test Fig18. Near the end of continuous pumping the well was encountered with a recharge boundary which resulted in the deflection of the time drawdown curve upwards. This can be clearly seen in Fig15.

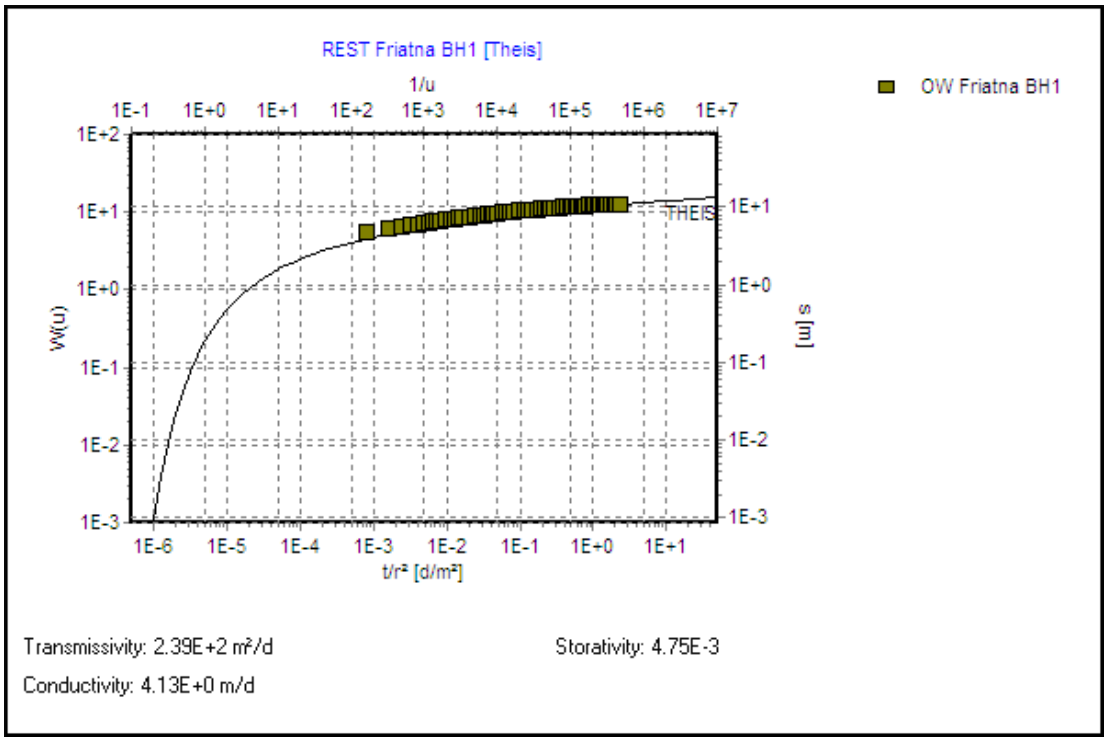


Figure 13 Time-drawdown graph of Friatna BH1 using Theis type curve

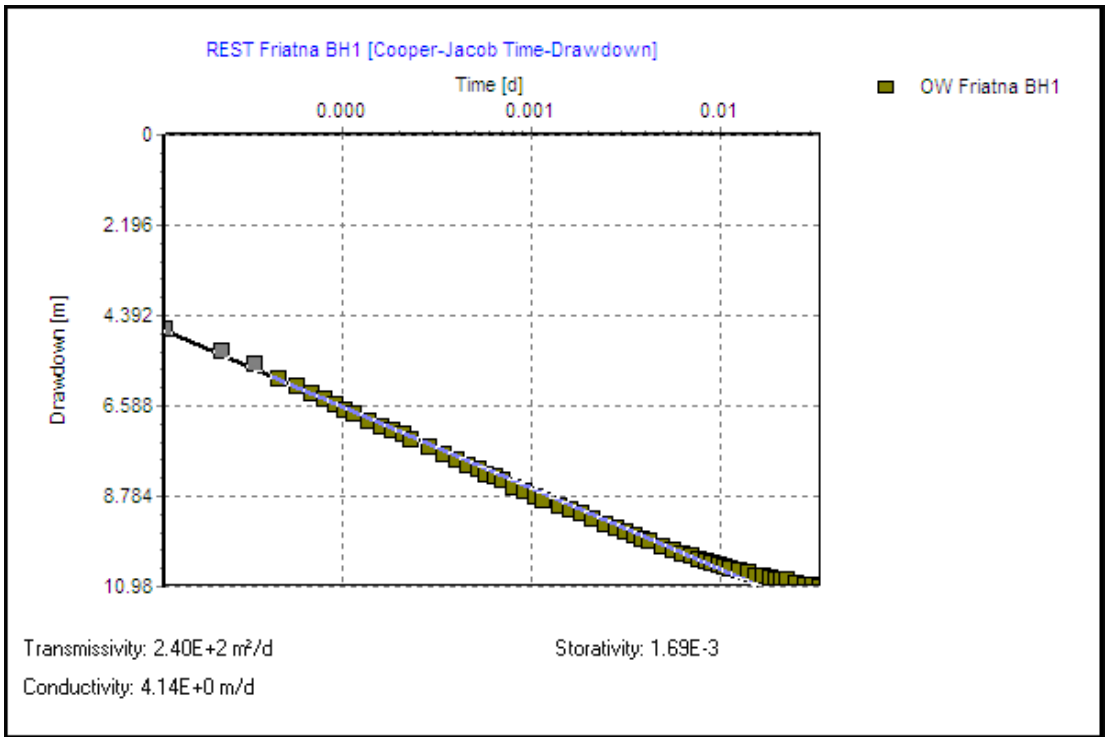


Figure 14 Time-drawdown graph of Friatna BH1 using Cooper-Jacob method

UNCONFINED AQUIFERS

The wells pumping unconfined aquifers are mainly selected based on their lithological logs, depth to water level and their curve types. Accordingly the methods of analysis are selected. 49 of the wells are taken as unconfined and have showed a best fit with Neuman type curve and are analyzed by using the Neuman method. However, in order to account for the decreasing saturated thickness all the wells pumping an unconfined aquifer are analyzed again using confined aquifer models, because the transmissivity values are underestimated due to the effect of decreased saturated thickness and their aquifer hydraulic parameters are obtained Table 7.

The time-drawdown curve of Wf Abergelle2 is presented in Figure 16 with Neuman type curve and in Fig 17 with Jacob correction method. From these Figures it can be observed that within 1.5 days of continuous pumping, the total observed drawdown was 13.61 meters. The time-drawdown plot of the field data shows best fit with Neuman type curve Fig 16 and with cooper-Jacob Graph after correction of the drawdown Fig 17 The hydraulic parameters

obtained using Neuman method are underestimated e.g. the transmissivity value obtained from Neuman method is 77m^2/day, however, it is about 748 m^2/day with Jacob correction.

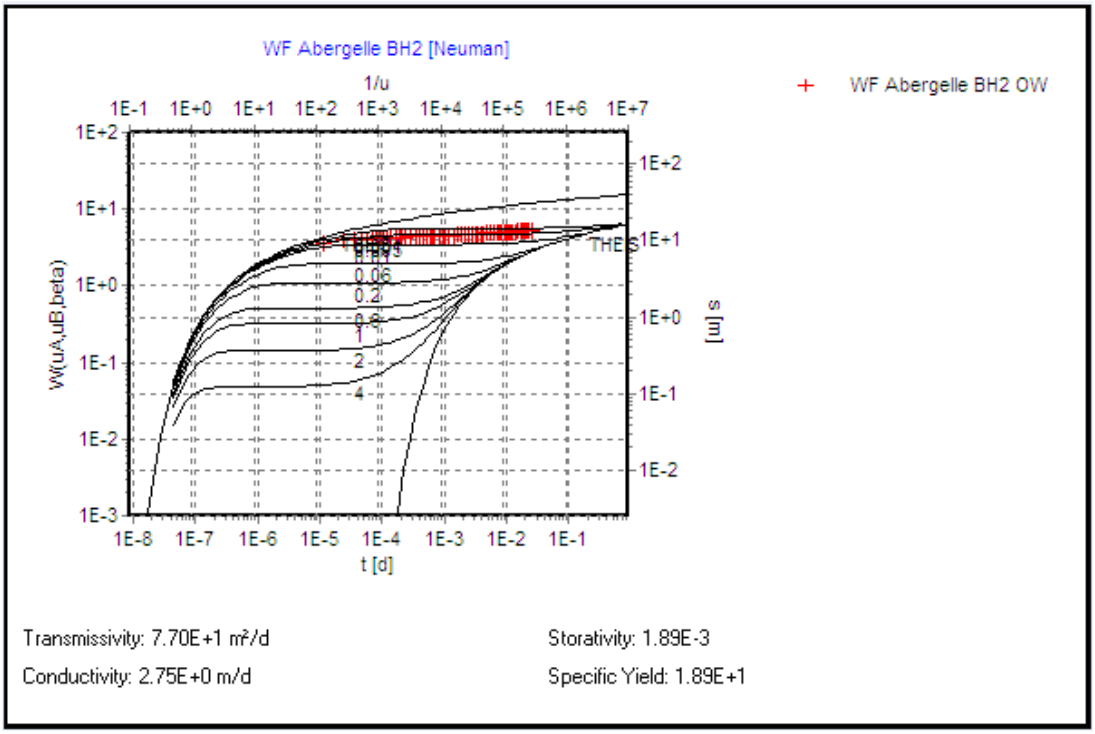


Figure 15 Time-drawdown graph of Wf Abergelle2 using Neuman type curve

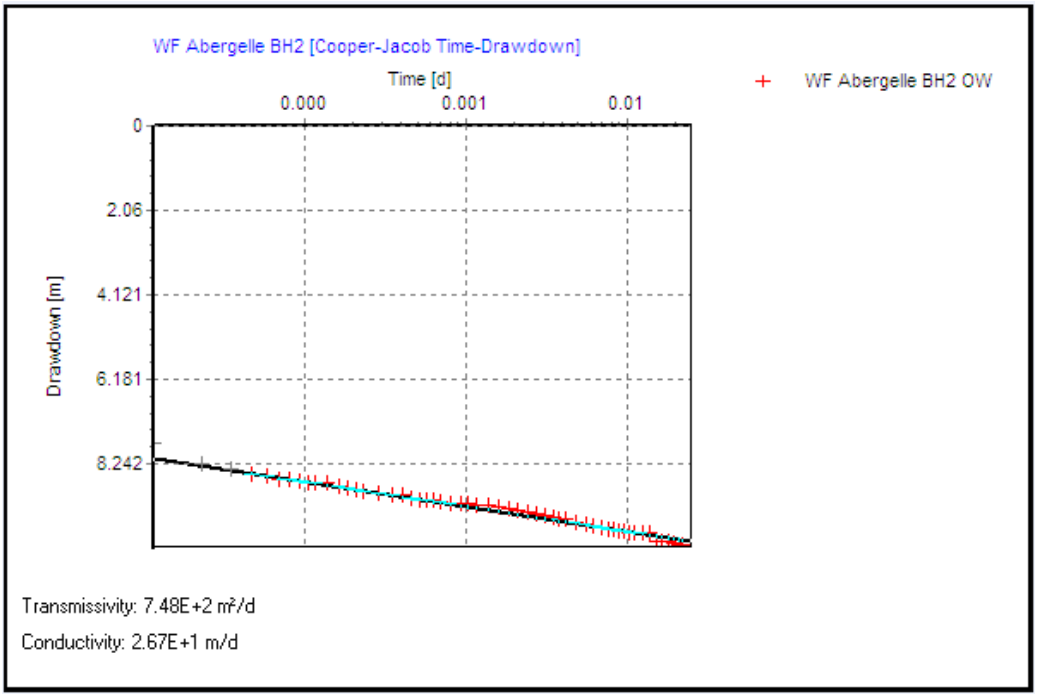


Figure 16 Time-drawdown graph of Wf Abergelle2 using Jacob correction method

7.2 RECOVERY DATA ANALYSIS

The recovery method is used to determine the aquifer hydraulic parameters after the cessation of pumping test from the raising water level. This rise in water level is known as residual drawdown (s'). Transmissivity values determined from Recovery-test measurements can provide an independent check on the results of the pumping test. Residual drawdown data can be more reliable than drawdown data because the recovery occurs at a constant rate, whereas constant discharge pumping is often difficult to achieve in the field. Residual drawdown data can be collected from both the pumping and observation wells. (ERSC. 642), AQTST user's manual. The Theis recovery solution method can be used for leaky, unconfined aquifers and aquifers with partially penetrating wells if additional limiting conditions are satisfied (Kruseman and de Ridder, 1990, p. 183). The recovery raw data of 135 wells are analyzed using aquifer test v3.5 software by Theis recovery analysis method. In this method the confined and unconfined aquifers are treated independently by controlling on the setting provided by the software. The transmissivity values calculated from recovery data are in good agreement with their corresponding transmissivity values determined from continuous pumping data Fig 20. The results of the analysis are presented in Table 7. The recovery curve of Friatna BH1 is presented in Figure 18, Figure 19. The well has recovered 91.25% within 12 hours time.

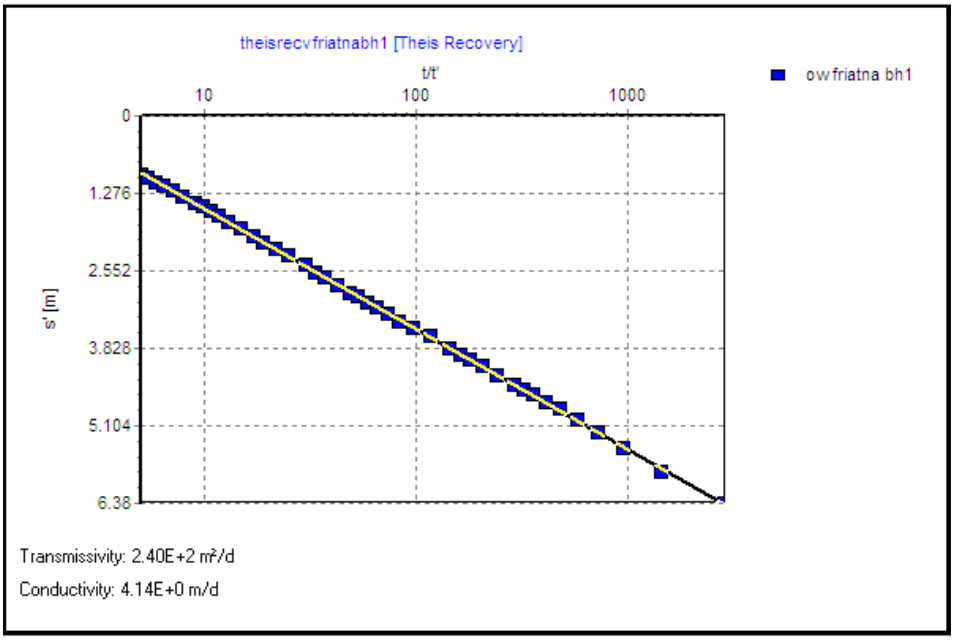


Figure 17 Recovery graph of Friatna BH1

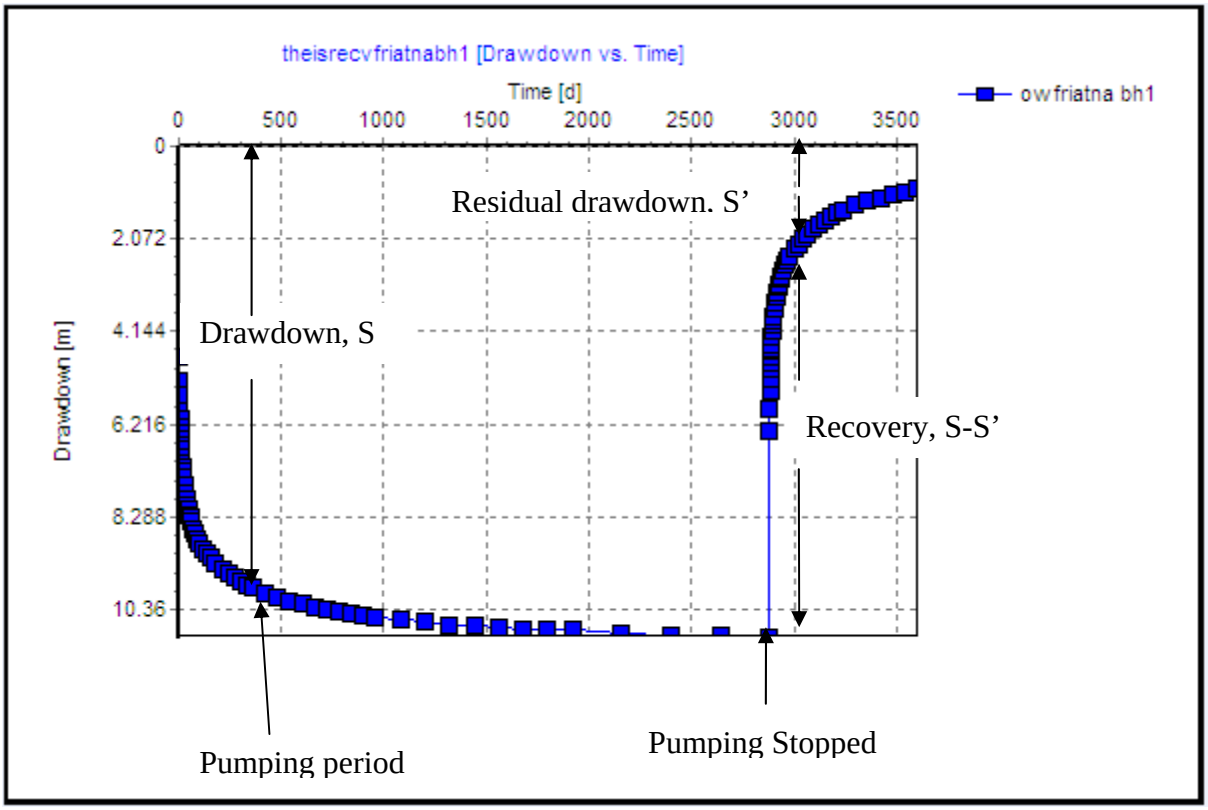


Figure 18 Time-drawdown plot of Friatna BH1 for pumping and non pumping conditions

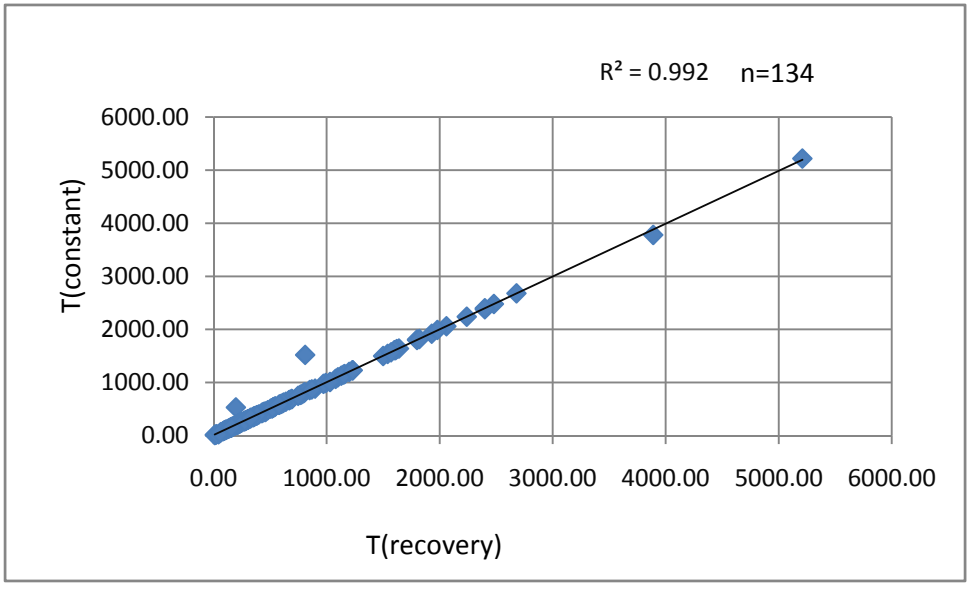


Figure 19 Transmissivity plots from Constant and Recovery data

8.0 DATA ORGANIZATION AND PREPARATION

All the collected pumping test and recovery raw data are analyzed and results are organized and tabulated for further interpretation according to their group and with their respective hydraulic parameters (Table 7.)

Aquifer hydraulic parameters determined from pumping test						Recovery test	
No	WELL_ID	E	N	T (m^2/d)	K (m/day)	T (m^2/d)	K (m/d)
1	RPW-004	587866	1399382	10.5	0.14	10.3	0.132
2	RPW-005	577889	1409202	401	11.1	400	11.1
3	RPW-006	577182	1408010	251	0.6	258	0.614
4	RPW-008	559048	1366594	17.8	0.3	17.6	0.296
5	RPW-012	581052	1404035	175	2.08	177	2.1
6	RPW-013	572677	1403437	254	89.1	255	8.94
7	RPW-014	582104	1403603	458	7.64	444	7.4
8	RPW-017	571732	1375106	279	3.32	279	3.32
9	RPW-019	581768	1400964	352	4.51	352	4.51
10	RPW-020	577596	1400661	242	3.44	245	3.40
11	RPW-021	571906	1363793	898	15	886	14.8
12	RPW-022	576837	1374986	12.1	0.29	15.2	0.365
13	RPW-023	568247	1400186	12.2	0.41		
14	RPW-024	574055	1399330	525	11	522	11
15	RPW-025	574144	1368595	448	4.98	448	4.98
16	RPW-026	570329	1389923	777	25.9	775	25.8
17	RPW-028	578718	1398109	672	8.13	671	8.12
18	RPW-030	573856	1396696	305	4.98	306	5.00
19	RPW-031	566678	1378864	1130	14.5	1130	14.4
20	RPW-032	576189	1395698	129	2.19	128	2.17
21	RPW-033	575022	1395075	351	6.8	350	6.77
22	RPW-034	576332	1394432	234	3.03	236	3.06
23	RPW-035	566991	1377439	305	4.24	309	4.29
24	RPW-036	574094	1392035	1620	51.8	1630	26.6
25	RPW-037	574690	1390976	309	5.27	308	5.24
26	RPW-038	574039	1389891	108	1.66	108	1.65
27	RPW-040	569910	1391794	101	2.01	105	2.11
28	RPW-042	572853	1372716	356	5.44	356	5.45
29	RPW-043	572369	1384905	152	1.94	153	1.96
30	RPW-044	569097	1378878	164	2.49	165	2.49
31	RPW-045	572436	1382113	84.4	1.41	84.8	1.41
32	RPW-046	569905	1381800	89.1	1.48	88.3	1.47
33	RPW-047	572052	1380755	197	4.1	531	11.1

34	RPW-048	570343	1380681	43.2	0.8	25.3	0.469
35	RPW-049	568921	1379801	222	3.71	220	3.67
36	RPW-050	571429	1379689	308	5.13	309	5.15
37	RPW-051	568031	1379400	187	2.6	186	2.58
38	RPW-052	570263	1378912	111	2.65	111	2.64
39	RPW-053	568862	1377910	155	2.35	150	2.28
40	RPW-054	567333	1378232	992	13.8	991	13.8
41	RPW-055	571864	1378166	288	3.69	286	3.67
42	RPW-056	567995	1377085	668	10.1	669	10.1
43	RPW-057	569431	1376222	213	3.55	215	3.58
44	RPW-058	571642	1376249	292	4.05	291	4.04
45	RPW-059	565861	1379159	1640	34.1	1640	34.2
46	RPW-060	566917	1374980	1420	20.10		
47	RPW-061	567200	1375899	190	3.95	191	3.98
48	RPW-062	566450	1374975	426	8.89	427	8.89
49	RPW-063	571462	1374198	194	2.36	195	2.37
50	RPW-064	564467	1373141	850	20.9	858	21.1
51	RPW-065	565658	1373049	2480	51.9	2480	51.8
52	RPW-066	566444	1372391	459	8.81	454	8.71
53	RPW-067	571726	1373354	273	4.73	277	4.8
54	RPW-068	572613	1371922	434	4.72	435	4.72
55	RPW-069	565204	1371005	375	6.95	374	6.93
56	RPW-070	570481	1371229	64.3	1.39	64.3	1.39
57	RPW-071	565705	1372178	1100	16.7	1100	16.6
58	RPW-072	572671	1370616	168	2.06	169	2.07
59	RPW-074	564898	1367281	353	6.55	353	6.56
60	RPW-075	561215	1368924	597	14.6	597	14.6
61	RPW-076	567162	1369865	334	4.31	336	4.33
62	RPW-077	565483	1368490	2060	49	2060	49.1
63	RPW-078	569076	1366877	325	10.8	322	10.7
64	RPW-079	568008	1367866	693	12	690	12
65	RPW-080	570393	1368715	445	10.9	446	10.9
66	RPW-081	566566	1367059	112	1.91	110	1.88
67	RPW-082	574045	1365777	639	7.28	638	7.27
68	RPW-083	565271	1365661	539	10.1	539	10.1
69	RPW-084	568850	1368728	93.5	2.25	93.5	2.25
70	RPW-085	564906	1363929	795	18.9	798	19
71	RPW-086	563445	1362750	1930	41.4	1920	41.1
72	RPW-087	567591	1361714	619	10.3	623	10.4
73	RPW-088	567019	1360930	206	3.5	206	3.50
74	RPW-090	563934	1356825	1230	19.1	1230	19.1
75	RPW-092	571968	1384297	357	5.41	352	5.33
76	RPW-093	567588	1359766	291	2.77	294	2.80

77	RPW-095	565153	1359042	137	2.1	136	2.09
79	RPW-096	566902	1358605	238	3.69	236	3.66
79	RPW-097	564016	1357876	518	11.1	515	11
80	RPW-098	562933	1357904	1160	25	1160	25.1
81	RPW-099	566904	1357791	530	5.65	536	5.72
82	RPW-100	565838	1357528	529	8.22	535	8.31
83	WF13/BH1	574502	1409298	1540	32.2	1540	32.1
84	WF13/BH2	575754	1407602	767	12.8	767	12.8
85	WF13/BH4	574837	1408721	2400	50	2380	49.6
86	WF13/BH5	575406	1408290	1800	42.9	1810	43.1
87	WF11/BH4	577896	1403786	277	4.2	273	4.13
88	WF9/BH1	569813	1400983	2680	49.7	2680	58.4
89	WF9/BH2	569708	1399528	1200	22.6	1200	22.6
90	WF9/BH3	569798	1400023	428	6.11	424	6.05
91	WF9/BH4	570553	1400160	2400	30.8	2400	30.7
92	WF2/V9	565921	1376322	805	19.2	817	19.5
93	WF4/BH1	567110	1381023	546	10.2	552	10.2
94	WF4/BH2	565885	1378789	1080	17.5	1070	17.3
95	WF4/BH3	564899	1378795	1800	50	1800	49.9
96	WF0/BH1	562709	1370793	689	28.7	689	23
97	WF0/BH2	562905	1370393	5210	124	5220	121
98	WF0/BH3	563923	1369802	233	5.55	233	5.55
99	WF0/BH4	562697	1368978	223	4.3	220	4.08
100	WF0/BH5	561903	1369790	810	16.9	1520	31.7
101	WF0/BH6	561399	1370777	1980	47.3	1990	47.5
102	WFO/BH7	561796	1370780	3890	92.6	3780	90.1
103	WF0/BH8	561409	1369799	1820	37.9	1820	38
104	WF1/V1	562872	1371640	273	7.81	274	7.61
105	WF1/V9	562713	1371855	1610	53.5	1610	53.7
106	WF1/V10	562681	1371183	972	32.4	976	32.5
107	WF5/BH1	563690	1366993	210	57.6	207	5.76
108	WF5/BH2v8	564103	1368593	611	14.6	611	14.6
109	WF5/BH3v3	563673	1367565	504	14	508	14.1
110	WF5/BH4v5	563905	1367793	155	3.22	150	3.13
111	WF6/BH3	563156	1366192	584	19.5	586	19.5
112	WF6/BH4	563912	1364685	1150	24	1150	24
113	WF7/BH1	564378	1363098	2240	46.6	2240	48.7
114	WF7/BH2	563863	1364133	1500	24.9	1500	23.4
115	WF Abergelle BH1	570017	1386373	479	7.49	478	7.70
116	WF Kalibso BH1	571787	1401448	213	3.74	210	3.68
117	WF GOBU BH1	564404	1358786	1600	40.1	1610	40.3
118	WF Abergelle BH2	573832	1365003	748	26.7	749	26.7
119	Galika Trading BH1	570245	1369978	365	9.13	367	9.17

120	WF-SAV/BH1	576764	1390173	386	6.89	386	6.89
121	WF-SAV/BH2	576732	1389596	384	7.39	381	7.62
122	WF-SAV/BH3	575944	1389641	519	6.49	518	6.56
123	WF-SAV/BH4	576495	1390581	308	4.82	309	4.83
124	Friatna BH1	577594	1403257	239	4.13	240	125
125	Tera BH1	571787	1401448	218	4.05	218	4.04
126	PZ1	581458	1402058	275	2.87	275	2.87
127	PZ2	585168	1402537	25.5	0.85	25.5	0.851
128	PZ3	569257	1377425	869	14	869	14.0
129	PZ4	565181	1379685	1570	52.4	1570	52.4
130	PZ5	572491	1373604	1230	21.5	1230	21.5
131	PZ7	574387	1361357	326	3.97	335	4.09
132	PZ9	562943	1365069	1030	26.8	1010	24.5
133	PBH1	571313	1415112	56.5	1.71	50.6	1.53
134	PBH3	587384	1411774	145	2.68	146	2.70
135	PBH7	568083	1385735	578	12	579	12.1
136	Dejena BH3	576046	1403659	157	2.62	157	2.62

Table 7 Analysis results of pumping and recovery tests

8.1 DETERMINATION OF AQUIFER PROPERTIES FROM PUMPING TEST

The aquifer properties are determined from drilling and pumping test data. These are well discharge, drawdown and specific capacity.

8.1.1 SPECIFIC CAPACITY

Specific capacity is defined as the well production per unit decline in head. Mathematically specific capacity is defined as, Sc = Q/Sw. where Q is the pumping rate (m^3/day), Sw is the measured drawdown (change in hydraulic head) in the well (m). It is generally reported as yield per unit of drawdown.

It is a function of aquifer setting, well setting and pumping duration. Attributes of the aquifer setting that can influence specific capacity include transmissivity, storativity and aquifer type (i.e. confined, unconfined, semi confined, boundaries, and fractured e.t.c.) (Mace, 2000), pp6.

The data used for the calculation of specific capacity are obtained from constant rate pumping test i.e. from the constant discharge rate used in the constant rate test and the pseudo steady state drawdown obtained at the end of constant rate test.

The pseudo steady state drawdown is the drawdown if the change in water level for a given time period becomes small at large pumping times, because water levels never theoretically reach pseudo steady state in a confined aquifer.

The specific capacity is calculated for 136 wells which are in different aquifer settings and having great variation in discharge rates (Table 8.)

No	BH ID	Location		Discharge	Measured drawdown	Corrected drawdown for decreased saturated thickness	Drawdown corrected for well loss	Specific capacity from measured data	Specific capacity corrected for decreased saturated thickness	Specific capacity corrected for well loss and decreased saturated thickness
		E	N	Q(M3/D)	Sw(m)	S'=S-(S2/2H)	Sw corrected	Sc	Sc Jacob corrected	Sc corrected
1	RPW-004	587866	1399382	518.40	42.34	30.76	30.76	12.24	16.85	16.85
2	RPW-005	577889	1409202	2030.40	7.36	6.61	6.61	275.87	307.28	307.28
3	RPW-006	577182	1408010	1209.60	24.63	24.63	24.63	49.11	49.11	49.11
4	RPW-008	559048	1366594	737.86	62.88	29.65	29.65	11.73	24.89	24.89
5	RPW-012	581052	1404035	2747.52	9.7	9.7	9.70	283.25	283.25	283.25
6	RPW-013	572677	1403437	1512.00	14.68	14.68	14.68	103.00	103.00	103.00
7	RPW-014	582104	1403603	4173.12	6.55	6.55	6.39	637.12	637.12	653.50
8	RPW-017	571732	1375106	4207.68	51.95	35.89	28.89	80.99	117.25	145.67
9	RPW-019	581768	1400964	2747.52	12.69	12.69	12.69	216.51	216.51	216.51
10	RPW-020	577596	1400661	2747.52	10.02	10.02	10.02	274.20	274.20	274.20
11	RPW-021	571906	1363793	5244.48	5.35	5.35	3.82	980.28	980.28	1371.65
12	RPW-022	576837	1374986	432.00	37.16	37.16	37.16	11.63	11.63	11.63
13	RPW-023	568247	1400186	1133.57	35	35	35.00	32.39	32.39	32.39
14	RPW-024	574055	1399330	2419.20	4.16	4.16	4.16	581.54	581.54	581.54
15	RPW-025	574144	1368595	3568.32	12.17	12.17	9.22	293.21	293.21	387.19
16	RPW-026	570329	1389923	3412.80	3.98	3.72	2.62	857.49	918.41	1303.76
17	RPW-028	578718	1398109	2419.20	3.45	3.45	3.45	701.22	701.22	701.22
18	RPW-030	573856	1396696	2073.60	8.42	8.42	8.42	246.27	246.27	246.27
19	RPW-031	566678	1378864	4795.20	2.95	2.95	2.65	1625.49	1625.49	1810.34
20	RPW-032	576189	1395698	2764.80	17.85	17.85	17.85	154.89	154.89	154.89
21	RPW-033	575022	1395075	2611.87	14.32	14.32	14.32	182.39	182.39	182.39
22	RPW-034	576332	1394432	2002.75	11.6	11.6	11.60	172.65	172.65	172.65
23	RPW-035	566991	1377439	9457.34	31.68	24.71	17.71	298.53	382.73	534.00
24	RPW-036	574094	1392035	2702.59	3.5	3.5	3.50	772.17	772.17	772.17
25	RPW-037	574690	1390976	2592.00	9.56	8.78	8.78	271.13	295.16	295.16

26	RPW-038	574039	1389891	2185.92	19.92	16.88	16.88	109.73	129.47	129.47
27	RPW-040	569910	1391794	2747.52	16.05	16.05	16.05	171.19	171.19	171.19
28	RPW-042	572853	1372716	4495.39	15.34	15.34	9.54	293.05	293.05	471.21
29	RPW-043	572369	1384905	2747.52	29.39	29.39	29.39	93.48	93.48	93.48
30	RPW-044	569097	1378878	4371.84	23.38	23.38	18.10	186.99	186.99	241.47
31	RPW-045	572436	1382113	2808.00	26.31	26.31	26.31	106.73	106.73	106.73
32	RPW-046	569905	1381800	2868.48	32.04	32.04	32.04	89.53	89.53	89.53
33	RPW-047	572052	1380755	2903.04	23.16	23.16	23.16	125.35	125.35	125.35
34	RPW-048	570343	1380681	1296.00	58.86	26.78	26.78	22.02	48.39	48.39
35	RPW-049	568921	1379801	4579.20	15.28	13.33	3.73	299.69	343.41	1227.50
36	RPW-050	571429	1379689	3818.88	10.59	10.59	7.41	360.61	360.61	515.32
37	RPW-051	568031	1379400	4622.40	18.7	18.7	13.21	247.19	247.19	349.95
38	RPW-052	570263	1378912	2903.04	39.86	39.86	39.86	72.83	72.83	72.83
39	RPW-053	568862	1377910	4795.20	17.47	17.47	17.47	274.48	274.48	274.48
40	RPW-054	567333	1378232	10459.58	20.25	20.25	13.25	516.52	516.52	789.40
41	RPW-055	571864	1378166	4173.12	17.64	17.64	16.77	236.57	236.57	248.78
42	RPW-056	567995	1377085	9784.80	22.54	22.54	15.54	434.11	434.11	629.65
43	RPW-057	569431	1376222	3136.32	20.48	20.48	10.55	153.14	153.14	297.42
44	RPW-058	571642	1376249	5624.64	16.68	16.68	9.68	337.21	337.21	581.06
45	RPW-059	565861	1379159	5019.84	5.26	4.97	2.93	954.34	1009.66	1712.85
46	RPW-060	566917	1374980	3196.80	3.98	3.98	3.98	803.22	803.22	803.22
47	RPW-061	567200	1375899	9457.34	40.5	40.5	33.50	233.51	233.51	282.31
48	RPW-062	566450	1374975	4371.84	14.67	14.67	12.67	298.01	298.01	345.05
49	RPW-063	571462	1374198	2937.60	12.9	12.9	12.90	227.72	227.72	227.72
50	RPW-064	564467	1373141	3024.00	8.37	7.51	7.51	361.29	402.73	402.73
51	RPW-065	565658	1373049	4704.48	6.92	6.42	5.08	679.84	732.86	926.43
52	RPW-066	566444	1372391	3352.32	9.78	9.78	6.32	342.77	342.77	530.54
53	RPW-067	571726	1373354	2702.59	15.48	15.48	15.48	174.59	174.59	174.59
54	RPW-068	572613	1371922	3110.40	10.63	10.02	10.02	292.61	310.53	310.53
55	RPW-069	565204	1371005	9174.82	29.13	21.27	16.26	314.96	431.29	564.39
56	RPW-070	570481	1371229	1382.40	47.09	23.15	23.15	29.36	59.71	59.71

57	RPW-071	565705	1372178	4704.48	6.4	6.4	5.02	735.08	735.08	936.52
58	RPW-072	572671	1370616	2704.32	48.63	48.63	48.63	55.61	55.61	55.61
59	RPW-074	564898	1367281	4661.28	21.13	21.13	12.48	220.60	220.60	373.43
60	RPW-075	561215	1368924	4147.20	8.34	8.34	5.31	497.27	497.27	780.59
61	RPW-076	567162	1369865	3352.32	8	8	5.37	419.04	419.04	624.23
62	RPW-077	565483	1368490	3594.24	4.56	4.31	2.31	788.21	833.46	1554.29
63	RPW078	569076	1366877	2747.52	15.1	11.30	11.30	181.95	243.15	243.15
64	RPW-079	568008	1367866	3844.80	5.95	5.95	4.04	646.18	646.18	950.96
65	RPW-080	570393	1368715	1123.20	2.54	2.46	2.46	442.20	456.38	456.38
66	RPW-081	566566	1367059	3456.00	22.66	22.66	15.71	152.52	152.52	220.01
67	RPW-082	574045	1365777	3532.03	13.63	13.63	10.76	259.14	259.14	328.23
68	RPW-083	565271	1365661	4320.00	8.65	8.65	1.58	499.42	499.42	2739.46
69	RPW-084	568850	1368728	2617.92	28.19	28.19	28.19	92.87	92.87	92.87
70	RPW-085	564906	1363929	9851.33	16.81	13.45	6.45	586.04	732.66	1528.29
71	RPW-086	563445	1362750	8054.21	45.82	45.82	38.82	175.78	175.78	207.48
72	RPW-087	567591	1361714	3594.24	6.3	6.3	4.30	570.51	570.51	835.87
73	RPW-088	567019	1360930	4320.00	15.29	15.29	10.70	282.54	282.54	403.77
74	RPW-090	563934	1356825	10022.40	19.49	16.54	9.54	514.23	606.00	1050.73
75	RPW-092	571968	1384297	2903.04	4.85	4.85	4.85	598.56	598.56	598.56
76	RPW-093	567588	1359766	3974.40	15.68	15.68	13.36	253.47	253.47	297.53
77	RPW-095	565153	1359042	3784.32	17.38	17.38	14.92	217.74	217.74	253.70
78	RPW-096	566902	1358605	3784.32	12.21	12.21	5.55	309.94	309.94	681.77
79	RPW-097	564016	1357876	3974.40	16.9	16.9	13.84	235.17	235.17	287.26
80	RPW-098	562933	1357904	3594.24	7.78	7.13	5.52	461.98	504.42	650.71
81	RPW099	566904	1357791	9676.80	18.62	18.62	11.62	519.70	519.70	832.77
82	RPW-100	565838	1357528	9331.20	22.2	22.2	18.11	420.32	420.32	515.32
83	WF13/BH1	574502	1409298.1	2937.60	2.58	2.51	2.51	1138.60	1170.05	1170.05
84	WF13/BH2	575754.1	1407602.4	3240.00	4.34	4.18	3.16	746.54	774.56	1025.13
85	WF13/BH4	574836.8	1408721	2747.52	3.76	3.61	3.61	730.72	760.51	760.51
86	WF13/BH5	575406.1	1408290	3784.32	2.44	2.37	1.02	1550.95	1597.35	3715.05
87	WF11/BH4	577895.9	1403785.7	3067.20	7.76	7.76	7.76	395.26	395.26	395.26

88	WF9/BH1	569813	1400983	3801.60	5.1	5.1	3.81	745.41	745.41	998.70
89	WF9/BH2	569708	1399528	3024.00	12.96	12.96	12.96	233.33	233.33	233.33
90	WF9/BH3	569798	1400023	2592.00	11.4	11.4	11.40	227.37	227.37	227.37
91	WF9/BH4	570553	1400160	3801.60	3.42	3.42	0.44	1111.58	1111.58	8584.31
92	WF2/V9	565921.4	1376322.4	3801.60	8.75	7.84	3.10	434.47	484.99	1227.02
93	WF4/BH1	567110	1381023	3412.80	7.08	7.08	4.47	482.03	482.03	763.31
94	WF4/BH2	565885.2	1378788.5	3974.40	3.38	3.29	2.06	1175.86	1208.81	1931.79
95	WF4/BH3	564899	1378795	3715.20	6.34	5.78	2.07	585.99	642.58	1795.82
96	WF0/BH1	562709.1	1370792.7	3024.00	5.12	4.57	4.57	590.63	661.15	661.15
97	WF0/BH2	562905	1370393	3456.00	3.15	3.15	2.26	1097.14	1097.14	1525.86
98	WF0/BH3	563922.8	1369802.1	3456.00	16.01	16.01	9.01	215.87	215.87	383.57
99	WF0/BH4	562696.5	1368977.6	3456.00	14.5	14.5	12.50	238.34	238.34	276.48
100	WF0/BH5	561902.6	1369790.4	3456.00	5.34	5.34	4.70	647.19	647.19	734.60
101	WF0/BH6	561399.4	1370776.7	3456.00	4.79	4.52	2.52	721.50	765.13	1373.14
102	WFO/BH7	561795.7	1370779.5	3801.60	1.76	1.72	0.60	2160.00	2206.23	6318.77
103	WF0/BH8	561408.5	1369799.3	3801.60	5.97	5.60	3.60	636.78	679.01	1056.37
104	WF1/V1	562871.8	1371639.7	3024.00	16.36	12.54	12.54	184.84	241.22	241.22
105	WF1/V9	562713.4	1371854.5	3024.00	3.12	2.96	2.96	969.23	1022.40	1022.40
106	WF1/V10	562680.6	1371182.6	3024.00	4.64	4.28	4.28	651.72	706.35	706.35
107	WF5/BH1	563690.3	1366992.6	2592.00	14.56	11.62	11.62	178.02	223.15	223.15
108	WF5/BH2v8	564103	1368592.9	3024.00	6.06	6.06	6.06	499.01	499.01	499.01
109	WF5/BH3v3	563672.5	1367565.2	3024.00	6.15	6.15	6.15	491.71	491.71	491.71
110	WF5/BH4v5	563905	1367793	3024.00	16.15	13.43	13.43	187.24	225.12	225.12
111	WF6/BH3	563155.7	1366191.7	3024.00	6.43	6.43	6.43	470.30	470.30	470.30
112	WF6/BH4	563912.4	1364684.5	3456.00	2.95	2.86	2.86	1171.53	1208.67	1208.67
113	WF7/BH1	564378.1	1363098.3	3801.60	1.65	1.62	0.32	2304.00	2344.29	12007.19
114	WF7/BH2	563863	1364132.9	3240.00	2.51	2.46	1.24	1290.84	1318.41	2613.37
115	WF Abergelle BH1	570017	1386373	3412.80	10.4	9.53	8.03	328.15	358.20	425.26
116	Kalibso plc BH1	571787	1401448	3067.20	11.01	11.01	11.01	278.58	278.58	278.58
117	WF GOBU BH1	564404	1358786	3343.68	3.07	2.95	2.05	1089.15	1132.61	1632.00
118	WF Abergelle BH2	573832	1365003	2479.68	13.61	10.30	10.30	182.20	240.69	240.69

119	Galika Trading BH1	570245	1369978	2937.60	15.83	15.83	15.83	185.57	185.57	185.57
120	WF-SAV/BH1	576764	1390173	2592.00	8.2	8.2	8.20	316.10	316.10	316.10
121	WF-SAV/BH2	576732	1389596	2592.00	6.96	6.96	6.96	372.41	372.41	372.41
122	WF-SAV/BH3	575944	1389641	2747.52	5.02	5.02	5.02	547.31	547.31	547.31
123	WF-SAV/BH4	576495	1390581	2764.80	7.63	7.63	7.63	362.36	362.36	362.36
124	Friatna BH/1	577594	1403257	2592.00	10.98	10.98	10.98	236.07	236.07	236.07
125	Tera BH1	571787	1401448	889.92	5.67	5.67	5.67	156.95	156.95	156.95
126	PZ1	581458	1402058	2903.04	12.71	12.71	12.71	228.41	228.41	228.41
127	PZ2	585168	1402537	172.80	5.95	5.95	5.95	29.04	29.04	29.04
128	PZ3	569257	1377425	3136.32	2.28	2.23	2.23	1375.58	1405.25	1405.25
129	PZ4	565181	1379685	2730.24	5.07	4.64	4.64	538.51	588.21	588.21
130	PZ5	572491	1373604	2764.80	1.05	1.05	1.05	2633.14	2633.14	2633.14
131	PZ7	574387	1361357	3006.72	14.42	14.42	14.42	208.51	208.51	208.51
132	PZ9	562943	1365069	2903.04	2.24	2.18	2.18	1296.00	1333.33	1333.33
133	PBH1	571313	1415112	388.80	8.84	7.06	7.06	43.98	55.04	55.04
134	PBH3	587384	1411774	483.84	3.34	3.34	3.34	144.86	144.86	144.86
135	PBH7	568083	1385735	302.40	1.75	1.72	1.72	172.80	176.01	176.01
136	Dejena BH3	576046	1403659	2747.52	21.85	21.85	21.85	125.74	125.74	125.74

Table 8 Analysis results of specific capacity before and after drawdown correction

8.1.2 DRAWDOWN

Drawdown is the measure of rate of decline in head (groundwater level) measured in a borehole during pumping test.

It can be expressed as $S_w = S_a + S_L$

Where Sw is drawdown observed in the well, S_a head loss in the aquifer and S_L the well loss (Mace, 2000) pp32.

The wells in the study area are grouped in to confined and unconfined aquifers; out of which 49 are unconfined and the remaining are confined aquifers.

The unconfined aquifers are analyzed using confined aquifer models to account for the decreasing saturation thickness.

For the saturation thickness aquifers, Jacob suggested correction of draw downs prior to application of confined aquifer models. Hence, the equivalent confined aquifer draw down; S_c, is expressed as $S_c = S_u - S_u^2/2m$ where S_u is the observed unconfined aquifer draw down and m is the initial saturation thickness in unconfined aquifer. He concluded that, if $s^2/2m < 3*10^{-3}m$, then the correction in the above equation is not necessary because the condition in the above equation is satisfied only in this case (Zekai Sen, 1995) pp241

All the wells grouped as pumping unconfined aquifers meet the condition expressed above i.e. $s^2/2m < 3*10^{-3}m$, so that their drawdown is corrected using the Jacob correction formula and then after the confined aquifer models are employed (Table 9.)

No	Well Id	E	N	S	H	S/H	S/H (%)	S'=S-(S^2/2H)	S_w^2	2H	S^2/2H	S^2/2H < 3*10^{-3}m
1	RPW-004	587866	1399382	42.34	77.40	0.55	54.70	30.76	1792.68	154.80	11.58	> 3*10^{-3}m
2	RPW-005	577889	1409202	7.36	36.00	0.20	20.44	6.61	54.17	72.00	0.75	> 3*10^{-3}m
3	RPW-008	559048	1366594	62.88	59.49	1.06	105.70	29.65	3953.89	118.98	33.23	> 3*10^{-3}m
4	RPW-017	571732	1375106	51.95	84.00	0.62	61.85	35.89	2698.80	168.00	16.06	> 3*10^{-3}m
5	RPW-026	570329	1389923	3.98	30.00	0.13	13.27	3.72	15.84	60.00	0.26	> 3*10^{-3}m
6	RPW-035	566991	1377439	31.68	72.00	0.44	44.00	24.71	1003.62	144.00	6.97	> 3*10^{-3}m
7	RPW-037	574690	1390976	9.56	58.72	0.16	16.28	8.78	91.39	117.44	0.78	> 3*10^{-3}m
8	RPW-038	574039	1389891	19.92	65.33	0.30	30.49	16.88	396.81	130.66	3.04	> 3*10^{-3}m
9	RPW-048	570343	1380681	58.86	54.00	1.09	109.00	26.78	3464.50	108.00	32.08	> 3*10^{-3}m
10	RPW-049	568921	1379801	15.28	60.00	0.25	25.47	13.33	233.48	120.00	1.95	> 3*10^{-3}m
11	RPW-059	565861	1379159	5.26	48.00	0.11	10.96	4.97	27.67	96.00	0.29	> 3*10^{-3}m
12	RPW-064	564467	1373141	8.37	40.67	0.21	20.58	7.51	70.06	81.34	0.86	> 3*10^{-3}m
13	RPW-065	565658	1373049	6.92	47.82	0.14	14.47	6.42	47.89	95.64	0.50	> 3*10^{-3}m
14	RPW-068	572613	1371922	10.63	92.10	0.12	11.54	10.02	113.00	184.20	0.61	> 3*10^{-3}m
15	RPW-069	565204	1371005	29.13	54.00	0.54	53.94	21.27	848.56	108.00	7.86	> 3*10^{-3}m
16	RPW-070	570481	1371229	47.09	46.32	1.02	101.66	23.15	2217.47	92.64	23.94	> 3*10^{-3}m
17	RPW-077	565483	1368490	4.56	42.00	0.11	10.86	4.31	20.79	84.00	0.25	> 3*10^{-3}m
18	RPW-078	569076	1366877	15.1	30.00	0.50	50.33	11.30	228.01	60.00	3.80	> 3*10^{-3}m
19	RPW-080	570393	1368715	2.54	40.88	0.06	6.21	2.46	6.45	81.76	0.08	> 3*10^{-3}m
20	RPW-085	564906	1363929	16.81	42.00	0.40	40.02	13.45	282.58	84.00	3.36	> 3*10^{-3}m
21	RPW-090	563934	1356825	19.49	64.35	0.30	30.29	16.54	379.86	128.70	2.95	> 3*10^{-3}m
22	RPW-098	562933	1357904	7.78	46.24	0.17	16.83	7.13	60.53	92.48	0.65	> 3*10^{-3}m
23	WF13/BH1	574502	1409298.1	2.58	48.00	0.05	5.38	2.51	6.66	96.00	0.07	> 3*10^{-3}m

24	WF13/BH2	575754.1	1407602.4	4.34	60.00	0.07	7.23	4.18	18.84	120.00	0.16	> $3*10^{-3}$m
25	WF13/BH4	574836.8	1408721	3.76	48.00	0.08	7.83	3.61	14.14	96.00	0.15	> $3*10^{-3}$m
26	WF13/BH5	575406.1	1408290	2.44	42.00	0.06	5.81	2.37	5.95	84.00	0.07	> $3*10^{-3}$m
27	WF2/V9	565921.4	1376322.4	8.75	42.00	0.21	20.83	7.84	76.56	84.00	0.91	> $3*10^{-3}$m
28	WF4/BH2	565885.2	1378788.5	3.38	62.00	0.05	5.45	3.29	11.42	124.00	0.09	> $3*10^{-3}$m
29	WF4/BH3	564899	1378795	6.34	36.00	0.18	17.61	5.78	40.20	72.00	0.56	> $3*10^{-3}$m
30	WF0/BH1	562709.1	1370792.7	5.12	24.00	0.21	21.33	4.57	26.21	48.00	0.55	> $3*10^{-3}$m
31	WF0/BH6	561399.4	1370776.7	4.79	42.00	0.11	11.40	4.52	22.94	84.00	0.27	> $3*10^{-3}$m
32	WFO/BH7	561795.7	1370779.5	1.76	42.00	0.04	4.19	1.72	3.10	84.00	0.04	> $3*10^{-3}$m
33	WF0/BH8	561408.5	1369799.3	5.97	48.00	0.12	12.44	5.60	35.64	96.00	0.37	> $3*10^{-3}$m
34	WF1/V1	562871.8	1371639.7	16.36	35.00	0.47	46.74	12.54	267.65	70.00	3.82	> $3*10^{-3}$m
35	WF1/V9	562713.4	1371854.5	3.12	30.00	0.10	10.40	2.96	9.73	60.00	0.16	> $3*10^{-3}$m
36	WF1/V10	562680.6	1371182.6	4.64	30.00	0.15	15.47	4.28	21.53	60.00	0.36	> $3*10^{-3}$m
37	WF5/BH1	563690.3	1366992.6	14.56	36.00	0.40	40.44	11.62	211.99	72.00	2.94	> $3*10^{-3}$m
38	WF5/BH4v5	563905	1367793	16.15	48.00	0.34	33.65	13.43	260.82	96.00	2.72	> $3*10^{-3}$m
39	WF6/BH4	563912.4	1364684.5	2.95	48.00	0.06	6.15	2.86	8.70	96.00	0.09	> $3*10^{-3}$m
40	WF7/BH1	564378.1	1363098.3	1.65	48.00	0.03	3.44	1.62	2.72	96.00	0.03	> $3*10^{-3}$m
41	WF7/BH2	563863	1364132.9	2.51	60.00	0.04	4.18	2.46	6.30	120.00	0.05	> $3*10^{-3}$m
42	WF Abergelle BH1	570017	1386373	10.4	62.00	0.17	16.77	9.53	108.16	124.00	0.87	> $3*10^{-3}$m
43	WF GOBU BH1	564404	1358786	3.07	40.00	0.08	7.68	2.95	9.42	80.00	0.12	> $3*10^{-3}$m
44	WF Abergelle BH2	573832	1365003	13.61	28.00	0.49	48.61	10.30	185.23	56.00	3.31	> $3*10^{-3}$m
45	PZ3	569257	1377425	2.28	54.00	0.04	4.22	2.23	5.20	108.00	0.05	> $3*10^{-3}$m
46	PZ4	565181	1379685	5.07	30.00	0.17	16.90	4.64	25.70	60.00	0.43	> $3*10^{-3}$m
47	PZ9	562943	1365069	2.24	40.00	0.06	5.60	2.18	5.02	80.00	0.06	> $3*10^{-3}$m

48	PBH1	571313	1415112	8.84	22.00	0.40	40.18	7.06	78.15	44.00	1.78	> $3*10^{-3}$m
49	PBH7	568083	1385735	1.75	48.00	0.04	3.65	1.72	3.06	96.00	0.03	> $3*10^{-3}$m

Table 9 Corrected drawdown using Jacob correction for wells tapping unconfined aquifers

8.1.3 Discharge Q (m^3/Day)

Discharge is the production of the wells in L^3/T, where L is unit of length and T unit of time. The discharge of the wells used for the analysis of aquifer hydraulic parameters and calculation of specific capacity is the constant discharge rate used during the constant rate test. It varies from well to well with minimum, maximum, average and median values of 172.8 m^3/d, 10459.58 m^3/d, 3541.987 m^3/d, and 3088.8 m^3/d respectively (Table 8.) As shown in Fig 21 most of the discharge rates used for specific capacity calculation are close either to their median or average values.

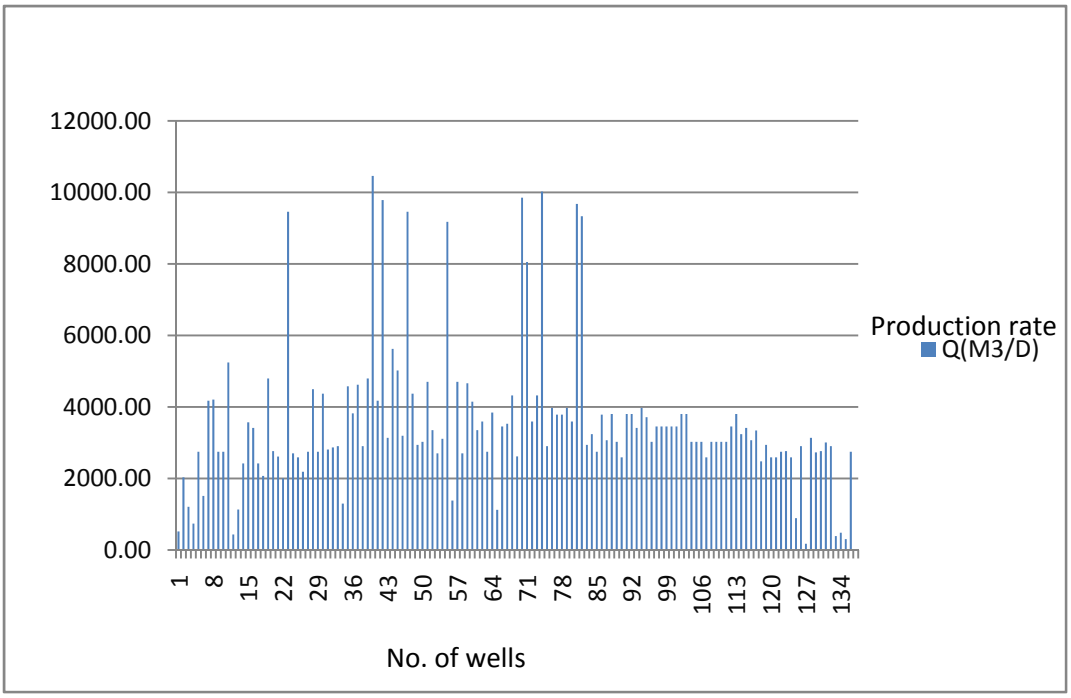


Figure 20 Production rates used for specific capacity tests in the raya valley aquifer

9.0 ESIMATING TRANSMISSIVITY FROM SPECIFIC CAPACITY AND BOREHOLE YIELD

There are three main approaches for estimating transmissivity from specific capacity analytical, empirical and Geostatistical methods (mace, 2000) pp.52. The three methods are employed to estimate transmissivity from specific capacity and are compared as to which method results in more accurate predictions.

9.1 ESIMATING TRANSMISSIVITY FROM SPECIFIC CAPACITY

9.1.1 ANALYTICAL METHOD

This approach only requires a single specific capacity value of specific capacity to estimate transmissivity. It uses mathematical equations based on the theory of groundwater flow. There are varieties of analytical solutions e.g. the Dupuit-Thiem steady state equation

$S_w = Q/2\pi TlnR/r_w$ where T is the transmissivity of the aquifer (m^2/day), R radius of influence of the pumping well (m) and r_w the radius of the well (m) so T can be solved from the above equation $T = (1/2\pi lnR/r_w)\ Q/S_w$. However the method employed for this purpose is the Theis non equilibrium equation. $Sc = 4\pi T/ (\ln (2.25Tt_p/r^2_wS))$ where S is the storativity of the aquifer, t_p the pumping time (day), r_w the radius of the well (m), T is the transmissivity of the aquifer (m^2/day)

The equation is based on the following assumptions – fully penetrating well; homogeneous, isotropic and porous media; negligible well loss and an effective radius equal to the radius of the production well (Walton, 1970) cited in Mace, 2000) pp11.

The above equation cannot be solved directly for transmissivity because T occurs in both numerator and denominator $T = Sc/4\pi\ln (2.25Tt_p/r^2_wS)$. It is solved iteratively by giving an initial guess of transmissivity value (the specific capacity value is a good initial guess) mace, 2000) to the right hand side of the equation. The value of T in the left hand of the equation is substituted back to the right hand of the equation. The operation is repeated until the difference between the value of T in the right hand side of the equation and the calculated T is small. This is done in a spread sheet with an iteration option.

The data requirements for this method are initial guess of T, pumping time, radius of well, and storativity (Table 11.)

Because this method assumes negligible well loss and fully penetrating well the output may be erroneous because in reality the measured drawdown in a well is a combined effect of well loss and aquifer loss. So the measured drawdown is corrected for well loss using Hantush-BierschenkWell Loss Solution method in Aquifer test. In this method the well loss constant "c" is determined from, the analysis of step drawdown test raw data of 63 boreholes, the slope of specific discharge vs. pumping rate plot. Before the start of the iteration process the well loss correction should be applied for wells with a pumping discharge of >36l/s (Mace, 2000) pp.

9.1.1.1 WELL LOSS CORRECTION

Well loss is the additional drawdown due to head loss from the resistance to flow into and inside the well. Well losses are generally due to well screen with insufficient open area, poor distribution of screen openings, and a poorly designed filter pack in the well annulus (after Driscoll, 1986, p.245)

Therefore well loss correction for 63wells whose production rates exceeding 36l/s is employed by analyzing step drawdown data using Hantush-Bierschenk Well Loss Solution. Borehole Rpw-074 is used for demonstration purpose Fig 22. The step test time-drawdown data of this borehole is plotted on semi-log graph and the slope of each line for each step is calculated from the change in drawdown (ΔS) and the time interval (the time from the beginning of each step at which the ΔS is measured for each step). The drawdown differences and the specified time interval are used to produce two coefficients: **B** and **C** (well loss coefficient) Fig 23. These coefficients can be used to estimate the expected drawdown inside a pumping well for a realistic discharge (Q) at a certain time (t) using the relation $S_w = BQ + (CQ'' + CQ^2)$. Where B is the proportionality constant for laminar flow in the formation, C'' is the proportionality constant for laminar well loss, and C is a proportionality constant for turbulent well loss. C'' is assumed to be negligible. Therefore the measured drawdown in the well is corrected by subtracting CQ^2 from the total drawdown in the well.

The measured draw downs in 49 wells pumping unconfined aquifers are also corrected for decreasing saturated thickness using the relation established by (Jacob, 1944)

$S_w cor = s_w - (s_w^2/2D)$ where S_{wcor} is the corrected draw down, S_w the measured draw down and D the original saturated thickness of the aquifer (Table 9.)

Specific capacity is then calculated for each well from discharge, Q (m^3/day) and the corrected drawdown for well loss and decreasing saturated thickness S_w (m).

The correction for partial penetration is not employed because almost all the wells drilled in the area are fully penetrating except 6 wells which are not fully penetrating. Although there are some techniques that correct for partial penetration effects they may not be valid if the percent of penetration is large (Driscoll, 1986) cited in Mace, 2000), hence the 6 wells are not corrected for partial penetration because the percent of penetration is assumed to be large based on the borehole data in their vicinity with fully penetrated aquifer sections.

The storativity value used in this analysis is assumed by taking the ranges of values for confined and unconfined aquifers i.e. 0.005 – 0.00005 and 0.01 – 0.3 (Mace, 2000), Fetter, 2001 and the averages within the range are taken.

The pumping times used in this analysis are taken from the constant rate test duration. The duration of the tests was not uniform in all wells (Table 10.)

No. of wells	Pumping time (day)	No. of wells with the specified time in (%)
92	3	68.6567
19	2	14.1791
2	1.33	1.49254
17	2.16	12.6866
3	1.5	2.23881
1	0.5	0.74627

Table 10 Pumping times for constant rate test

To avoid the error introduced due to variation in pumping times of the constant test the mean test time is used for the analysis and it is 2.67 days.

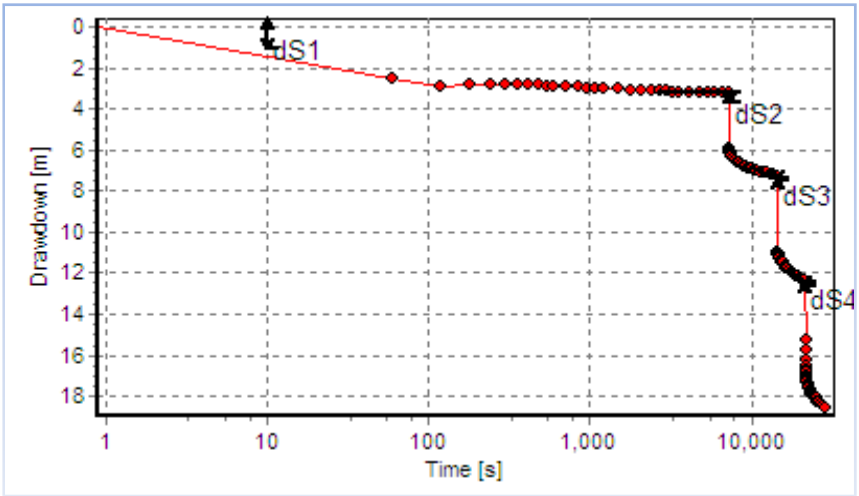


Figure 21 Step drawdown plot for well RPW-074

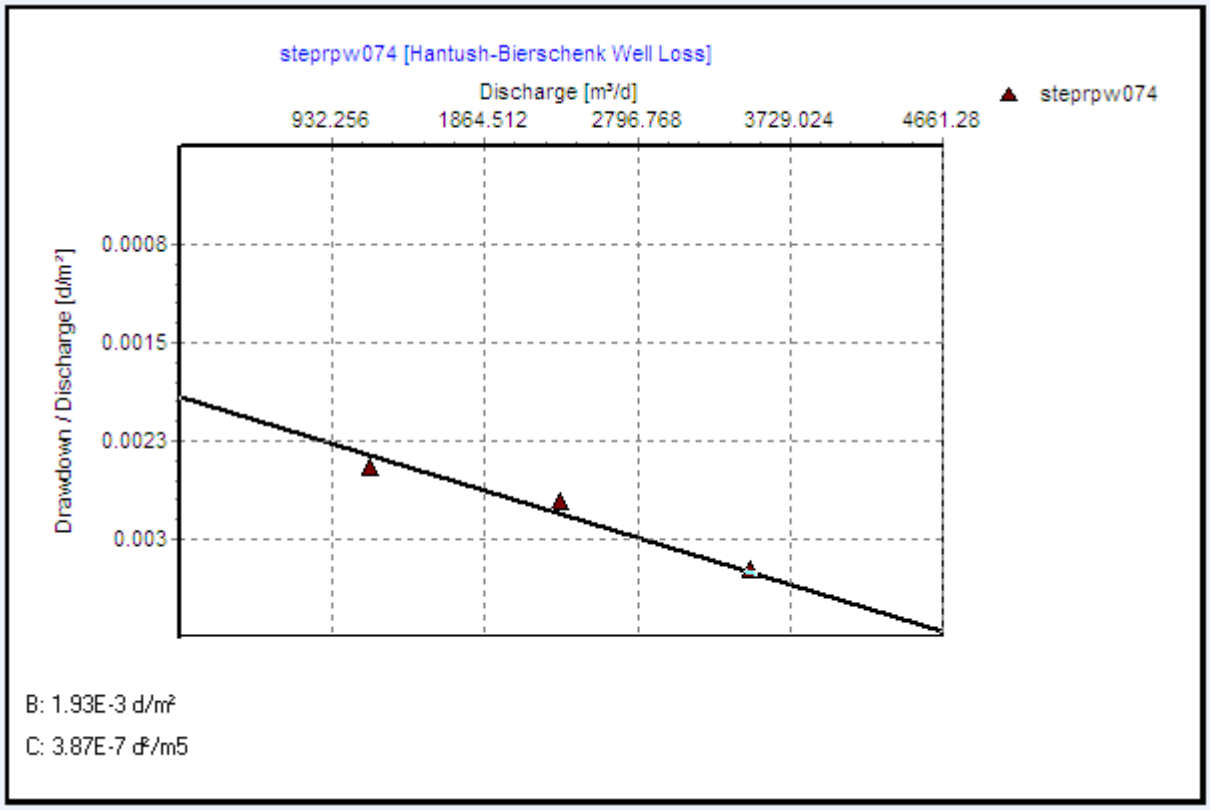


Figure 22 Head loss constant in the formation B and well loss constant, C determined from step test

No	Well Id	X	Y	Pumping time (day)	D (inch)	r(m) (AVRG)	Storativity average	Specific capacity (m^2/d) corrected
1	RPW-004	587866	1399382	3	12" & 8"	0.13	0.0025	16.85
2	RPW-005	577889	1409202	3	10" & 8"	0.11	0.0650	307.28
3	RPW-006	577182	1408010	3	12" & 8"	0.13	0.0650	49.11
4	RPW-008	559048	1366594	3	12" & 8"	0.13	0.0650	24.89
5	RPW-012	581052	1404035	3	10" & 8"	0.11	0.0025	283.25
6	RPW-013	572677	1403437	3	10" & 8"	0.11	0.0650	103.00
7	RPW-014	582104	1403603	3	10" & 8"	0.11	0.0025	653.50
8	RPW-017	571732	1375106	3	10" & 8"	0.11	0.0650	145.67
9	RPW-019	581768	1400964	3	10" & 8"	0.11	0.0025	216.51
10	RPW-020	577596	1400661	3	10" & 8"	0.11	0.0025	274.20
11	RPW-021	571906	1363793	3	12" & 8"	0.13	0.0025	1371.65
12	RPW-022	576837	1374986	3	12" & 8"	0.13	0.0650	11.63
13	RPW-023	568247	1400186	3	10" & 8"	0.11	0.0650	32.39
14	RPW-024	574144	1368595	3	10" & 8"	0.11	0.0025	581.54
15	RPW-025	570329	1389923	3	10" & 8"	0.11	0.0025	387.19
16	RPW-026	578718	1398109	3	10" & 8"	0.11	0.0650	1303.76
17	RPW-028	573856	1396696	3	10" & 8"	0.11	0.0025	701.22
18	RPW-030	566678	1378864	3	10" & 8"	0.11	0.0025	246.27
19	RPW-031	576189	1395698	3	12" & 8"	0.13	0.0025	1810.34
20	RPW-032	575022	1395075	3	10" & 8"	0.11	0.0025	154.89
21	RPW-033	576332	1394432	3	10" & 8"	0.11	0.0025	182.39
22	RPW-034	566991	1377439	3	10" & 8"	0.11	0.0025	172.65
23	RPW-035	574094	1392035	3	14" & 10"	0.15	0.0025	534.00
24	RPW-036	574690	1390976	3	10" & 8"	0.11	0.0650	772.17
25	RPW-037	574039	1389891	3	10" & 8"	0.11	0.0025	295.16
26	RPW-038	569910	1391794	3	10" & 8"	0.11	0.0025	129.47
27	RPW-040	572853	1372716	3	10" & 8"	0.11	0.0025	171.19
28	RPW-042	572369	1384905	3	12" & 8"	0.13	0.0025	471.21
29	RPW-043	569097	1378878	3	10" & 8"	0.11	0.0650	93.48
30	RPW-044	572436	1382113	3	10" & 8"	0.11	0.0025	241.47
31	RPW-045	569905	1381800	3	10" & 8"	0.11	0.0025	106.73
32	RPW-046	572052	1380755	3	10" & 8"	0.11	0.0650	89.53
33	RPW-047	570343	1380681	3	10" & 8"	0.11	0.0025	125.35
34	RPW-048	568921	1379801	3	10" & 8"	0.11	0.0650	48.39
35	RPW-049	571429	1379689	3	12" & 8"	0.13	0.0025	1227.50
36	RPW-050	568031	1379400	3	10" & 8"	0.11	0.0025	515.32
37	RPW-051	570263	1378912	3	12" & 8"	0.13	0.0025	349.95
38	RPW-052	568862	1377910	3	10" & 8"	0.11	0.0025	72.83
39	RPW-053	567333	1378232	3	12" & 8"	0.13	0.0025	274.48
40	RPW-054	571864	1378166	3	14" & 10"	0.15	0.0650	789.40
41	RPW-055	567995	1377085	3	10" & 8"	0.11	0.0025	248.78
42	RPW-056	569431	1376222	3	14" & 10"	0.15	0.0650	629.65

43	RPW-057	571642	1376249	3	10" & 8"	0.11	0.0650	297.42
44	RPW-058	565861	1379159	3	12" & 8"	0.13	0.0025	581.06
45	RPW-059	567200	1375899	3	12" & 8"	0.13	0.0025	1712.85
46	RPW-060	566917	1374980	3	10" & 8"	0.11	0.0025	803.22
47	RPW-061	571462	1374198	3	14" & 10"	0.15	0.0025	282.31
48	RPW-062	564467	1373141	3	12" & 8"	0.13	0.0025	345.05
49	RPW-063	565658	1373049	3	10" & 8"	0.11	0.0025	227.72
50	RPW-064	566444	1372391	3	10" & 8"	0.11	0.0650	402.73
51	RPW-065	571726	1373354	3	12" & 8"	0.13	0.0650	926.43
52	RPW-066	572613	1371922	3	10" & 8"	0.11	0.0025	530.54
53	RPW-067	565204	1371005	3	10" & 8"	0.11	0.0025	174.59
54	RPW-068	570481	1371229	3	10" & 8"	0.11	0.0025	310.53
55	RPW-069	565705	1372178	3	14" & 10"	0.15	0.0025	564.39
56	RPW-070	572671	1370616	3	10" & 8"	0.11	0.0025	59.71
57	RPW-071	564898	1367281	3	12" & 8"	0.13	0.0650	936.52
58	RPW-072	561215	1368924	3	10" & 8"	0.11	0.0025	55.61
59	RPW-074	567162	1369865	3	12" & 8"	0.13	0.0025	373.43
60	RPW-075	565483	1368490	3	12" & 8"	0.13	0.0025	780.59
61	RPW-076	569076	1366877	3	10" & 8"	0.11	0.0025	624.23
62	RPW-077	568008	1367866	3	10" & 8"	0.11	0.0650	1554.29
63	RPW-078	570393	1368715	3	8"	0.10	0.0650	243.15
64	RPW-079	566566	1367059	3	10" & 8"	0.11	0.0025	950.96
65	RPW-080	574045	1365777	3	10"	0.13	0.0650	456.38
66	RPW-081	565271	1365661	3	10" & 8"	0.11	0.0025	220.01
67	RPW-082	568850	1368728	3	10" & 8"	0.11	0.0025	328.23
68	RPW-083	564906	1363929	3	12" & 8"	0.13	0.0025	2739.46
69	RPW-084	563445	1362750	3	10" & 8"	0.11	0.0025	92.87
70	RPW-085	567591	1361714	3	14" & 10"	0.15	0.0025	1528.29
71	RPW-086	567019	1360930	3	14" & 10"	0.15	0.0025	207.48
72	RPW-087	563934	1356825	3	10" & 8"	0.11	0.0025	835.87
73	RPW-088	571968	1384297	32	10" & 8"	0.11	0.0025	403.77
74	RPW-090	567588	1359766	3	14" & 10"	0.15	0.0650	1050.73
75	RPW-092	565153	1359042	3	10" & 8"	0.11	0.0025	598.56
76	RPW-093	566902	1358605	3	12" & 8"	0.13	0.0025	297.53
77	RPW-095	564016	1357876	3	12" & 8"	0.13	0.0650	253.70
78	RPW-096	562933	1357904	3	10" & 8"	0.11	0.0025	681.77
79	RPW-097	566904	1357791	3	10" & 8"	0.11	0.0025	287.26
80	RPW-098	565838	1357528	3	10" & 8"	0.11	0.0025	650.71
81	RPW-099	574502	1409298	2	14" & 10"	0.15	0.0025	832.77
82	RPW-100	575754	1407602	2	14" & 10"	0.15	0.0025	515.32
83	WF13/BH1	574837	1408721	2	Steel 8"	0.10	0.0650	1170.05
84	WF13/BH2	575406	1408290	2	8" Steel	0.10	0.0025	1025.13
85	WF13/BH4	577896	1403786	1.33	10" Steel	0.13	0.0650	760.51
86	WF13/BH5	569813	1400983	2	10" Steel	0.13	0.0650	3715.05
87	WF11/BH4	569708	1399528	2.16	10" PVC	0.13	0.0650	395.26
88	WF9/BH1	569798	1400023	2.16	8" Steel	0.10	0.0025	998.70
89	WF9/BH2	570553	1400160	2	8" Steel	0.10	0.0650	233.33
90	WF9/BH3	565921	1376322	2	8" Steel	0.10	0.0650	227.37

91	WF9/BH4	567110	1381023	2	8" Steel	0.10	0.0025	8584.31
92	WF2/V9	565885	1378789	1.33	8" Steel	0.10	0.0025	1227.02
93	WF4/BH1	564899	1378795	2	10" Steel	0.13	0.0025	763.31
94	WF4/BH2	562709	1370793	2.16	10" Steel	0.13	0.0025	1931.79
95	WF4/BH3	562905	1370393	2.16	10" Steel	0.13	0.0650	1795.82
96	WF0/BH1	563923	1369802	2.16	10" PVC	0.13	0.0025	661.15
97	WF0/BH2	562697	1368978	2.16	8" Steel	0.10	0.0650	1525.86
98	WF0/BH3	561903	1369790	2.16	8" Steel	0.10	0.0025	383.57
99	WF0/BH4	561399	1370777	2.16	8" Steel	0.10	0.0025	276.48
100	WF0/BH5	561796	1370780	2.16	8" Steel	0.10	0.0025	734.60
101	WF0/BH6	561409	1369799	1.5	8" Steel	0.10	0.0025	1373.14
102	WFO/BH7	562872	1371640	2.16	10" Steel	0.13	0.0650	6318.77
103	WF0/BH8	562713	1371855	2.16	8" Steel	0.10	0.0650	1056.37
104	WF1/V1	562681	1371183	2.16	8" PVC	0.10	0.0025	241.22
105	WF1/V9	563690	1366993	2.16	8" PVC	0.10	0.0025	1022.40
106	WF1/V10	564103	1368593	2.16	10" PVC	0.13	0.0025	706.35
107	WF5/BH1	563673	1367565	2.16	10" Steel	0.13	0.0650	223.15
108	WF5/BH2v8	563905	1367793	2.16	8" PVC	0.10	0.0025	499.01
109	WF5/BH3v3	563156	1366192	2.16	10" Steel	0.13	0.0025	491.71
110	WF5/BH4v5	563912	1364685	2	10" Steel	0.13	0.0025	225.12
111	WF6/BH3	564378	1363098	2	10" Steel	0.13	0.0025	470.30
112	WF6/BH4	563863	1364133	2	8" Steel	0.10	0.0025	1208.67
113	WF7/BH1	570017	1386373	2	8" Steel	0.10	0.0650	12007.19
114	WF7/BH2	571787	1401448	2	8" Steel	0.10	0.0025	2613.37
115	WF Abergelle BH1	564404	1358786	1.5	8" PVC	0.10	0.0025	425.26
116	Kalibso plc BH1	573832	1365003	1.5	8" PVC	0.10	0.0025	278.58
117	WF GOBU BH1	570245	1369978	2	8" PVC	0.10	0.0650	1632.00
118	WF Abergelle BH2	576764	1390173	3	8" PVC	0.10	0.0650	240.69
119	Galika Trading BH1	576732	1389596	3	8" PVC	0.10	0.0025	185.57
120	WF-SAV/BH1	575944	1389641	3	10" PVC	0.13	0.0025	316.10
121	WF-SAV/BH2	576495	1390581	3	10" PVC	0.13	0.0025	372.41
122	WF-SAV/BH3	577594	1403257	2	10" PVC	0.13	0.0025	547.31
123	WF-SAV/BH4	571787	1401448	0.5	10" PVC	0.13	0.0025	362.36
124	Friatna BH/1	581458	1402058	3	8"	0.10	0.0025	236.07
125	Tera BH1	585168	1402537	2	8"	0.10	0.0025	156.95
126	PZ1	569257	1377425	3	8"	0.10	0.0025	228.41
127	PZ2	565181	1379685	3	8"	0.10	0.0650	29.04
128	PZ3	572491	1373604	3	8"	0.10	0.0025	1405.25
129	PZ4	574387	1361357	3	8"	0.10	0.0650	588.21
130	PZ5	562943	1365069	3	8"	0.10	0.0025	2633.14
131	PZ7	571313	1415112	3	8"	0.10	0.0025	208.51
132	PZ9	587384	1411774	3	8"	0.10	0.0025	1333.33
133	PBH1	568083	1385735	2	8"	0.10	0.0650	55.04
134	PBH3	576046	1403659	2	8"	0.10	0.0025	144.86
135	PBH7	568083	1385735	2	8"	0.10	0.0025	176.01
136	Dejena BH3	576046	1403659	2	10"PVC	0.13	0.0025	125.74

Table 11 Data requirements for estimating Transmissivity from specific capacity using analytic

Iteration process is applied on the Theis and others, 1963 non equilibrium formula in a spread sheet to estimate transmissivity from specific capacity using the above listed parameters. It is found that the estimated Transmissivity is in good agreement with the measured Transmissivity (Fig. 24). The value of the specific capacity is used as an initial guess for transmissivity. The estimated and measured values of transmissivity are plotted against each other and fitted with a regression line with a power relation, $R^2 = 0.963$, n = 79, indicating the analytic formula is non linear. The closeness of the goodness of fit to unity implies that the analytical solution is a very good estimator of transmissivity from specific capacity.

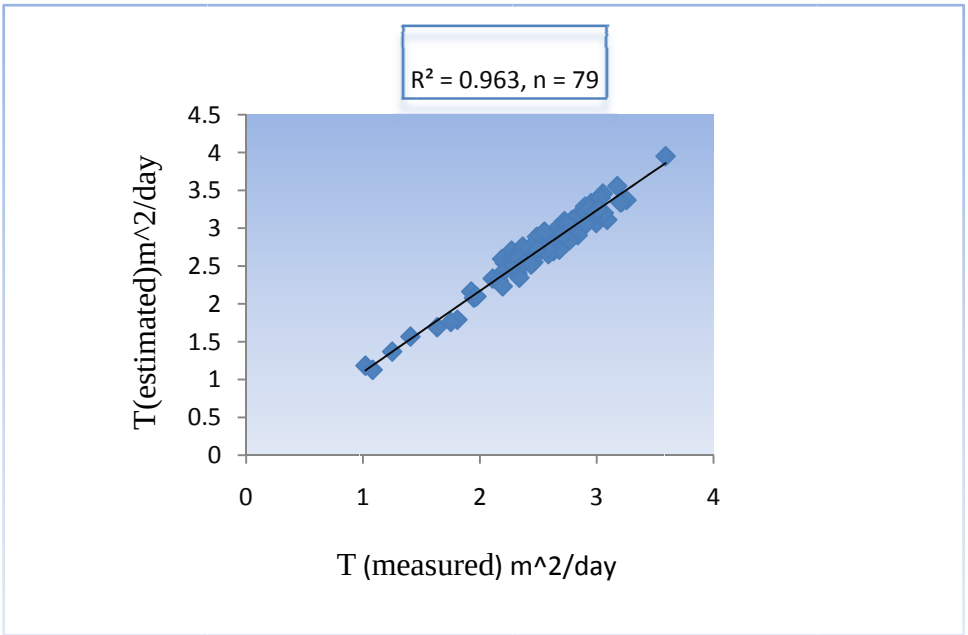


Figure 23 comparison of measured T and estimated T from analytic method

9.1.2 THE EMPIRICAL METHOD

This approach involves empirically relating paired values of transmissivity and specific capacity data measured in the same well.

To apply this method at least 25 measured pairs of transmissivity and specific capacity data are required to establish a linear relationship between the two parameters (Mace, 2000) pp 52.

This is done by defining $Yi = b_0 + b_1x_i$, in the present case $Y_i = \log T_i$ and $X_i = \log ((S_c)_i)$ (Davis, 1986), Mace and others 1999).

The specific capacity and transmissivity pairs used for this analysis are measured from the same well; and the specific capacity data are calculated from the pumping rate applied in the constant rate pumping test and the measured drawdown from the same test. The measured drawdown from wells tapping an unconfined aquifer are corrected for decreasing saturated thickness using Jacob correction Table 9, and the Transmissivity data are also analyzed by using Aquifer test 3.5 software applying either theis, cooper Jacob and confined aquifer models with Jacob correction depending on the aquifer type.

Log transformation is applied to the data to improve the normality of the data, to stabilize the variance, to transform the data from skewed to symmetric distribution and there by improve the goodness of fit (R^2) value.

For this analysis 79 pairs of log transformed values of specific capacity and transmissivity data are plotted against each other and fit a least squares regression line through them.

Therefore log transmissivity can be directly estimated from the best fit regression equation.

The best fit regression equation through the data pairs is T= 1.064Sc - 0.151 with a goodness of fit (R^2 = 0.96) (Fig 25) using linear relationship between log transformed values of both parameters. By rearranging this equation in to $T = 10^{-0.151}Sc^{1.064}$ or $T= 0.85Sc^{1.064}$ it is possible to estimate an untransformed transmissivity directly from this relation. Therefore, the regression equation can be a better estimator of Transmissivity for a single specific capacity data and from this equation we can see that the relationship between transmissivity and specific capacity might be non linear.

In addition to this, the correlation between transmissivity and specific capacity show similar goodness of fit with power and 2^{nd} order polynomial Fig 26, Fig 27

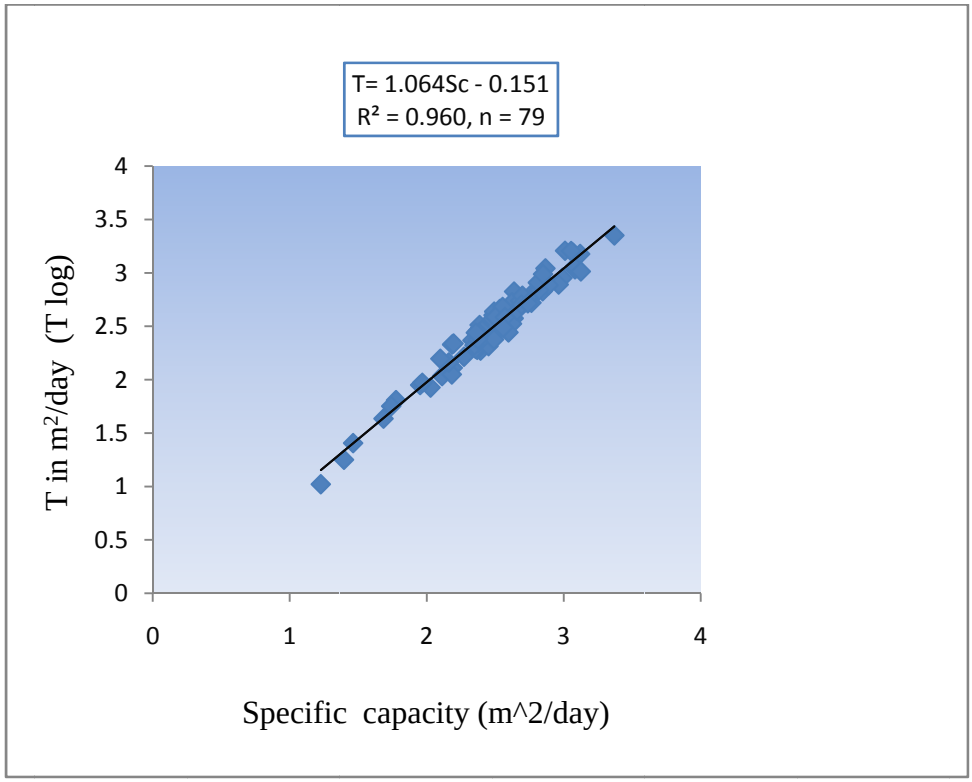


Figure 24 Empirical relation between log transformed Transmissivity and log transformed Specific capacity with a linear relationship

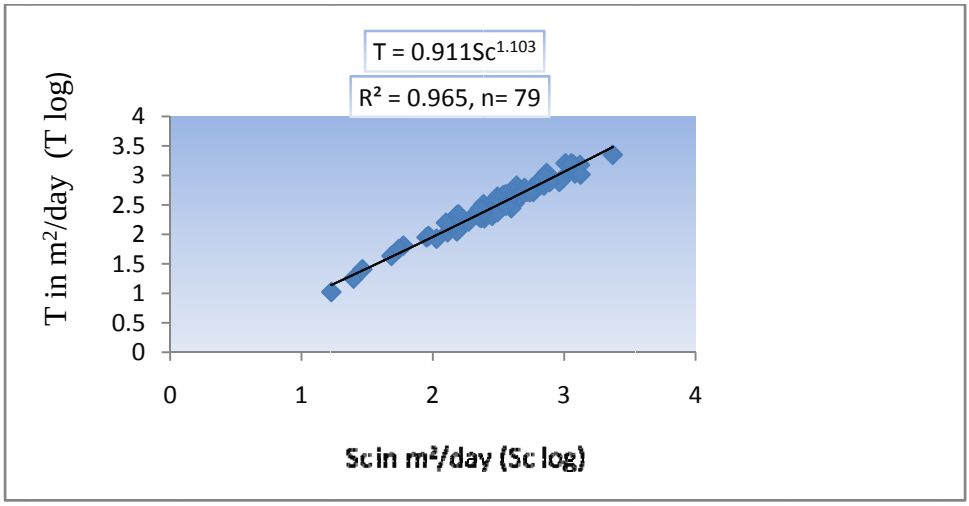


Figure 25 Empirical relationship between log transmissivity and log specific capacity with a power relationship

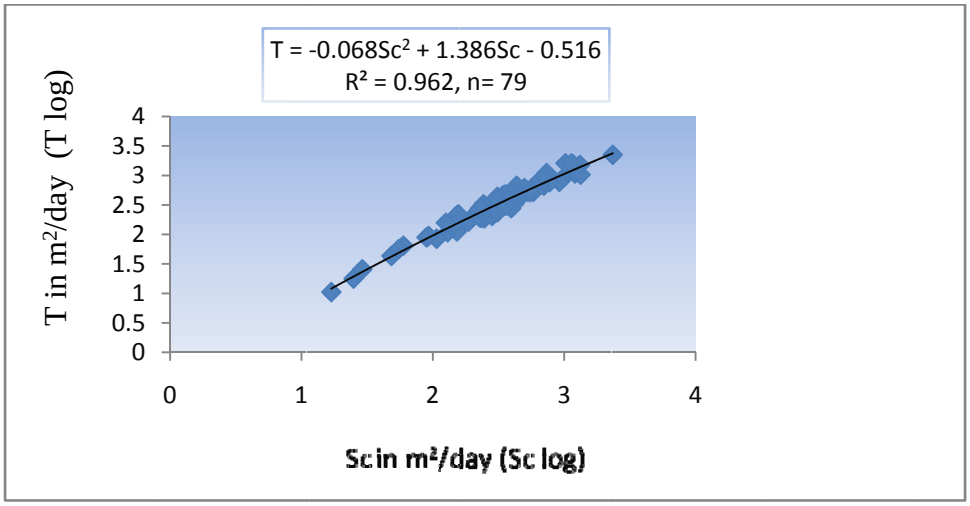


Figure 26 Empirical relationship between log transmissivity and log specific capacity with a 2nd order polynomial Relationship

9.1.2.1 RESULTS OF COMPARISON BETWEEN ESTIMATES OF TRANSMISSIVITY USING ANALYTICAL AND EMPIRICAL APPROACHES

To evaluate the relative accuracy of transmissivity estimated using analytic relationship against transmissivity estimated using empirical relationship the mean absolute error $|\overline{\varepsilon}|$ and the mean error ε should be determined between log transformed values of measured and estimated transmissivity for both relations (Mace and others 1999 pp 23)

$$|\overline{\varepsilon}| = \frac{}{} \qquad \text{and } \varepsilon = \frac{}{}$$

Where n is the number of values, Tm - transmissivity determined from pumping test analysis, Te - transmissivity estimated from specific capacity.

Therefore to compare the transmissivity estimated using both relations the mean absolute error and the mean error between the estimates and the measured values of log-transformed transmissivity are determined. The mean absolute error and mean error for transmissivity estimated using the analytic approach are 0.21 and -0.21 respectively. A mean absolute error of 0.21 means that, on average, the estimated value of transmissivity is within a factor of 1.6 of the measured value (determined by taking the inverse log of 0.21)

The mean absolute error and mean error for transmissivity estimated using the empirical approach are 0.073 and 0.00021 respectively. A mean absolute error of 0.073 indicates that, on average, the estimated value of transmissivity is within a factor of 1.18 of the measured value (determined by taking the inverse log of 0.073). The closeness of the mean error to zero indicates that the estimates may not have a systematic error towards overestimating or underestimating transmissivity.

9.1.3 THE GEOSTATISTICAL METHOD

Geostatistics is a statistical approach for working with spatially distributed data that considers the spatial location of a point and its correlation with a spatially distributed data that considers the spatial location of a point and its correlation with nearby points (Mace, 2000) pp23

This method is employed to estimate transmissivity from specific capacity based on 135 data pairs of transmissivity and specific capacity measured in the same well. The purpose of this work is to produce interpolated map of transmissivity and to compare with the other approaches discussed above. The transmissivity is estimated from specific capacity using cokriging and the spatial characteristics is quantified using semivariograms between transmissivity points and specific capacity points and with crossvariogram between transmissivity and specific capacity.

This is done using ArcGis 9.3 software by a Geostatistics analyst wizard. The regressed relationship will be used to estimate transmissivity from locations where only specific capacity is measured.

In cokriging, the degree of correlation between transmissivity and specific capacity and the special structure of the correlation are considered in the cross semivariograms (Mace, 2000), pp27. A transmissivity, $Z^*(x_0)$, can be estimated at a point , x_0, from the measured values of transmissivity ($Z(x_i)$ for I = 1,…n) and specific capacity ($Y(x_k)$ for k = 1,…,m) using $Z^*(x_0) = \sum_{i=1}^{n} \lambda i\, Z(xi)) + \sum_{k=1}^{m} \lambda k\, Y(xk)$ where the weights, λ, must satisfy $\sum_{i=1}^{n} \lambda i = 1$ & $\sum_{k=1}^{m} \lambda k = 0$, (Mace, 2000) pp27.

The prediction map of transmissivity is prepared in two stages. In the first stage it is created using default parameters in ArcGis by Geostatistics wizard; in the second stage the final transmissivity map is created after passing through the following steps which are employed

to improve the quality of the final transmissivity map predicted from specific capacity data based on 135 data pairs of transmissivity and specific capacity measured in the same well.

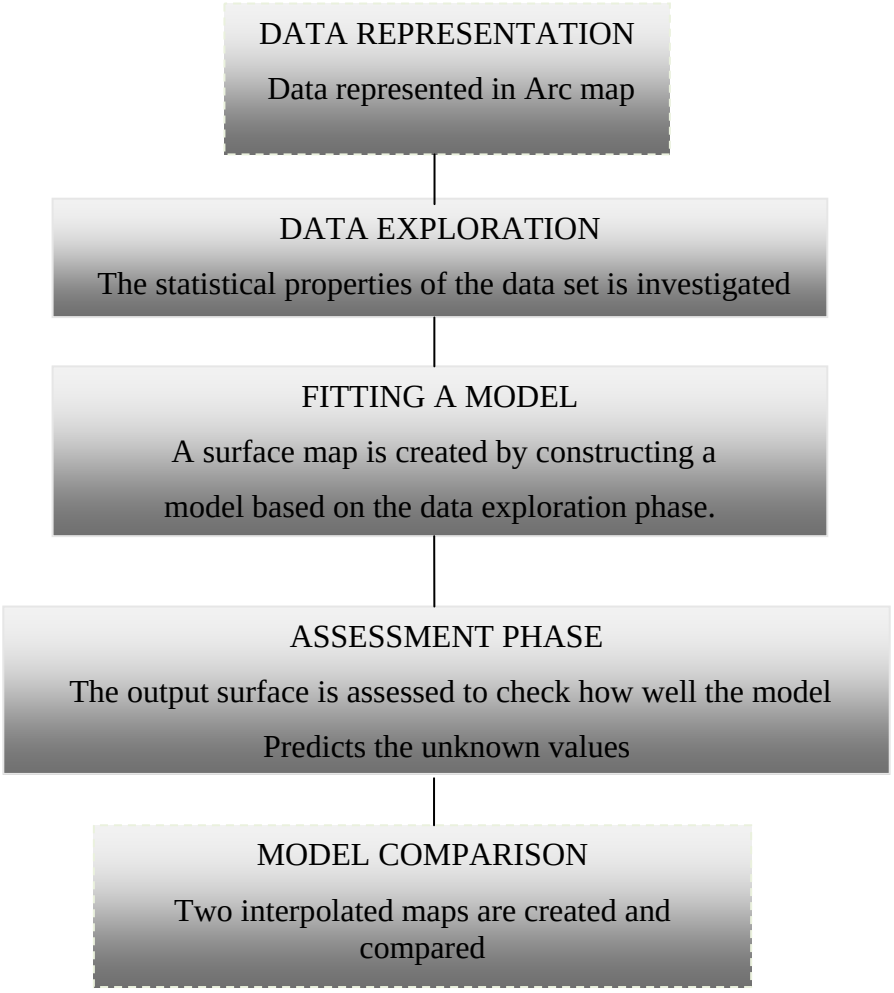


Figure 27 flow chart on the analysis of data sets using geostatistical approach

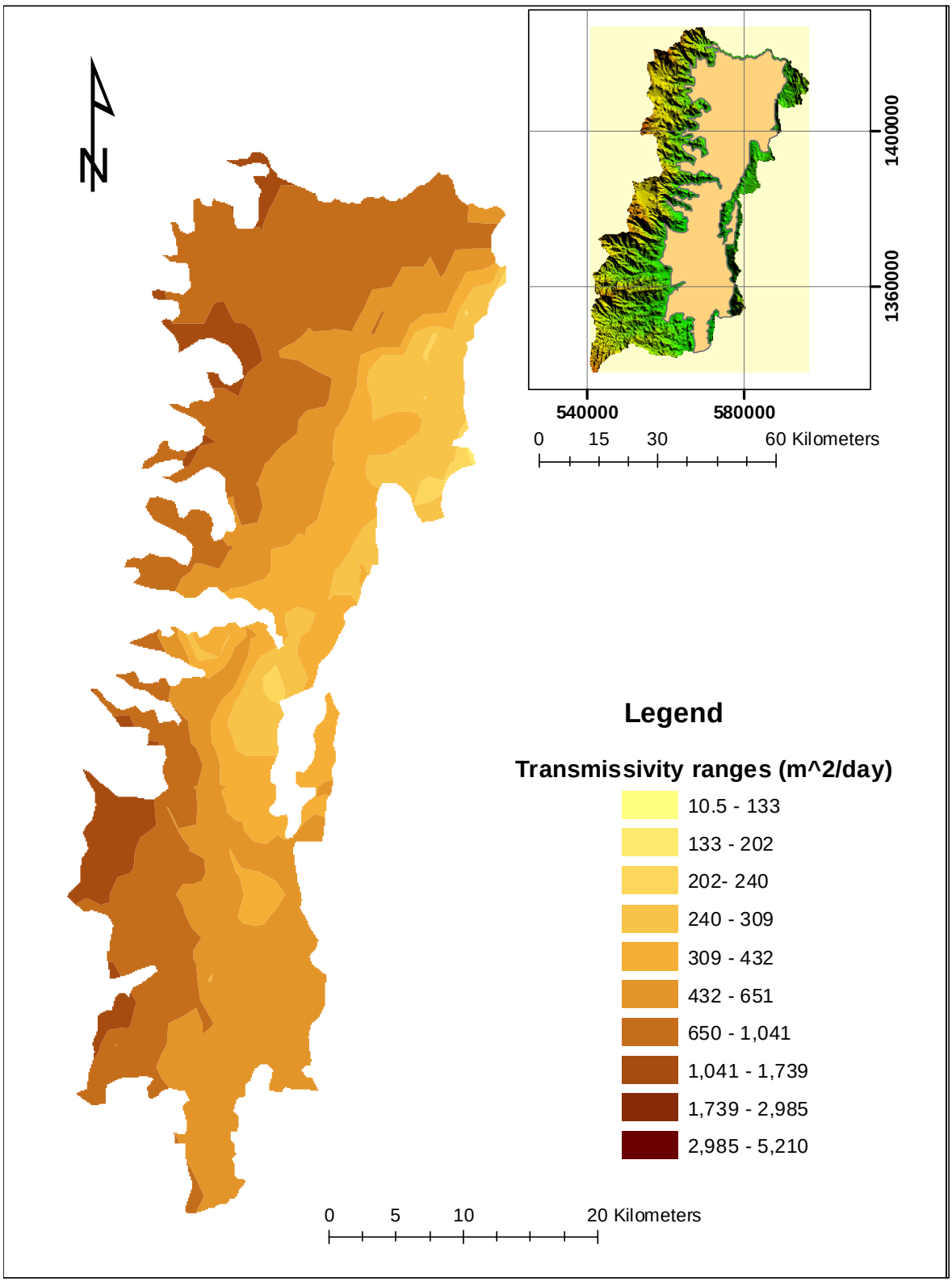


Figure 28 Transmissivity map created with default parameters in Arc Gis

9.1.3.1 DATA EXPLORATION

After creating the prediction map with default parameters in ArcGis the data values are explored for further refinement.

9.1.3.2 HISTOGRAM

The histograms of transmissivity and specific capacity show that the skewed (asymmetric) nature of both parameters, therefore to improve the final output surface the two parameters are log transformed and the distribution of the data values approach to a nearly normal distribution (Fig 30-33.)

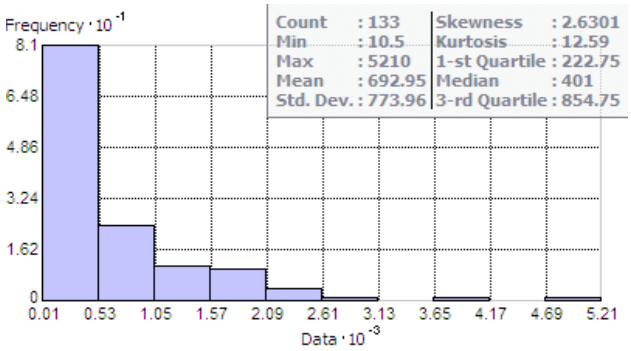


Figure 29 Histogram for T with Skewed distribution

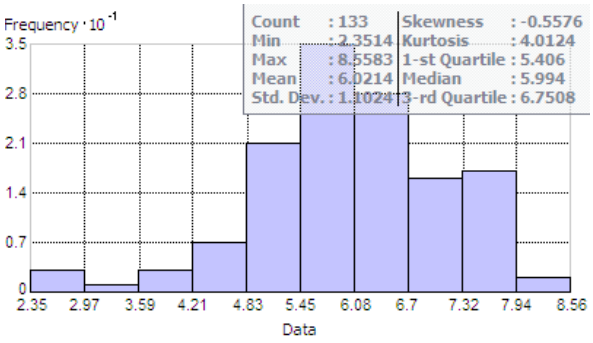


Figure 30 Histogram for T with log transformed Values and nearly normal distribution

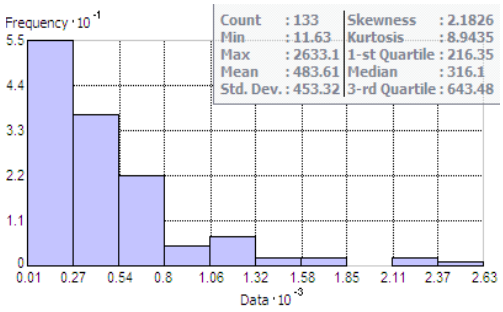


Figure 31 Histogram for Sc with Skewed distribution transformed

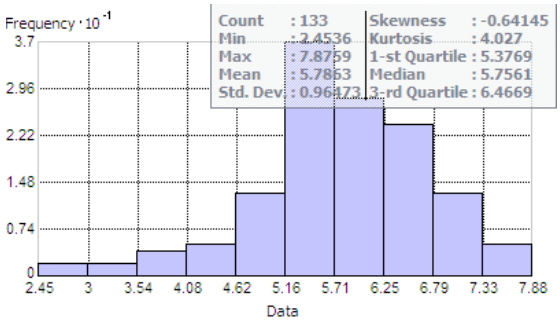


Figure 32 Histogram for Sc with log Values and nearly normal distribution

The right tail in the histogram shows a relatively small number of transmissivity data with high values these are selected in both the histogram and in the default transmissivity surface map (Fig 34)

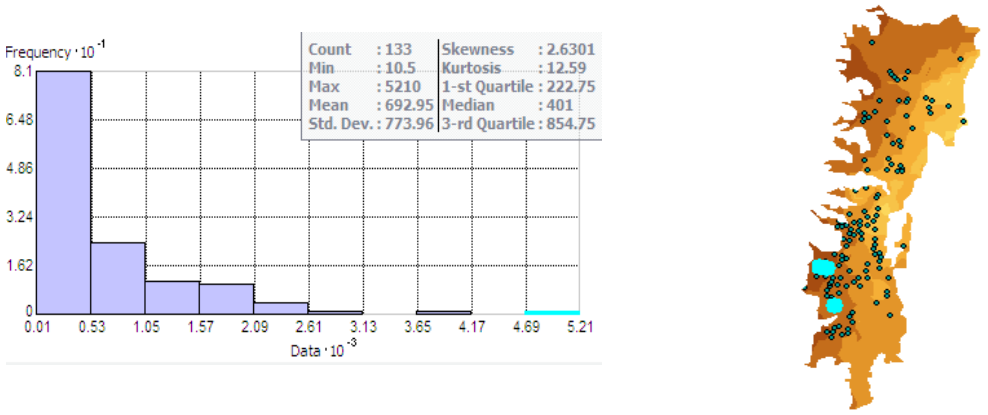


Figure 33 Transmissivity with higher values shown on the histogram and default Transmissivity map

9.1.3.3 QQ PLOT

A QQ plot is a graph of the quantiles of the distribution of two different distributions plotted against each other. For identical distributions the plot will be a straight line. The plots help to compare the quantiles of Transmissivity and specific capacity values with the quantiles of a standard normal distribution. Therefore the quantiles of both the transmissivity and specific capacity values are not normally distributed therefore both are log transformed to make them normal before using cokriging interpolation technique (Fig 35-38.)

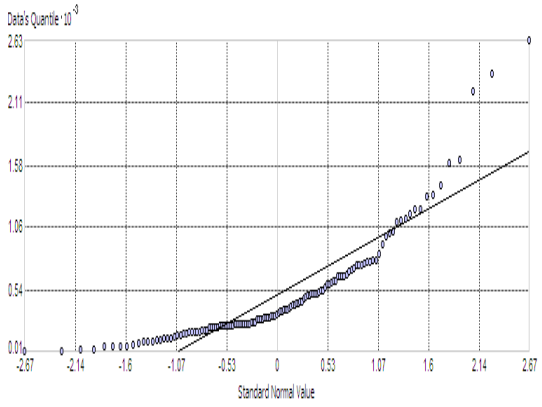


Figure 34 QQ plot for Sc

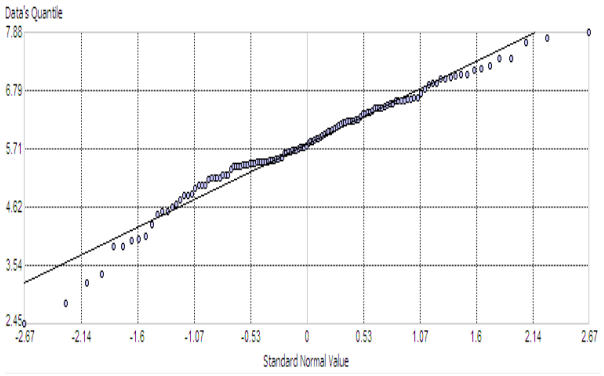


Figure 35 Normal QQ plot for Sc log transformed

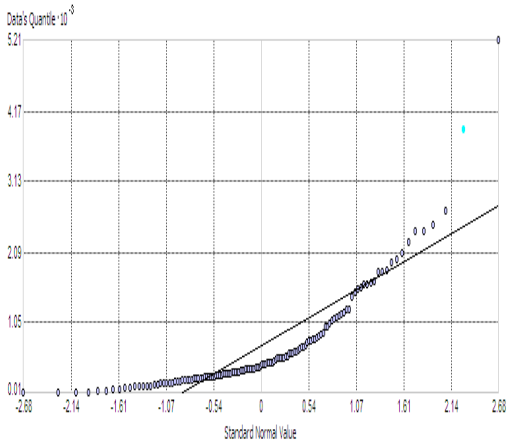


Figure 36 QQ plot for T

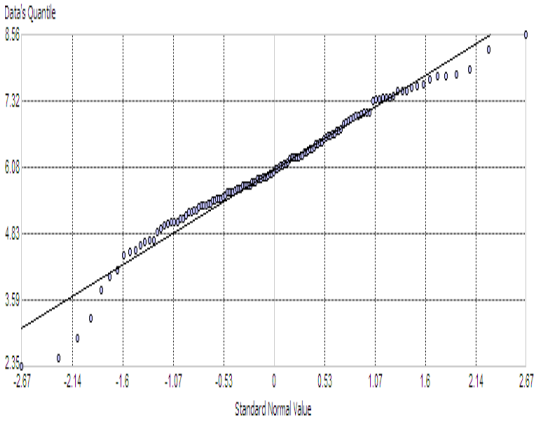


Figure 37 Normal QQ plot for T log transformed

9.1.3.4 IDENTIFYING GLOBAL TRENDS

A nearly u shaped trend surface (green colored) with a nearly NE-SW orientation is observed at 30^0 rotation angle this signifies the existence of a trend with higher values at the west (southwest) which could be attributed to the existence of higher transmissivity values at western margin of the study area because the trend surface has higher value at the western tip of the curve. Therefore a second order polynomial could be the best choice for fitting the global trend and this will be removed on the final map in order to reduce the influence of the trend on the residuals i.e. the short range variation and concentrate on these residuals (Fig 39.)

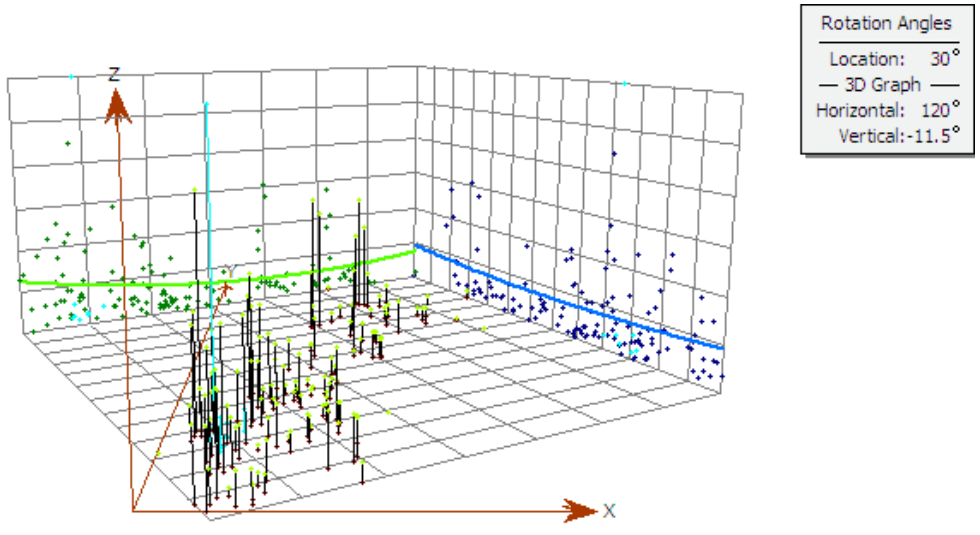
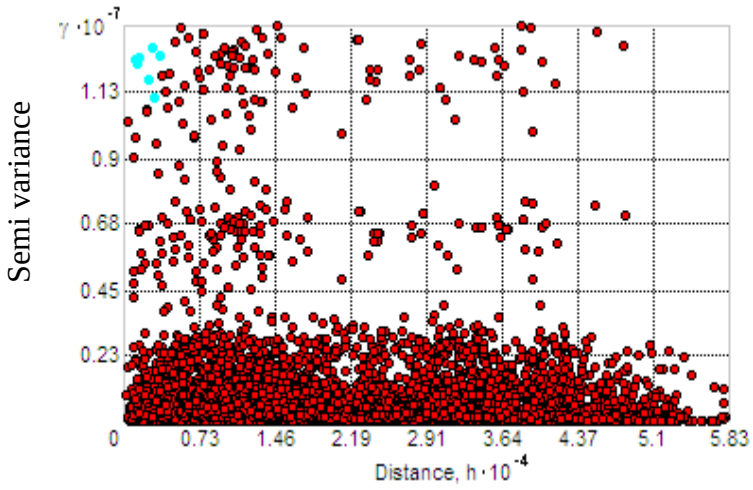


Figure 38 Trend surface for both transmissivity and specific capacity points

9.1.3.5 SEMIVARIOGRAM (COVARIANCE) CLOUD

In this portion the semivariogram cloud is assessed to examine the evidence of auto correlation and directional influences

Locations that are closer together are expected to be more alike than locations distant from each other. In this semivariogram 4 groups of data pairs are clearly observed. The 1st group is characterized by low semi variance values and smaller distance between pairs; 2nd group is characterized by closer distance but high semi variance values. These groups are found in areas with high transmissivity values around Alamata town these are paired with low transmissivity values nearby. This is the reason for high semi variance values Fig 40 the 2nd group are selected in the map. The 3rd groups are characterized by high semivariogram values and high distance values. These pairs of points are separated by longer distances than the previous ones. They have high semivariogram values due to large difference in transmissivity values at the pairs (Fig 41.) The 4th group is defined by low semi variance values and high distance values between transmissivity pairs Fig 42 this is because nearly similar values of transmissivity pairs are paired, but with longer distance between pairs.



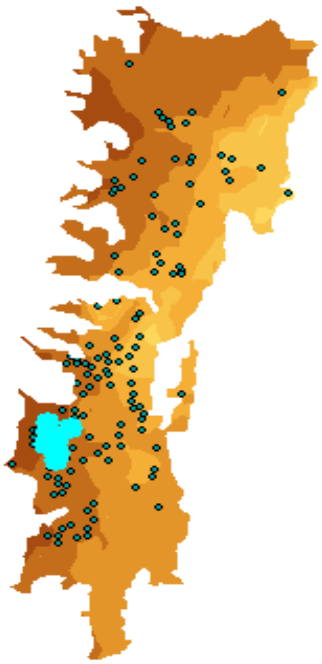
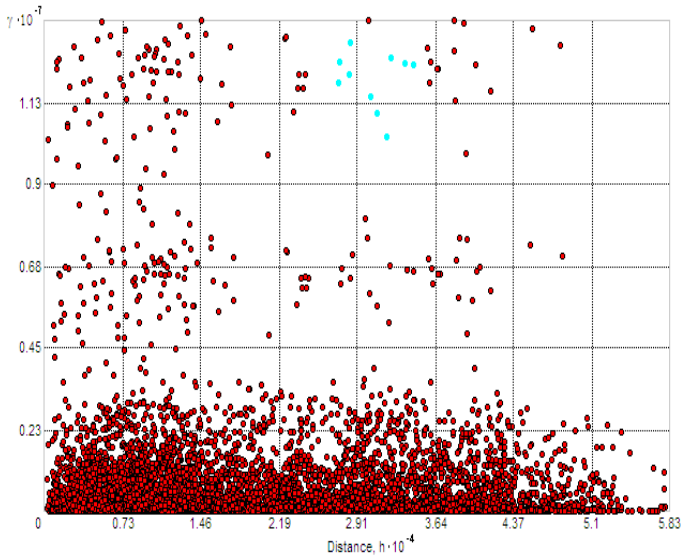


Figure 39 Semivariogram cloud for transmissivity



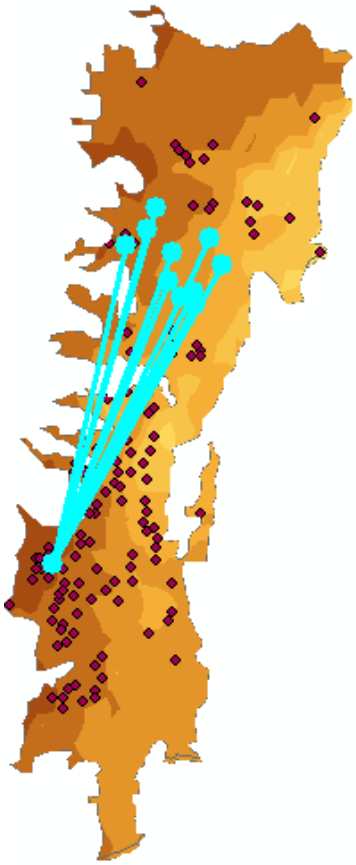


Figure 40 Semivariogram cloud for transmissivity

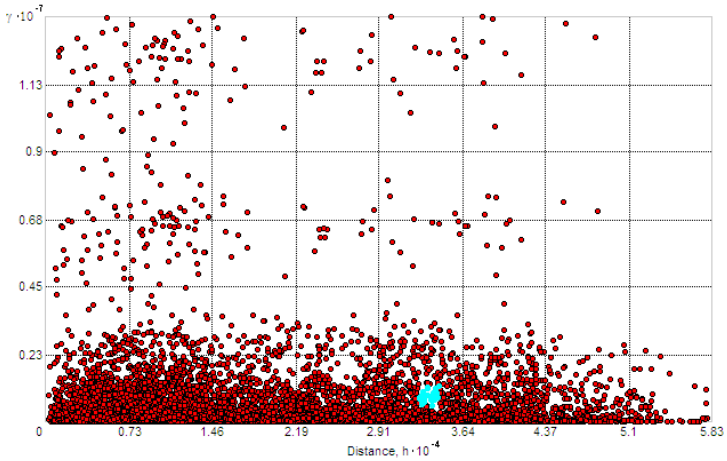




Figure 41 Semivariogram cloud for transmissivity

From the exploration phase the evidence of auto correlation of transmissivity pairs between themselves is assessed as defined in the semivariogram. The same is also true for specific capacity pairs.

9.1.3.6 CROSS COVARIANCE CLOUD

The cross covariance between transmissivity and specific capacity pairs is also assessed in the cross variogram for the evidence of cross correlation between the pairs (Fig 43.)

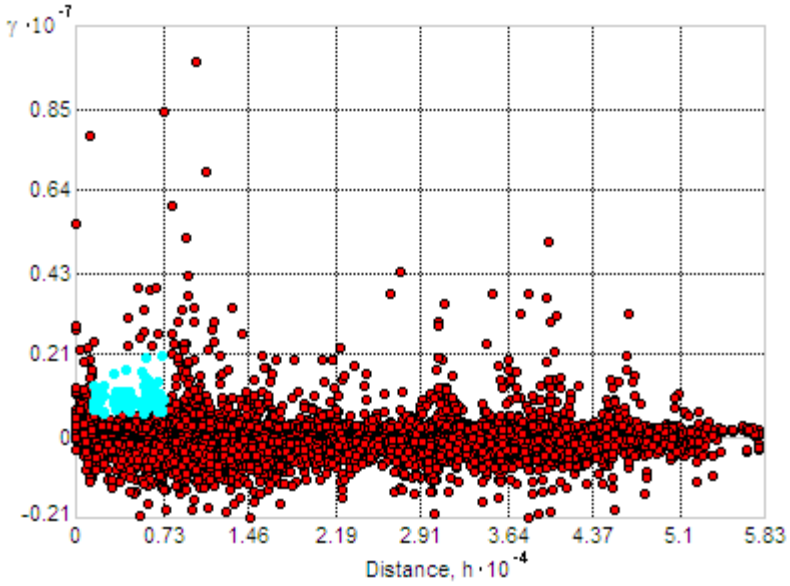
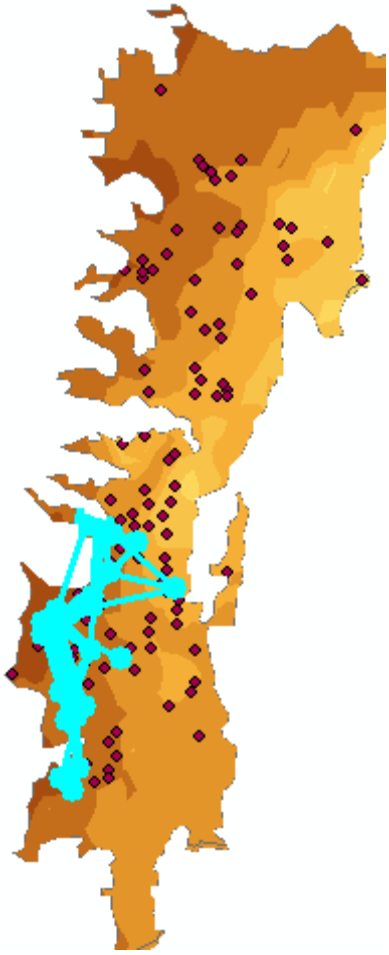


Figure 42 cross variogram between transmissivity and Specific capacity



9.1.3.7 MAPPING TRANSMISSIVITY

The data sets are explored with semivariogram and crossvariogram and are checked for directional influences and the presence of global trends, and are verified with QQ plots and histograms to understand the normality and distribution of the data sets respectively in the above section. Therefore those observations are incorporated and improved in the final map (Fig 44.)

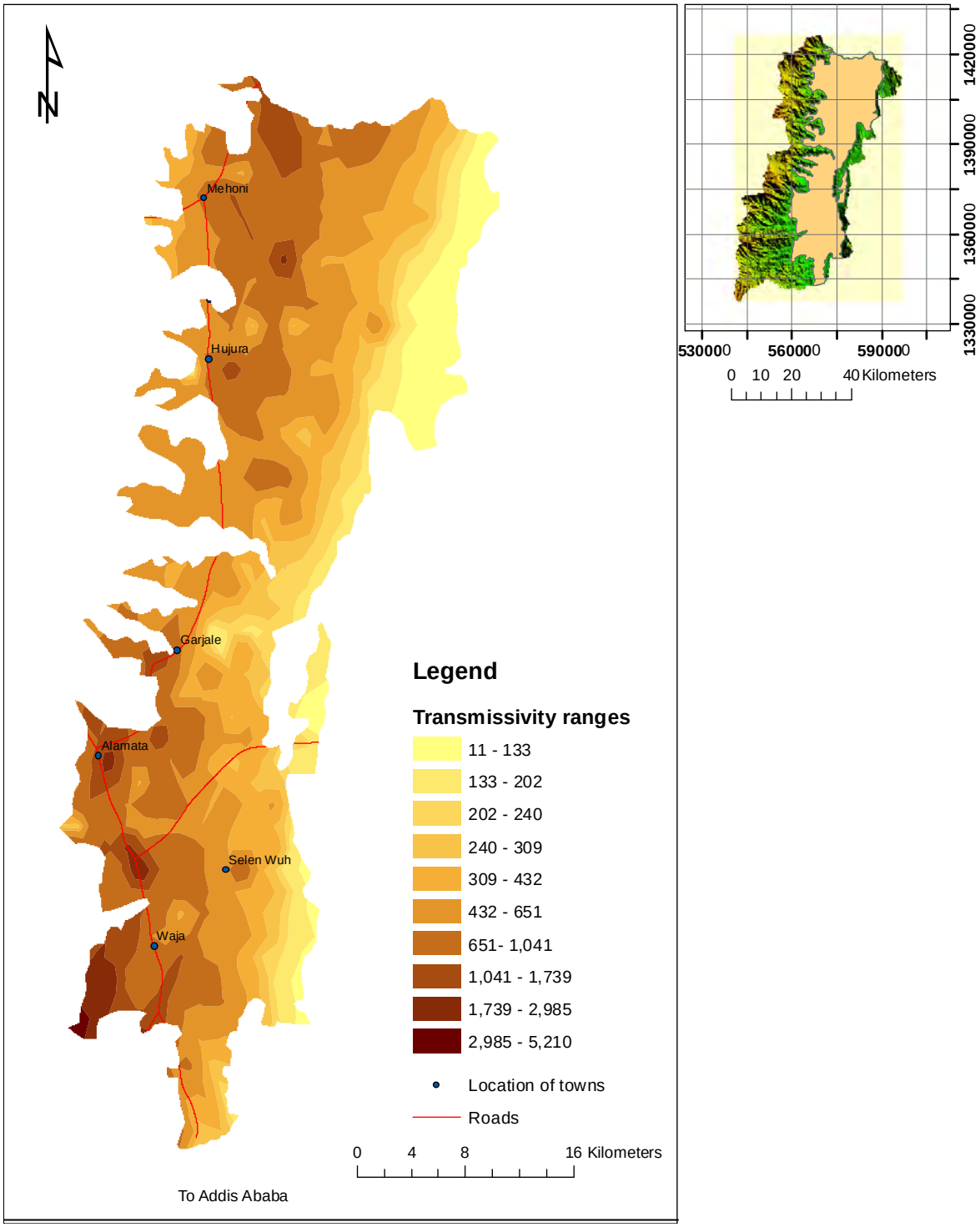


Figure 43 Predicted Transmissivity map of the study area

9.1.3.8 MODEL COMPARISON

Two interpolated maps are created and compared. The best map which provides the best prediction of the unknown values is selected. The first interpolated map of transmissivity is created directly with the default parameters in ArcGis 9.3 with a regression function of T = 0.100Sc + 533.876 with the following prediction errors: mean = -25.78, root mean square = 739, average standard error 795.1, mean standardized = -0.03214 and root-mean-square standardized = 0.9305 from a total sample of 135 pairs of transmissivity and specific capacity using the default spherical model. The final map of transmissivity is created after passing through the exploration phase with a regression function of T = 0.631Sc + 217.926 with the following prediction errors: mean = 4.627, root mean square = 540.6, average standard error 654.7, mean standardized = 0.006123 and root-mean-square standardized = 0.9437. Therefore based on the mean error, RMS, average standardized error, mean standardized error and RMS standardized error the final map has reduced error parameters therefore it has a relatively improved prediction of transmissivity from specific capacity and it is fit with a circular model.

9.1.3.9 CROSSVALIDATION RESULT FOR TRANSMISSIVITY

The cross validation between the measured and predicted values of transmissivity are done in Geostatistics by removing the measured values of all points and predict the transmissivity of these locations based on the other predicted values

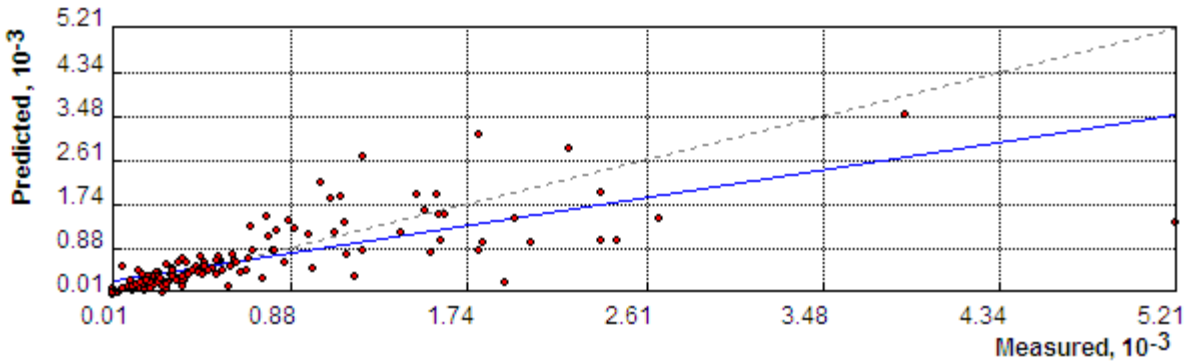


Figure 44 cross validation result for transmissivity

The predicted values of transmissivity may range as large as a factor of 1.5 to 5 orders of the measured transmissivity.

9.1.4.0 HYDRAULIC CONDUCTIVITY

The hydraulic conductivity is also treated by Geostatistical approach using ordinary kriging method and explored in the same manner as above after creating with the surface of hydraulic conductivity with default parameters in Arc GIs (Fig. 46)

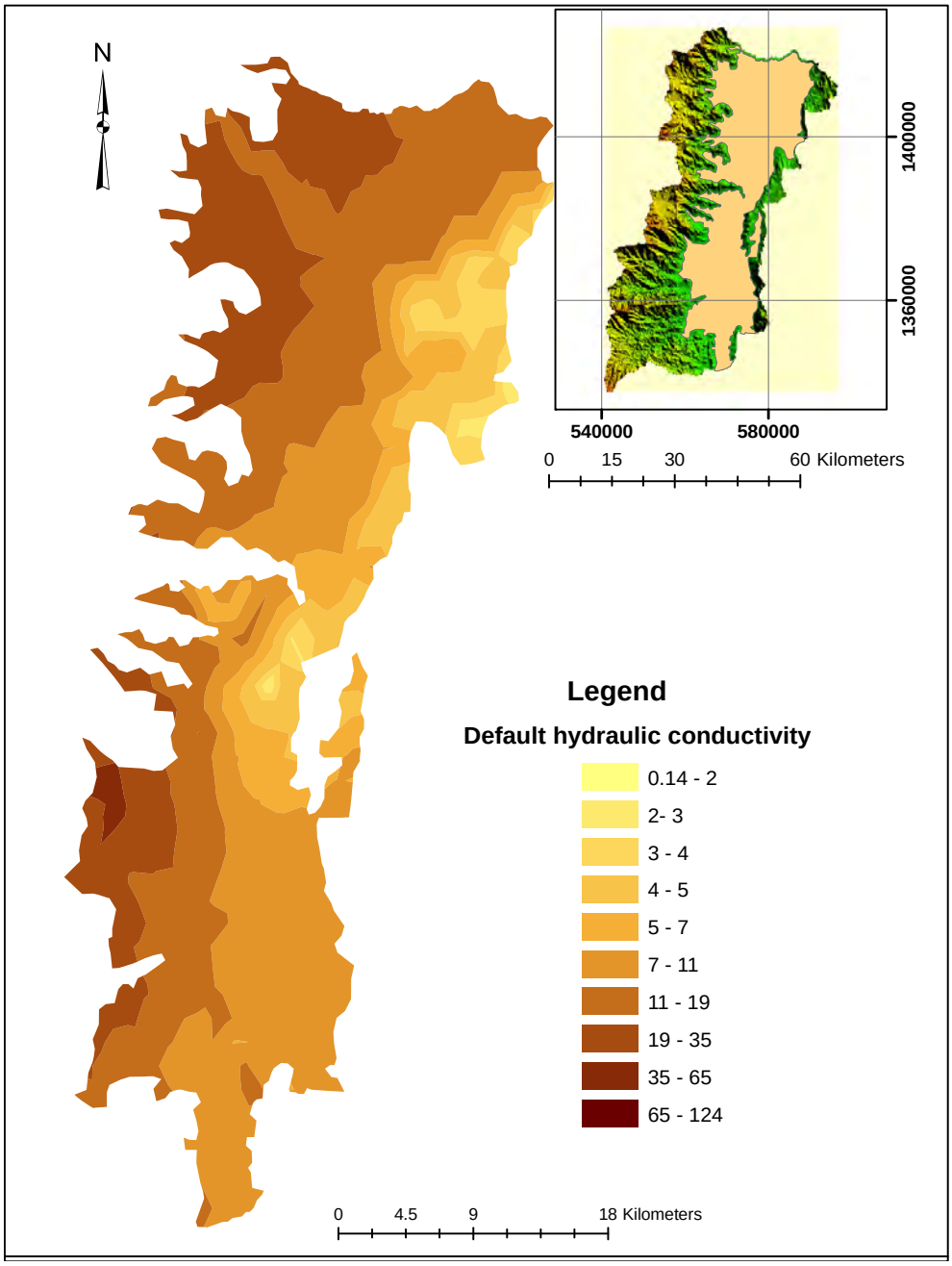


Figure 45 Default hydraulic conductivity map

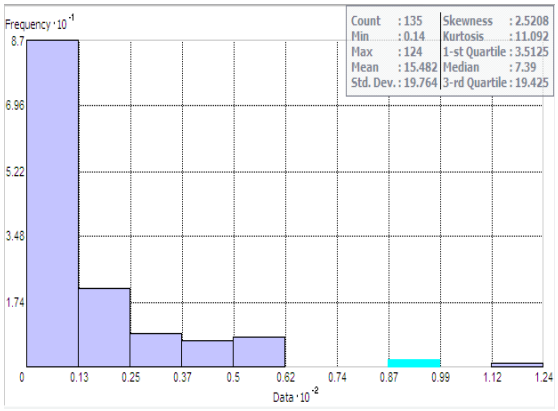


Figure 46 Histogram for hydraulic conductivity Skewed distribution



Figure 47 Hydraulic conductivity created by default Parameters in Arc GIS

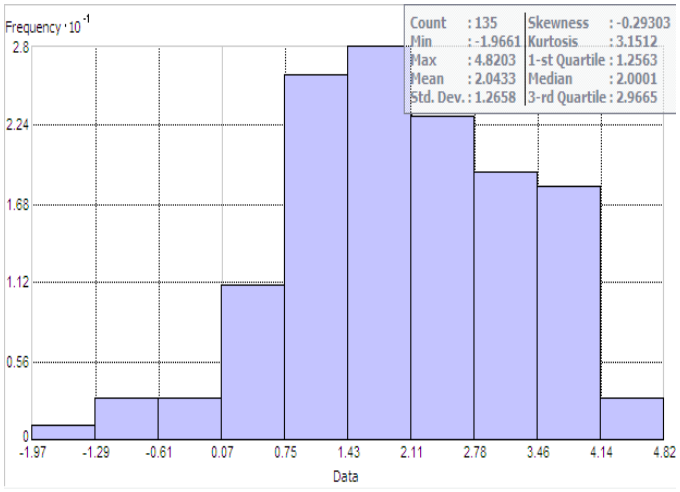


Figure 48 Histogram of hydraulic conductivity with normal distribution after log transformation

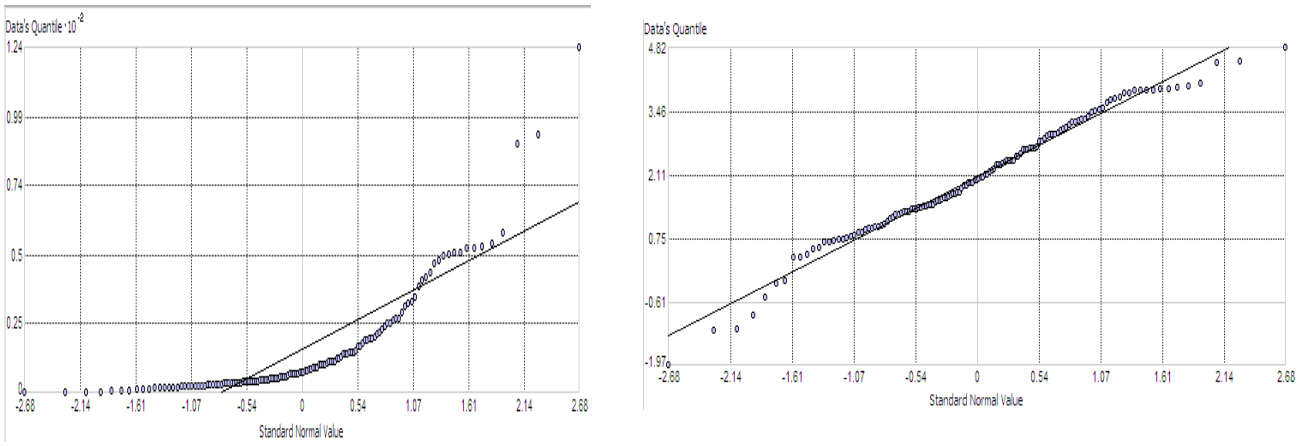


Figure 49 Quantile distribution plots before and after log transformation

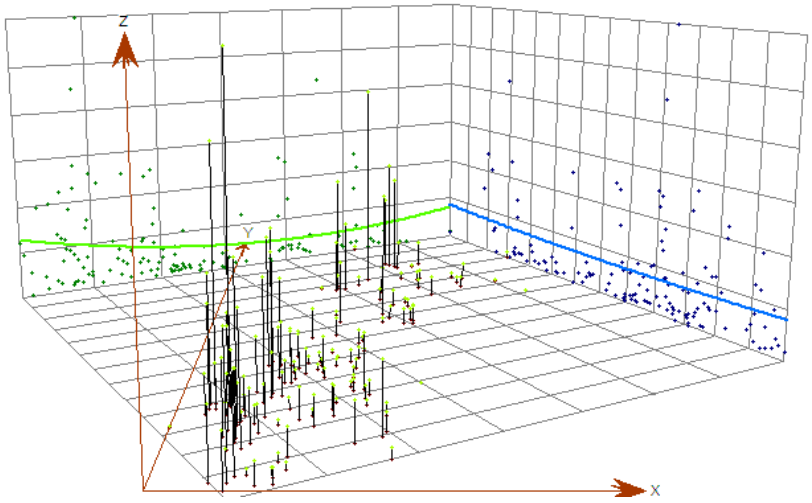


Figure 50 Trend Analysis plot for Hydraulic conductivity with a nearly u shape trend Identified in the E-W direction

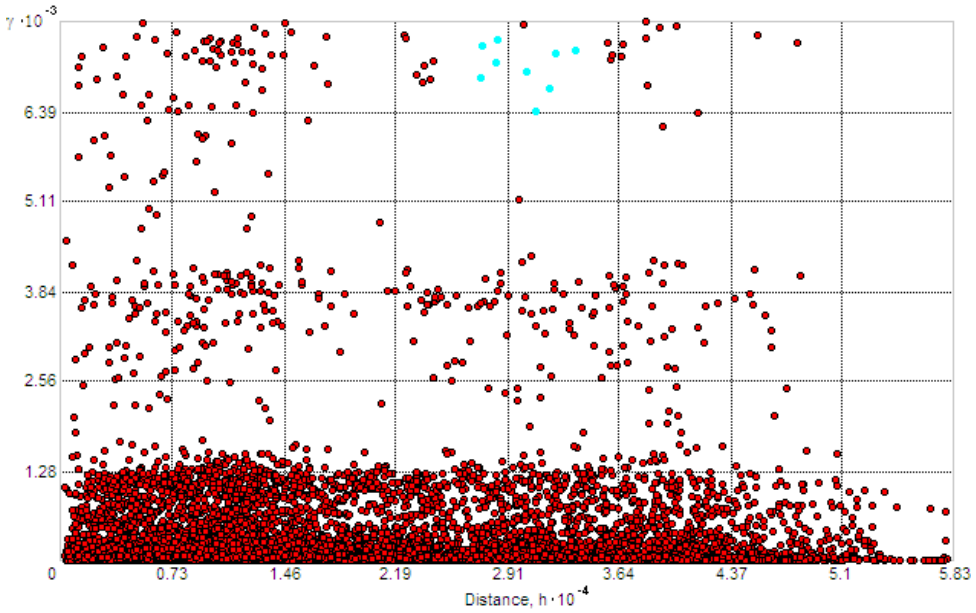


Figure 51 Semivariogram cloud for hydraulic conductivity showing 4 semi variance groups between hydraulic Conductivity pairs



Figure 52 Data pairs of hydraulic conductivity related with distant pairs

9.1.4.1 MAPPING HYDRAULIC CONDUCTIVITY

The data sets are explored with semivariogram and are checked for directional influences and the presence of global trends, and are verified with QQ plots and histograms to understand the normality and distribution of the data sets respectively in the above section. Therefore those observations are incorporated and improved in the final map.

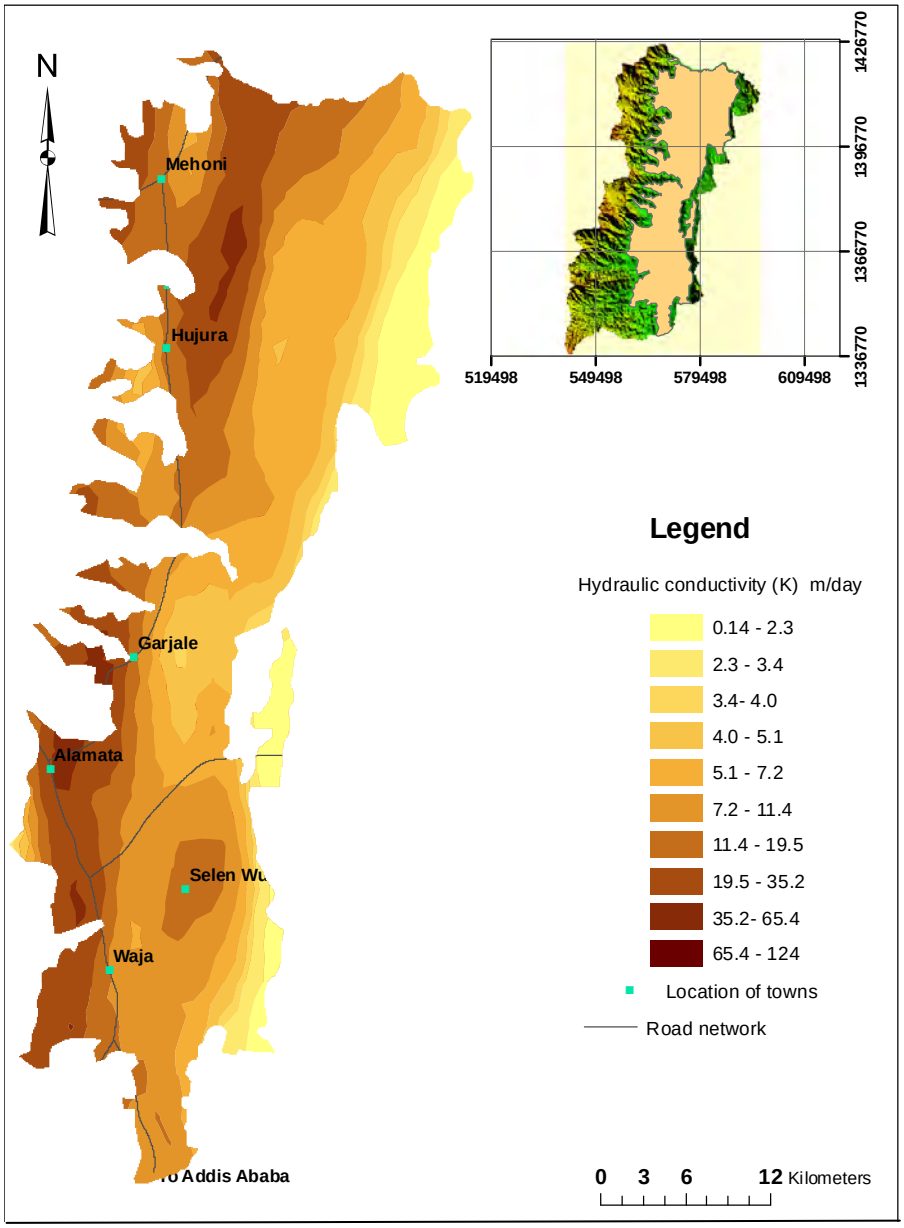


Figure 53 Predicted map of Hydraulic conductivity

9.1.4.2 MODEL COMPARISON

Two interpolated maps are created and compared. The best map which provides the best prediction of the unknown values is selected. The first interpolated map of hydraulic conductivity is created directly with the default parameters in ArcGis 9.3 with a regression function of $E_{stimated} = 0.105K_{measured} + 525.597$ with the following prediction errors: mean = -30.24, root mean square = 734.2, average standard error 796.3, mean standardized = -0.0376 and root-mean-square standardized = 0.923from a total sample of 135 hydraulic conductivity data Fig. The final map of hydraulic conductivity is created after passing through the exploration phase with a regression function of $E_{stimated} = 0.208K_{measured} +9.007$ with the following prediction errors: mean = 0.001127, root mean square = 22.95, average standard error 23.78, mean standardized = -0.1941 and root-mean-square standardized = 1.1. Therefore based on the mean error, RMS, average standardized error, mean standardized error and RMS standardized error the final map has reduced error parameters therefore it has a relatively improved prediction of hydraulic conductivity from measured hydraulic data and it is fit with a circular model and interpolated by ordinary kriging.

9.2 ESTIMATING TRANSMISSIVITY FROM BOREHOLE YIELD

Transmissivity can also be estimated from the empirical relationship between transmissivity and borehole yield data; although the quality of yield data are relatively lower than specific capacity and transmissivity data due to different cases they can be helpful to be a fair indicator of aquifer productivity in the absence of transmissivity and specific capacity. To establish an empirical relationship between transmissivity and discharge rate 50 pairs of transmissivity and discharge rate data measured from the same borehole. The bore yield data are those used in the constant rate pumping test.

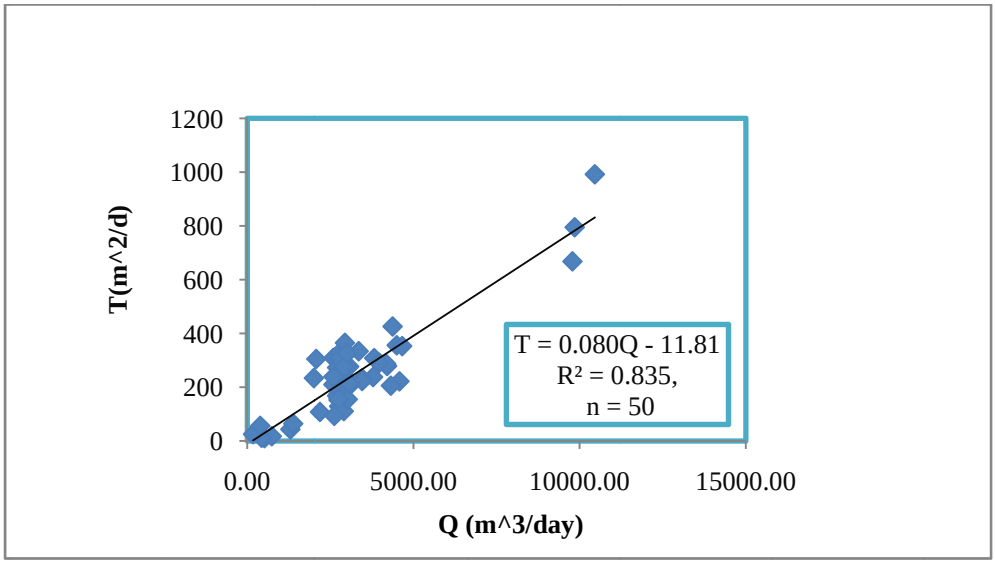


Figure 54 Empirical relationship between Transmissivity and discharge rate with linear fit

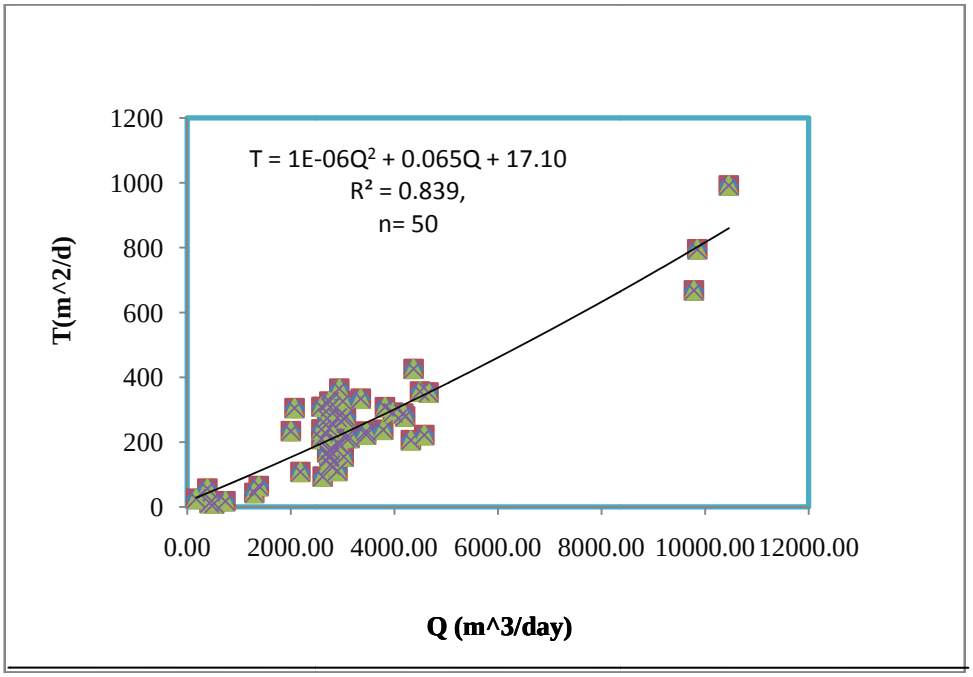


Figure 55 Empirical relationship between Transmissivity and discharge rate with polynomial fit

10.0 GEOPHYSICAL DATA ANALYSIS

10.1 VERTICAL ELECTRICAL SOUNDING

Direct resistivity sounding can be used to map the vertical and horizontal resistivity distribution in an area and it can also be applied to predict the aquifer hydraulic parameters in areas without available well information; stated another way it can be used to extrapolate pumping test information to an area.

The theory of and mathematical expressions used for exploration of groundwater by geolelectrical methods are well established (e.g. Bhattacharya and Patra, 1968; Koefoed, 1979; Keller and Frischknecht, 1966) (Cited in hessed 2-917) pp920. The Schlumberger array method of Vertical Electric Sounding (VES) has been applied both for obtaining the electrical resistivity distribution of the unconsolidated aquifers in the Raya valley and for extrapolating pumping test analysis results to areas with no well information; for this purpose 25 vertical electrical sounding raw data are analyzed using win resist v 1.0 and IPI2Win (Lite) v 3.0 softwares using the iterative and automatic inversion techniques after dividing the study area in to representative 6 sections. The selected sections have boreholes and VES conduced nearby them. The VES points have a spread length of 500 to 750 meters. So it is assumed this separation could investigate deeper levels.

The depth of investigation in a Schlumberger sounding conFiguration typically varies between 0.25 AB to 0.5 AB (Roy and Elliot, 1981) (Cited in hessed 2-917 pp 920

Mathematically, electrical current flow (*J*) in a conducting medium is governed by Ohm's law and groundwater flow in a porous medium Darcy's law, both having similar forms of equation:

$J = -\sigma \, dv/dr$ and $q = -kdh/dr$

Where *J*, V, *r*, *q*, *K*, *h* are respectively the current density (amps per unit area), electrical conductivity (Siemens/m = reciprocal resistivity, ohm m or Ωm), electrical potential (volts), distance (meters), specific discharge (discharge per unit area), hydraulic conductivity (or

permeability; m/s) and hydraulic head (m). The analogy between these two macroscopic phenomena is widely accepted (Freeze and Cherry, 1979; Fitts, 2002).

If a prism of homogeneous and isotropic aquifer material having a unit cross-sectional area and thickness h, Q = KIA (from Darcy's law and J = σE from Ohm's law, can be combined to get T = KσR = KS/σ Niwas and Singhal (1981) (cited in Ekwe and others, 2006) pp123, Tirzo and Salehzade) pp8.

Where T = Aquifer transmissivity

R = Transverse resistance of the aquifer

S = Longitudinal conductance

The parameters R and S are commonly called Dar- Zarrouk parameters and are designated by S = h/ρ and R = hρ where h and ρ are the thicknesses and resistivities of the individual layers (Ersc 731)

In areas of similar geologic setting and water quality, the product, Kσ remains fairly constant (Niwas and Singhal, 1981. Thus knowing K values for existing boreholes and σ values extracted from the sounding interpretation for the aquifer at borehole locations, it has been possible to determine transmissivity and its variations from place to place, including those areas without boreholes.

Thus, the electrical method provides a powerful analogue and tool for groundwater exploration and modeling.

10.1.1 DATA PROCESSING

There are around 200 VES data out of which 25 VES which were taken nearby boreholes are selected for this purpose. Accordingly the study area is divided in to 7 geolelectrical groups. Each group is characterized by a representative geo electric section containing 3-5 VES points. The geo electric sections are fairly distributed starting from Waja town southern part of the study area through Alamata, Gerjale, Kara, Kukuftu and Mehoni areas northwards. For each section, based on the information of lithological logs of boreholes drilled in the area the geolelectrical layers are identified on the basis of single VES points analysis and correlation with the hydrolithologic units. The whole subsurface layers are categorized in to 4 major groups; the top layer, the unsaturated zone, the saturated horizon

and the bed rock. This approach is applied during the construction of geoelectric sections, because the hydro lithologic units in the study area have an alternating nature of the water bearing and non water bearing formations creating a number of inter layered groups. This is the most difficult part of the interpretation i.e. considering each water bearing and non water bearing layers for calibration; because most of the geophysical softwares consider the minimum number of layers or the least error (error reduction approach). Therefore due to this draw back the minimum number of layers approach is employed for the interpretation yielding the average aquifer resistivity at the VES locations, however, this has resulted in an over estimated electrical thickness. Therefore based on borehole log data calibration the VES data are again interpreted by iteration process using Win Resist version 1.0 and Ipi2win geophysical data processing softwares. The former software is employed after establishing initial model parameters based on borehole lithological data. The 2nd software is employed for automatic preliminary analysis of the VES data to get a knowhow on the distribution of subsurface resistivity parameters. Then the final layer parameters are determined iteratively with the least fitting error (2-3%) using win resist 1 software. The Ipi2win software is also employed for some of the VES data using automatic inversion method with least number of layers and least fitting error. In both interpretation methods some parameters like depth are fixed according to the real subsurface information obtained from borehole litho logs Annex 5.

10.1.2 INTERPRETATION AND CALIBRATION

The processed VES data are interpreted and calibrated based on borehole lithological data at or near the VES locations. The interpretation and calibration of VES LV72 Fig 58 and borehole RPW-021 Fig. 59 shows a good agreement between the observed and calibrated and interpreted data Table 12.

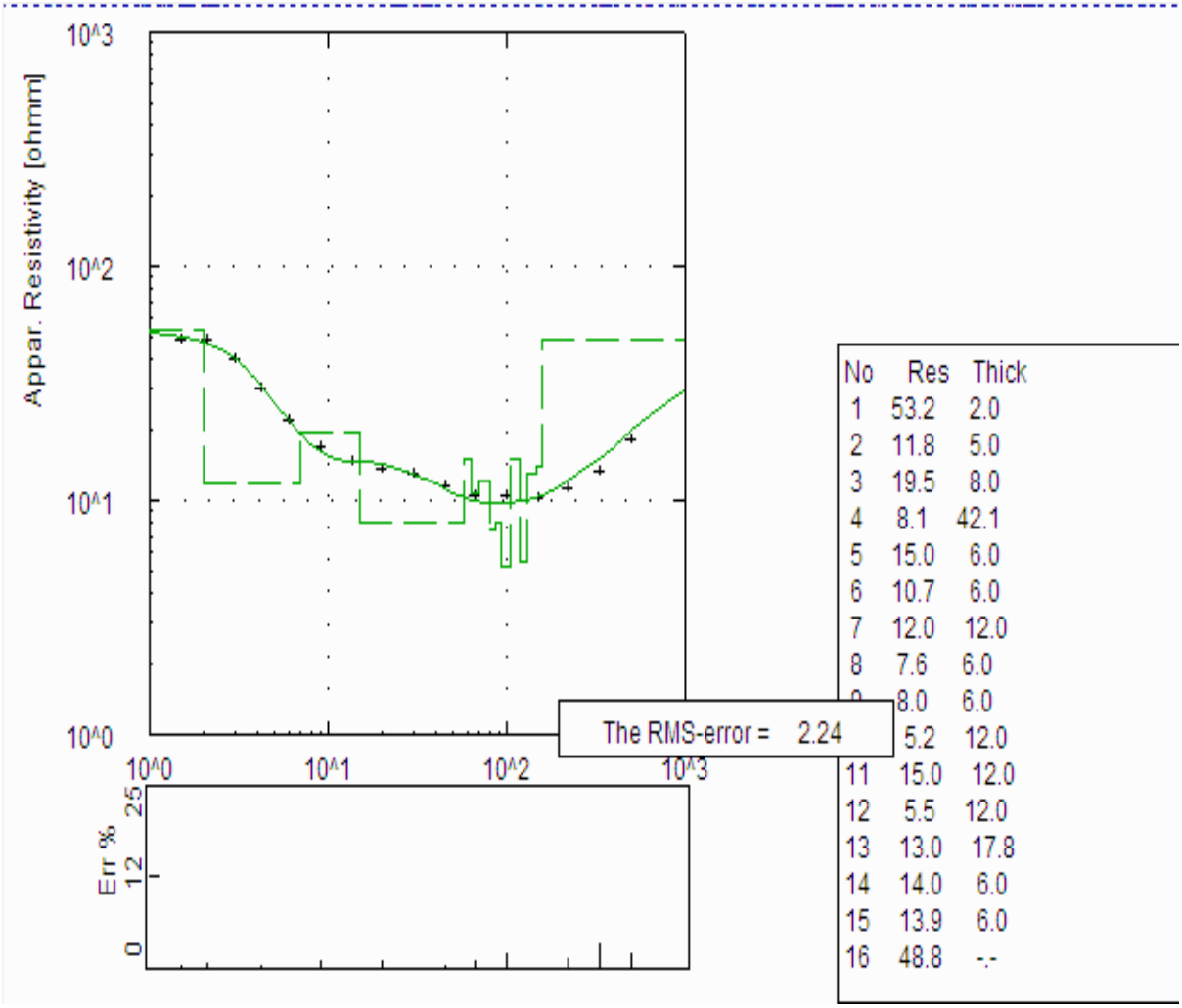


Figure 56 VES LV72 for BH RPW-021

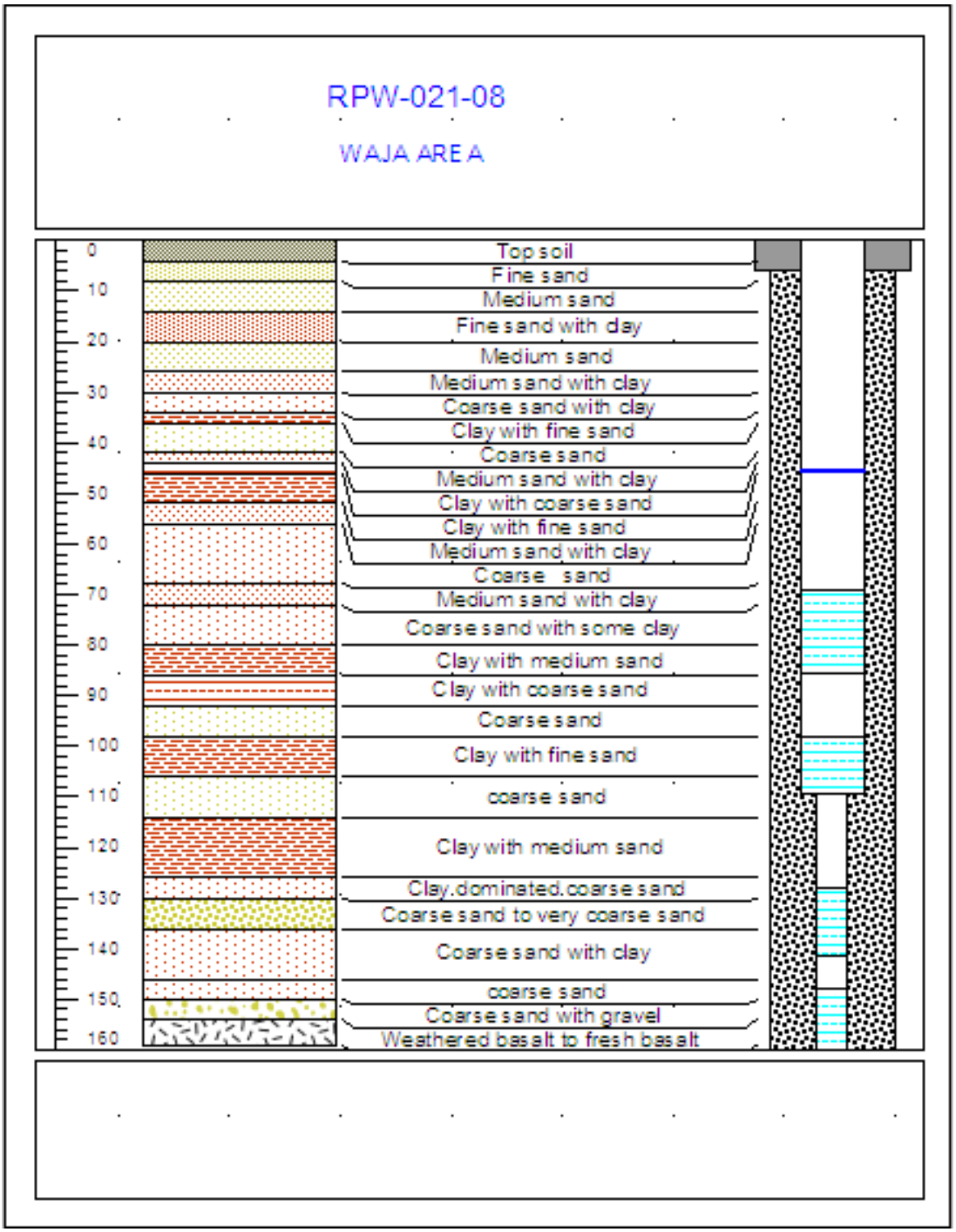


Figure 57 Borehole lithological log of RPW-021

Well data			VES data		
No.	Depth (m)	Lithologic Description	Resistivity (Ωm)	Depth(m)	Interpretation
1	0-4	Top soil	53.2	0-2	Dry top soil
2	4-8	Fine Sand	11.8	2-7	Dry fine sand
3	8-14	Medium Sand	19.5	7-15	Dry medium sand
4	14-56	Fine, medium to coarse sand with Clay	8.1	15-57.1	Dry fine, medium to coarse sand with clay
5	56-68	Coarse sand	15.0	57.1-63.1	Saturated coarse sand
6	68-72	Medium to coarse sand	10.7	63.1-69.1	Saturated medium to coarse sand
7	72-80	Coarse sand with some clay	12	69.1-81.1	Saturated coarse sand with
8	80-86	Clay with medium sand	7.6	81.1-87.1	saturated
9	86-92	Clay with coarse sand	8.0	87.1-93.1	saturated
10	92-106	Clay with fine sand and coarse sand	5.2	93.1-105.1	saturated
11	106-114	Coarse sand	15.0	105.1-117.1	saturated
12	114-130	Clay with medium sand and clay dominated coarse sand	5.5	117.1-129.1	saturated
13	130-146	Coarse sand to very coarse sand and coarse sand with clay	13.0	129.1-146.9	saturated
14	146-150	coarse sand	14.0	146.9-152.9	saturated
15	150-154	Coarse sand with gravel	13.9	152.9-158.9	Saturated coarse sand with gravel and weathered basalt
16	154-159	Basalt	48.8	∞	Massive basalt

Table 12 Calibration of VES LV72 based on lithological log of BH RPW-021 Waja area.

10.2 GEO ELECTRICAL INVESTIGAION

The primary purpose of resistivity method is primarily to measure the potential differences on the surface due to the current flow in the subsurface and therefore to have a relative estimation of the area's hydraulic parameters (porosity and water distribution e.t.c.)

All the selected geolelectrical soundings have a current electrode separation of 500-750 meters. In order to visualize the subsurface resistivity distribution and variation with respect

to depth and spatially 7 geo electrical sections are constructed having in mined to cover the whole area extent. In addition to these all the selected VES points for the construction of geoelectric sections are taken at borehole locations in order to take the advantage of calibration Fig 60.

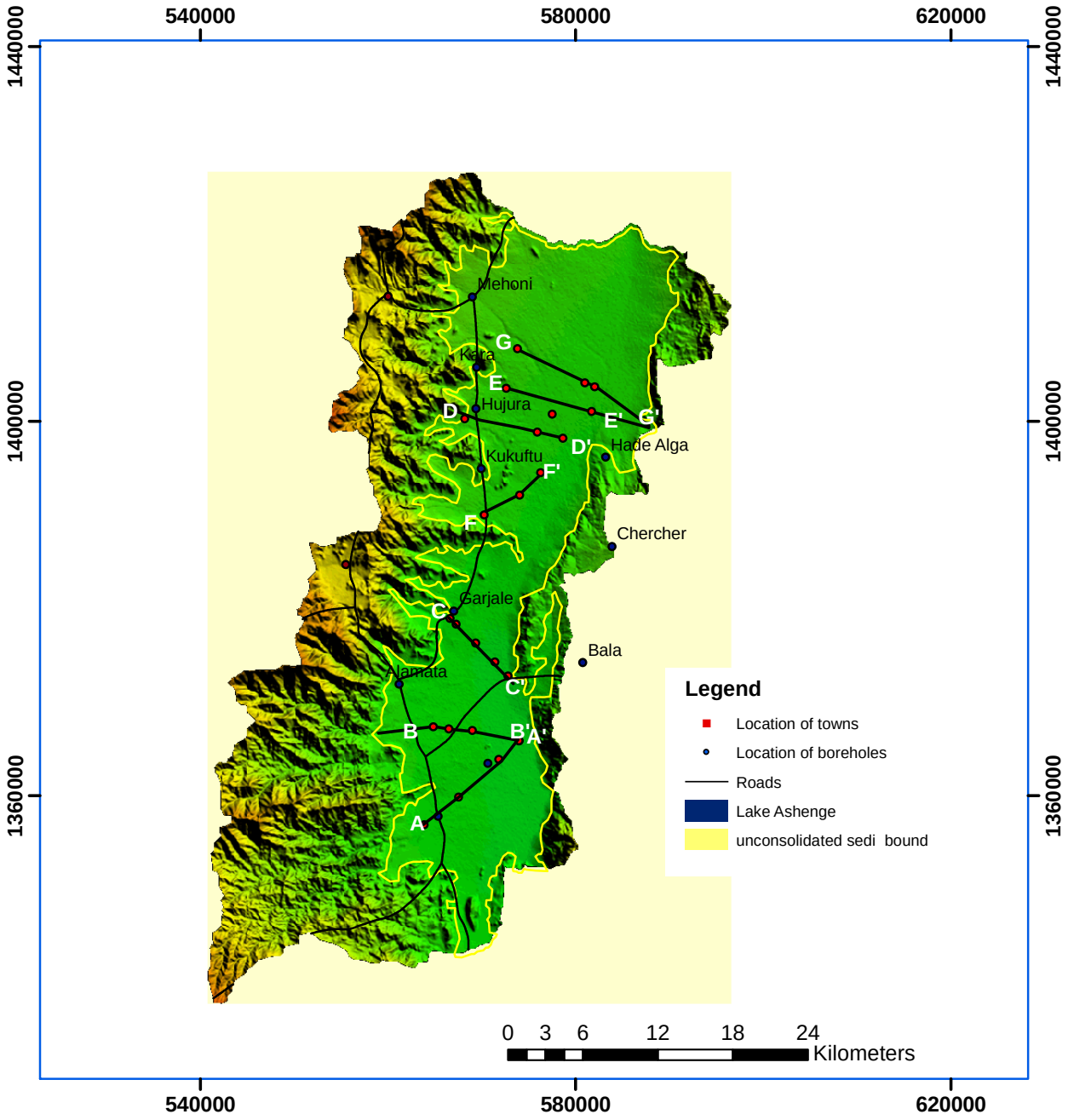


Figure 58. Location map of boreholes and VES points

N.B. In all the geoelectric cross sections clay layers are not included because they are not Mappable with the specified scale, besides hey are no more aquifers.

10.2.1 Geo-electrical section Waja area along A-A' (SW-NE)

From this Geoelectric section (Fig. 61) 4 layers are identified. The top most layer of the section is composed of undifferentiated top soil with a thickness of 2-4meters. The 2nd layer is characterized by dry fine, medium to coarse sand with clay content increasing northeast wards. This layer has a thickness of 43-75 meters and the maximum thickness is observed at BH RPW-093 location (VES RV3). This layer is underlain by the saturated zone which is composed of inter beds of fine, medium to coarse sand and clay. In this layer the southeastern part of the section is purely sand, however northeast wards the clay containing beds dominate. The thickness of this layer ranges from 53-88m, where the maximum thickness is observed at VES location LV64 (BH RPW-082) and at the central part.

10.2.2 Geo-electrical section Alamata area along B-B' (W-E)

In this geo-electrical section also 4 layers are identified Fig 62. The top layer of the section is composed of 4-2 meters thick top soil. The second layer is composed of dry fine to coarse grained sand and has a thickness of 32-78 meters. This layer is underlain by the saturated horizon which is dominantly composed of coarse sand to gravel and pebble in the western part of the section BH RPW-074 (VES LV52) and fine to medium and coarse sand with clay inter beds in the remaining part of the section. The coarsening of grain size is observed towards west and depth wise. However, the maximum thickness of unconsolidated sediments can be seen in the eastern part of the section. The basaltic bed rock is encountered at all VES stations forming an undulating subsurface topography, with depressions at BH locations RPW-081 and RPW-082 where relatively thick sediments are accumulated. These subsurface undulations could be results of faulting with an orientation of N-S and dipping to the east.

10.2.3 Geo-electrical section Gerjale area along C-C' (NW-SE)

In this geo-electrical section 4 layers are identified Fig.63 The top layer of the section is composed of 1-6 meters thick top soil. The second layer is composed of dry fine to coarse grained sand where coarse deposits are found in the north western part of the section at BH

RPW-031 and fine, medium to coarse sand towards south east. This layer has a thickness of 53-62.8 meters. It is underlain by the saturated horizon which is dominantly composed of coarse sand to gravel, pebble and boulder with inter beds of clay in the north western part of the section BH RPW-031 (VES LV52) and fine to medium and coarse sand with some clay in the central part of the section and inter beds in the remaining part of the section. The south eastern tip of the section at RPW-042 there are inter beds of medium to coarse sand, gravel and clay. Coarsening of grain size is observed towards North West and south east and depth wise. However, the maximum thickness of unconsolidated sediments can be seen in the north western direction between boreholes RPW-031 and RPW-054 and towards south eastern part at BH location RPW- 063. The basaltic bed rock is encountered at all VES stations forming an undulating subsurface topography, with depressions at BH locations RPW-054 and RPW-063 where relatively thick sediments are accumulated. These subsurface undulations could be results of faulting with an orientation of NE-SW and dip direction towards south east.

10.2.4 Geo-electrical section Hujura area along D-D' (WNW-ESE)

From this Geoelectric section (Fig.64) 4 layers are identified. The top most layer of the section is composed of undifferentiated top soil and clay with a thickness of 2-14meters. The 2nd layer is characterized by dry fine, medium to coarse sand with some clay. This layer has a nearly proportional thickness with an average of 51 meters. This layer is underlain by the saturated zone which is composed of inter beds of coarse sand, gravel and boulder in the WNW and ESE part of the cross section, however the ESE area is characterized by inter beds of clay; and the middle part of the section is composed of clay dominated fine to medium sand and gravel. The thickness of this layer ranges from 25-102m, where the maximum thickness is observed at VES location RV-75 (BH RPW-028). The depth to bed rock and thickness of unconsolidated sediments increases towards ESE

10.2.5 Geo-electrical section Kara area along E-E' (NW-SE)

In this Geo-electric section 4 layers are identified (Fig 65). The top most layer of the section is composed of undifferentiated top soil with a thickness of 4-6 m. The 2nd layer is characterized by dry fine, medium to coarse sand with some clay. The thickness of this layer increases from NW to SE. This layer is underlain by the saturated zone which is composed of inter beds of coarse sand, gravel and boulder. This layer shows fining SE wards. The NW part of the section which is characterized by gravel to boulder materials is free of clay. The middle part of the section is composed of fine, medium to coarse sand, gravel and boulders highly dominated with clay inter beds, however the SE part of the cross section is characterized by fine, medium to coarse sand dominated by clay inter beds. The basaltic bedrock gets deeper towards the SE direction. Similarly the saturated thickness increases in the same direction. The variation of depth to bed rock along NW-SE could be the result of faulting with an orientation of NE-SW and dip direction towards SE. This fault might be responsible for the creation of depression in the SE part of the cross section which is down thrown.

10.2.6 Geo-electrical section Kukuftu area along F-F' (SW-NE)

In this geo-electrical section also 4 layers are identified Fig 66. The top layer of the section is composed of 4-6 meters thick top soil. The second layer is composed of dry fine to coarse grained sand and has a thickness of 50-70 meters. This layer is underlain by the saturated horizon which is dominantly composed of coarse deposits of sand to gravel and pebble in the south western part of the section BH RPW-026 (VES LV151) and medium to coarse sand with clay inter beds in the remaining part of the section. The coarsening of grain size is observed towards south west and depth wise. However, the maximum thickness of unconsolidated sediments can be seen in the north eastern part of the section. The basaltic bed rock is encountered at all VES stations forming a raised subsurface topography in the SW part of the section and a depression towards NE at BH RPW-034 location.

10.2.7 Geo-electrical section Mehoni area along G-G' (NW-SE)

The geo-electrical section along this line also contains 4 layers Fig 67. The top layer of the section is composed of 2-6 meters thick top soil. The second layer is composed of dry fine to coarse grained sand with some clay lenses towards south east and has a thickness of 58-65 meters. This layer is underlain by the saturated horizon which is dominantly composed of coarse deposits of gravel and pebble inter layered with fine sand in the north western part of the section BH RPW-007 (VES RV49) and coarse sand and gravel with clay inter beds in the central part of the section at BH RPW-012 and the remaining part of the section is characterized by medium to coarse grained sand dominated by clay. The coarsening of grain size is observed towards North West and depth wise. However, the maximum thickness of unconsolidated sediments can be seen in the south eastern part of the section at BH RPW-012 location. The basaltic bed rock is encountered at all VES stations forming a raised subsurface topography towards NW and a depression towards south east The variation of depth to bed rock along NW-SE could be the result of faulting with an orientation of NE-SW and dip direction towards SE. This fault might be responsible for the creation of depression in the SE part of the cross section which might be down thrown.

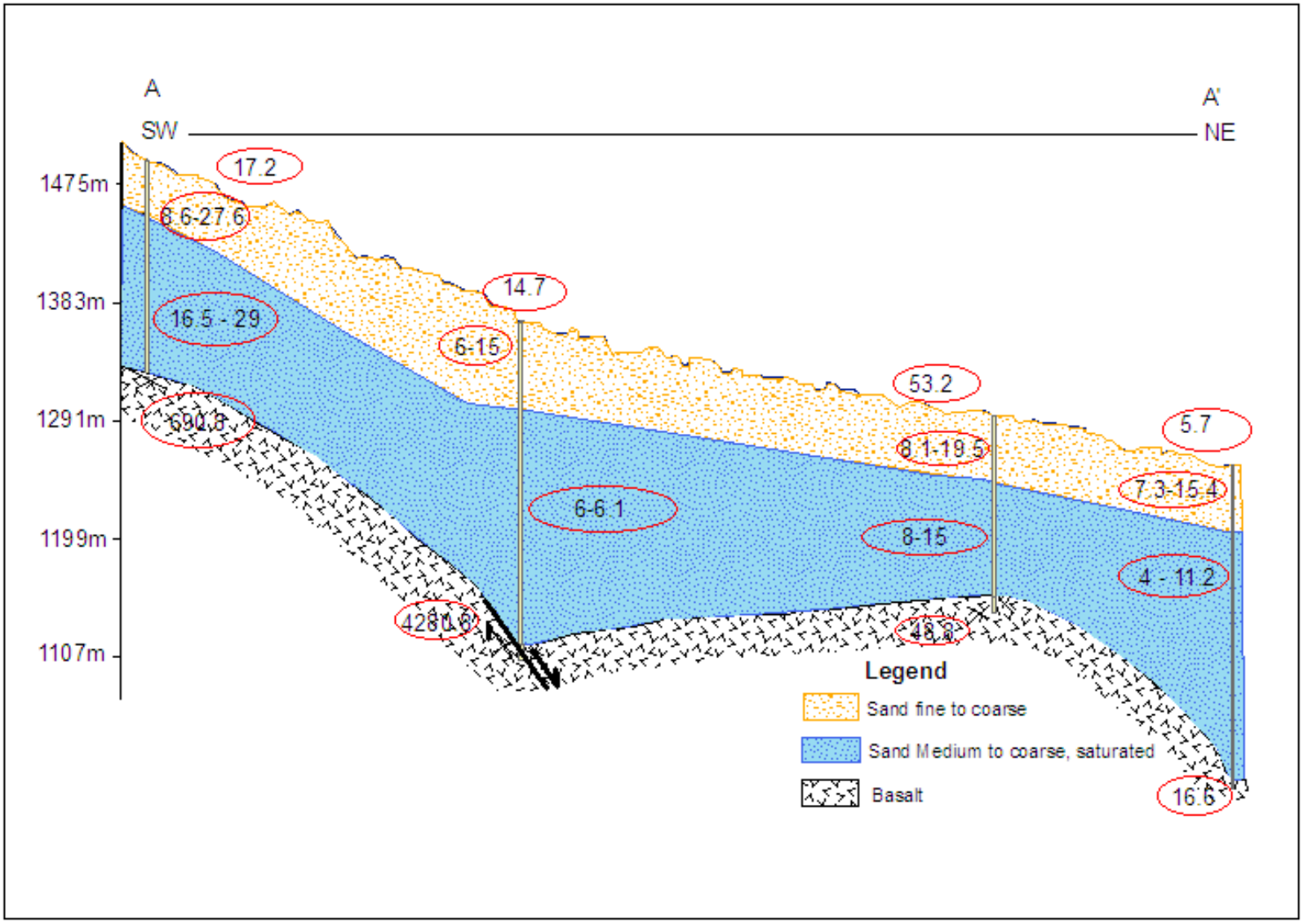


Figure 59 Geo-electric section Waja area along A-A'

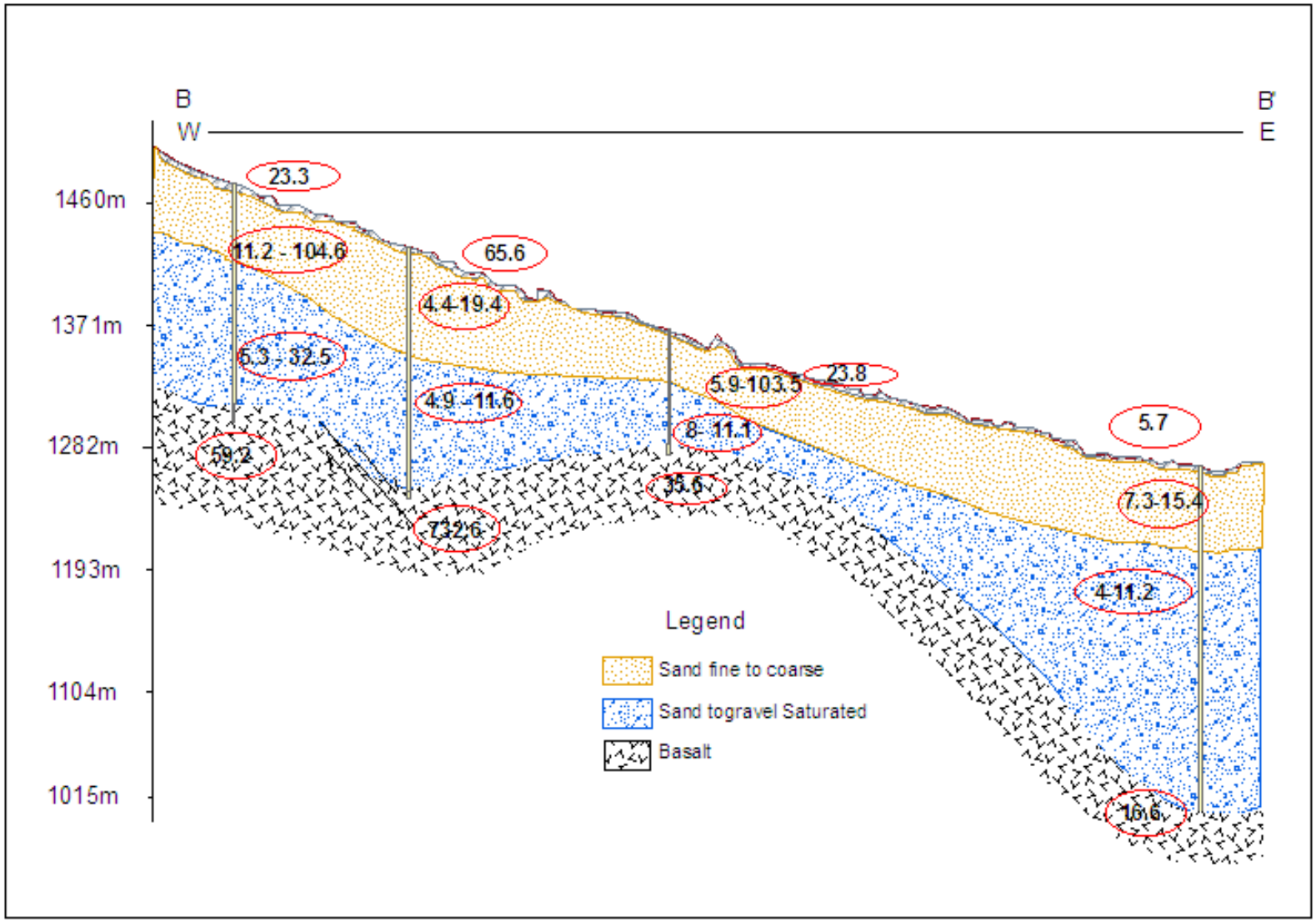


Figure 60 Geo-electric section Alamata area along B-B'

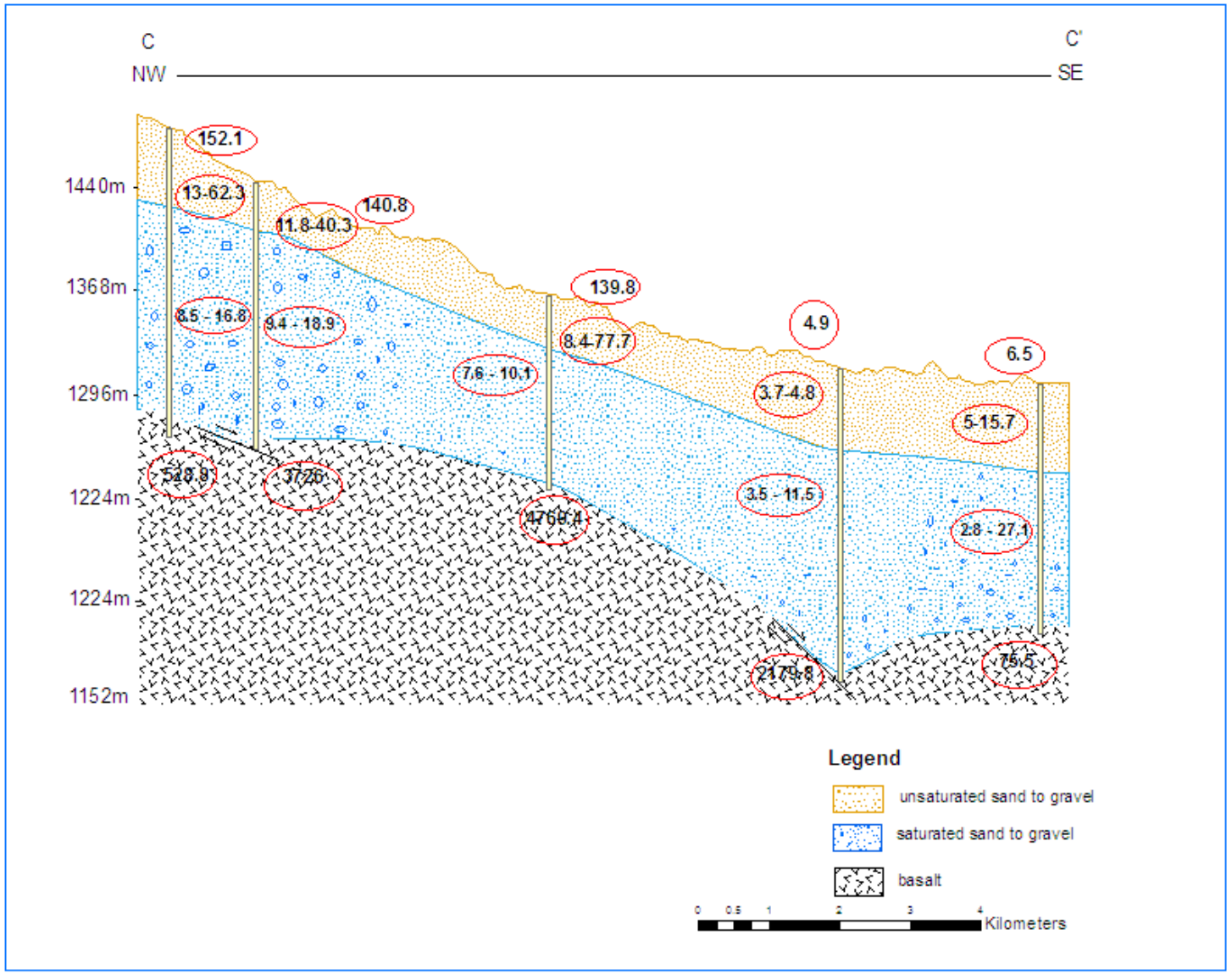


Figure 61 Geo-electric section Gerjelle area along C-C'

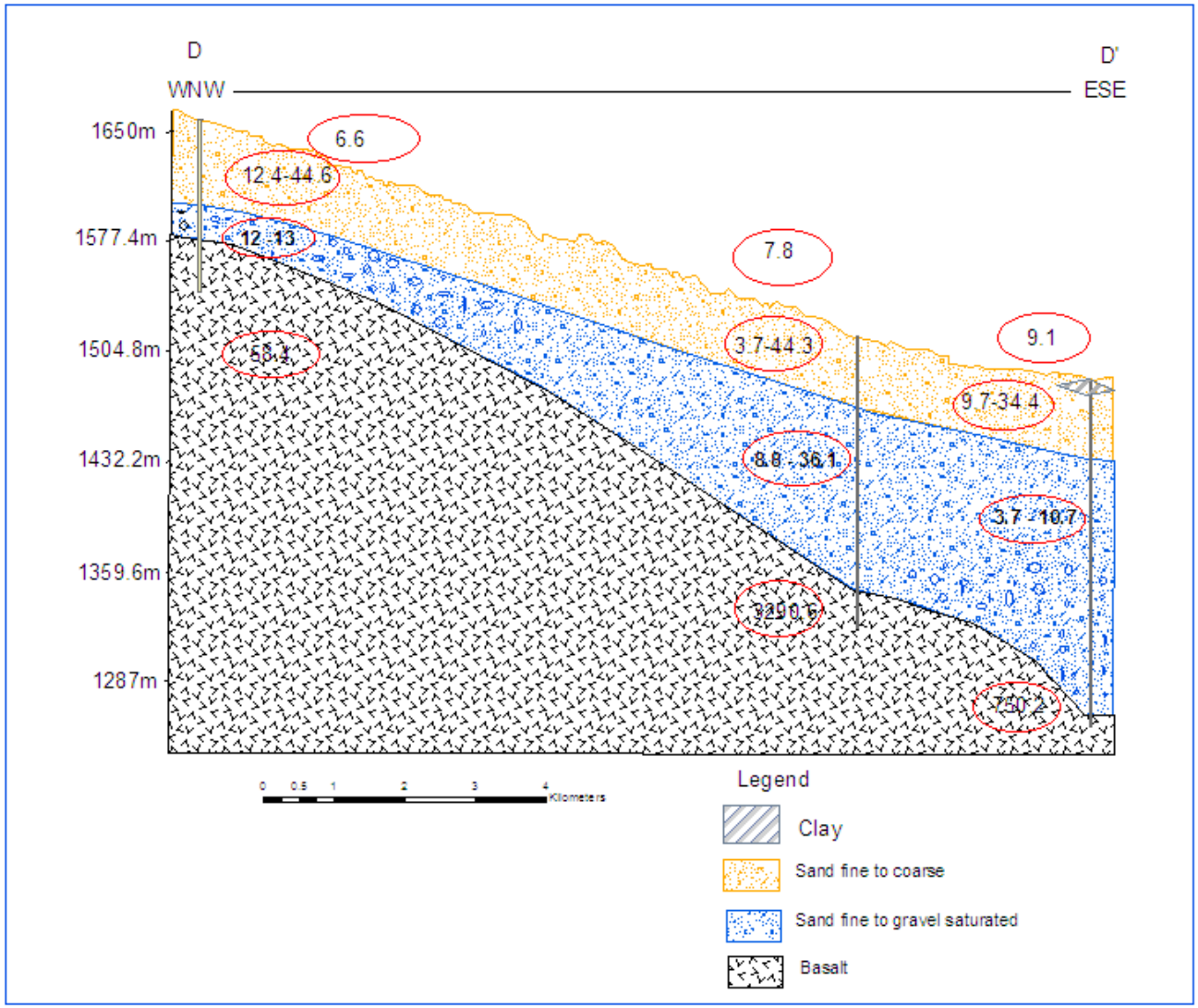


Figure 62 Geo-electric section Hujura area along D-D'

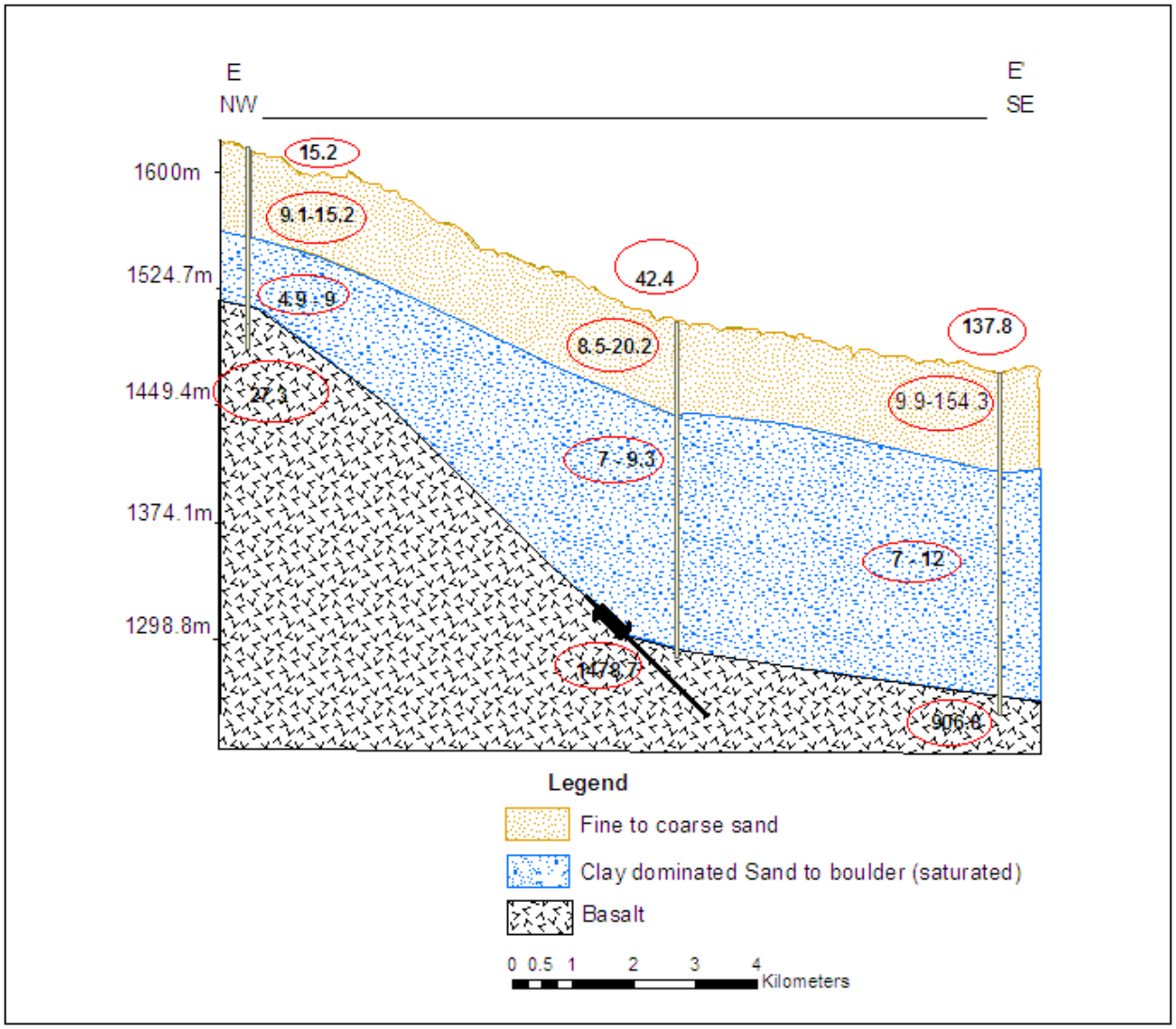


Figure 63 Geo-electric section Kara area along E-E'

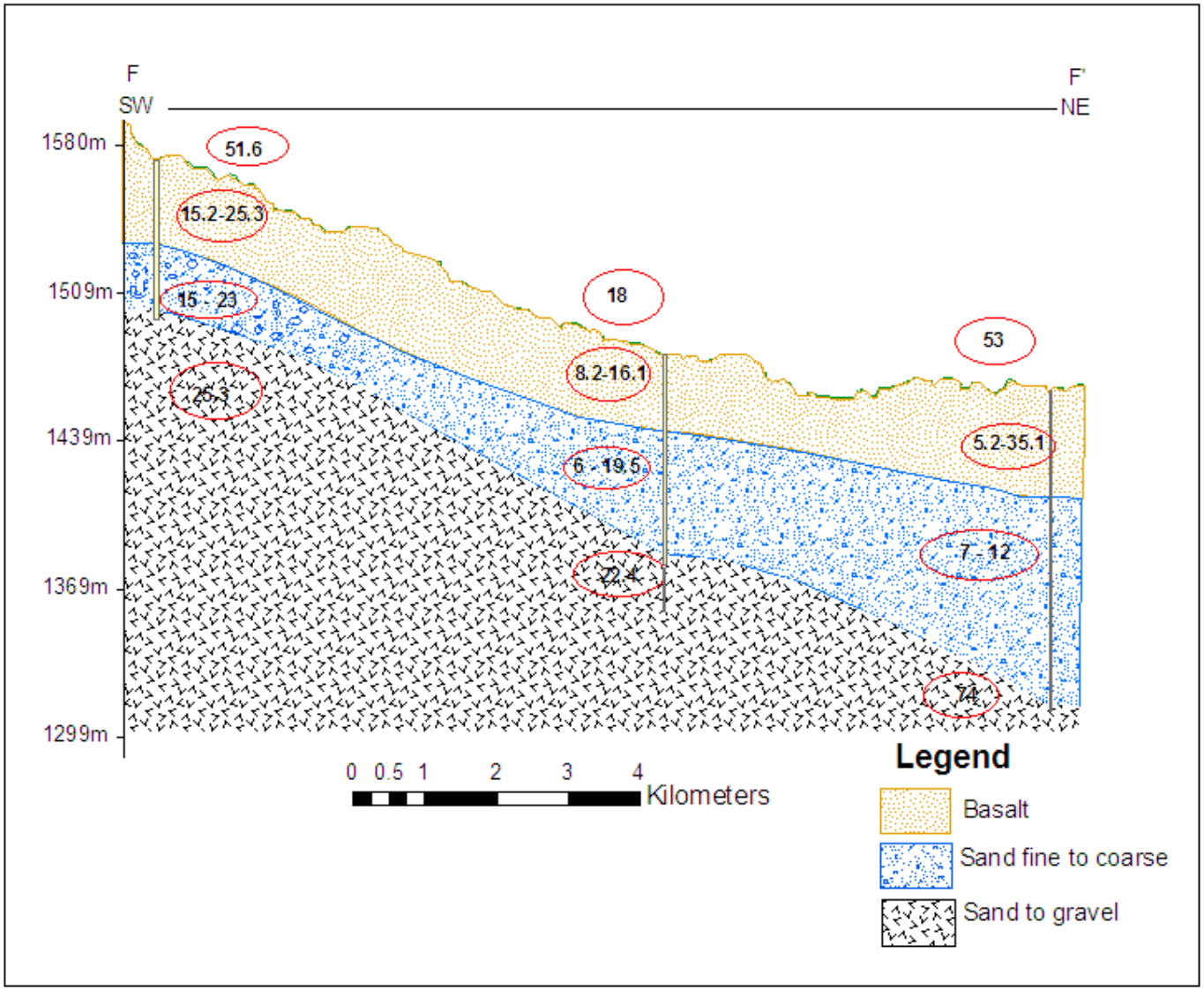


Figure 64 Geo-electric section Kukuftu area along F-F'

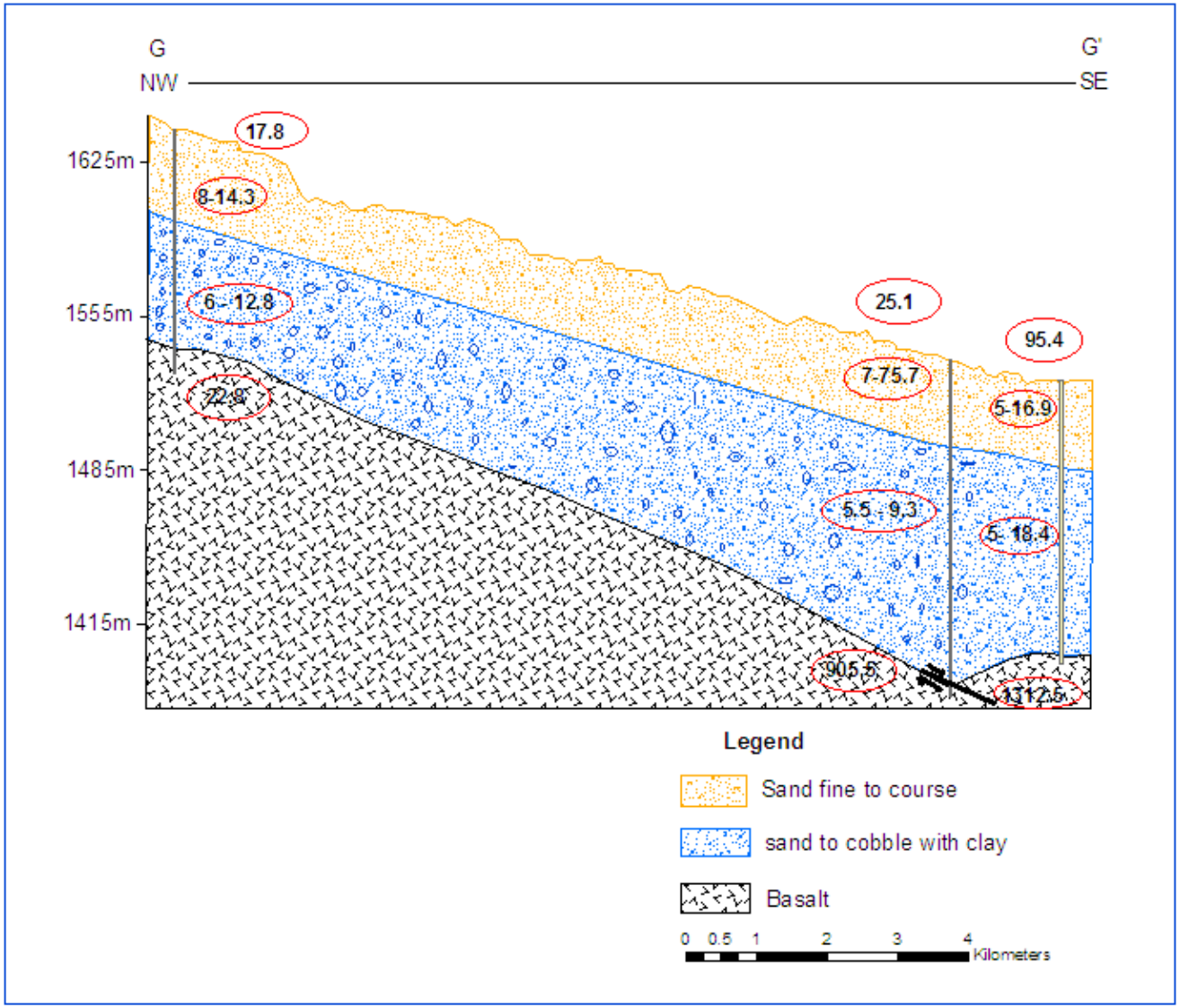


Figure 65 Geo-electric section Kukuftu area along F-F'

10.3 RESULTS OF THE GEOELECTRICAL INVESTIGATIONS

The geolelectrical cross sections discussed above helped to qualitatively visualize the distributions and variations of the resistivities of the unconsolidated sediments depth wise and laterally. The resistivity values of the unconsolidated sediments in Waja area Fig 61, Gerjelle area Fig 63 and Alamata area Fig 62 are observed to be low; this could be attributed to the existence of a relatively higher EC values Fig 68. In addition to this the dominancy of the clayey materials in these areas mainly in the central and eastern part in reference to the valley margins of these localities could also have a contribution to the lowering of the resistivity values. The higher EC values in these areas can also be confirmed by the ground water level map of the raya valley Fig 5. The ground water flow direction is generally from N-S and locally from E-W i.e. towards these areas. Therefore the high EC values are supportive to this reality. High EC values are observed closer to the surface water outlet and probably also the ground water out let. These areas which are characterized by high EC values are also characterized by for e.g. Gerjelle area by swamps which could have a contribution to high salinity, Alamata area is also closer to Gerjelle and Waja area is also characterized by near surface groundwater levels which might have an influence to salinity due to evaporation effects.

Based on all geo-electric cross sections the high resistivity values of the unconsolidated saturated formations could be related to the coarse deposits gravel to boulder size (18-36.1Ωm) and the intermediate value ranges to sand (fine to coarse grained) (10-17Ωm) and the very low resistivity ranges (2.8-10 Ωm) to clay and clay dominated sand to gravel mixes characterized by high EC values appendix 5

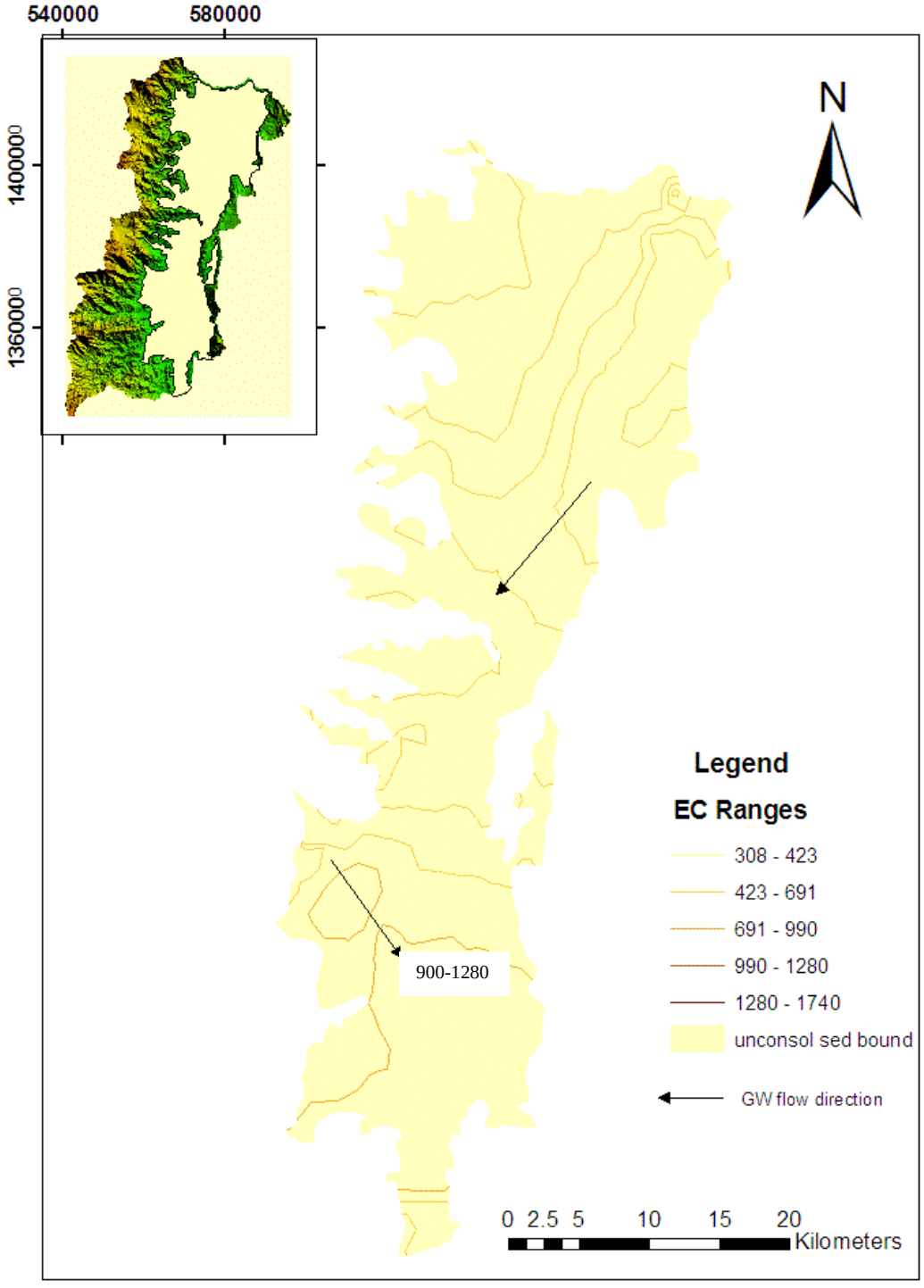


Figure 66 EC contours

10.4 EMPIRICAL RELATION BETWEEN TRANSMISSIVITY AND TRANSVERSE RESISTANCE

The area is characterized by a thick and prolific aquifer zone, tapped by many productive boreholes and wells. This is due to the composition of the aquifer zone, which consists of unconsolidated medium to coarse grained sands and gravel.

Calibration resistivity soundings, performed at wells where pumping tests were carried out, allowed the determination of Transmissivity values. Figure shows the Transmissivity, T versus Transverse Resistance R, plot.

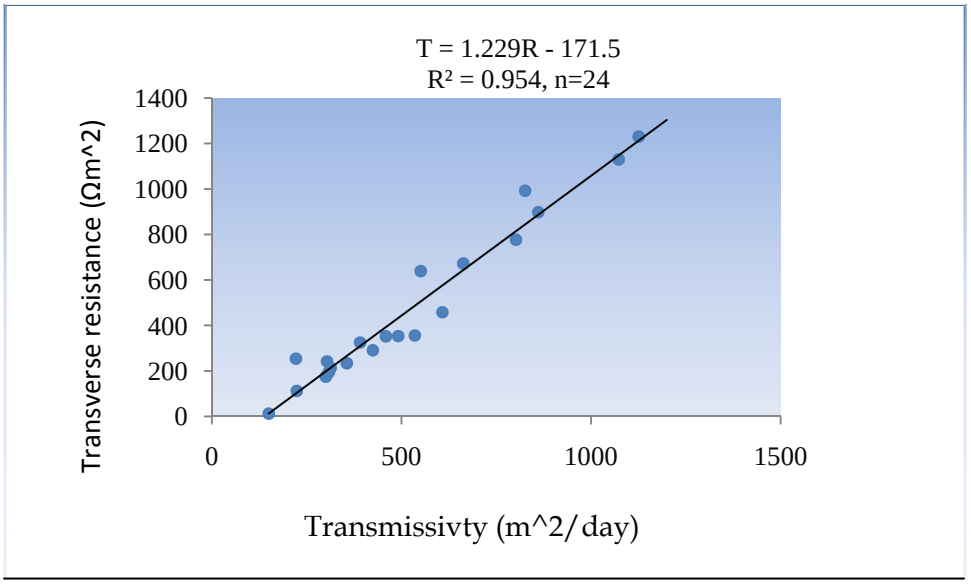


Figure 67 Transmissivity versus Transverse resistance plot

The Equation which relates T and R is an empirical relation between T and R obtained by using linear regression techniques.

T = 1.229R - 171.5

This is practically a straight line, within the range of values used. For higher values of transverse resistance the value of transmissivity will also be high, this type of case happens only in unconsolidated sediments where water content increases with increase in grain size

of sediments, however in hard rock terrain water content increases with decrease in resistivity.

10.5 ELECTRICAL CONDUCTIVITY (EC)

The conductivity (or specific conductance) of an electrolyte solution is a measure of its ability to conduct electricity. The SI unit of conductivity is micro Siemens per centimeter (S/cm).

In many cases, conductivity is linked directly to the total dissolved solids (T.D.S.) The typical conversion of conductivity to the total dissolved solids is done assuming that the solid is sodium chloride: 1 µS/cm is then an equivalent of about 0.6 mg of NaCl per kg of water. (From Wikipedia, the free encyclopedia)

Conductivity is the reciprocal (inverse) of electrical resistivity, ρ, and has the SI units of Siemens per meter $\sigma = \frac{1}{\rho}$. ($S \cdot m^{-1}$)

Conductivity measurements in water are often reported as specific conductance, which is the conductivity of the water at 25 °C.

There are 109 EC measurements from wells in the study area with min, max, mode, median and average values of 308, 1740, 415.78, 618.5 and 665.73 in µS/cm respectively. Because the median and the average values are close the data set is normally distributed. Generally, relatively higher values of EC are observed in the southern part of the study area. This seems reasonable as the ground water flow direction is generally from north to south higher EC values are expected in this area (Fig. 69)

11.0 CONCLUSION AND RECOMMENDAION

11.1 CONCLUSION

The study quantified the variability and spatial distribution of transmissivity and hydraulic conductivity.

The results of this study will be useful for developing numerical ground-water-flow models to predict the future availability of the water resource. The main conclusions of the analysis results of this study are:

- Analysis results of raw pumping test data from a data set of 135 boreholes show that the maximum and minimum transmissivity obtained is 2.74E+03m2/day and 5.40E-03m2/day respectively and a median value of 3.23E+02m2/day this indicates the heterogeneity of the aquifer materials as indicated by their variation in the values of transmissivity.
- Transmissivity and hydraulic conductivity vary laterally within formations.
- Lateral variations of transmissivity and hydraulic conductivity have spatial continuity.
- The analytical approach can be used to estimate transmissivity from specific capacity if the limiting conditions are satisfied. The estimated T values showed strong correlation with measured T values with a power function and with $R^2 = 0.96$
- The empirical approach has also resulted a strong correlation between transmissivity and specific capacity $T= 0.85Sc^{1.064}$, $R^2 = 0.96$ and it can be applied in alluvial basins where only specific capacity data are available. This has similar forms with (Mace and others, 1999)

  Correlation results $T =1.99Sc^{0.84}$ with the correlation coefficient, $R^2 = 0.91$ and Graham and others, 2007 with correlation results $T= 1.6(Q/S)^{0.93}$ with ($r^2 = 0.8$, n=116) in hard rock aquifers and Razack[a] and Huntley[b], 1991 with correlation results $T = 0.36 (Q/S)^{0.67}$T &Sc in (m^2/sec) in an alluvial basin (Haouz plain, Morocco)
- The transmissivity estimated using the analytical and empirical methods are compared based on the mean error and mean absolute error between the estimates and the measured values of log-transformed transmissivity are determined. The mean absolute error and mean error for transmissivity estimated using the analytic approach are 0.21 and -0.21 respectively. A mean absolute error of 0.21 means that, on average, the estimated value of transmissivity is within

a factor of 1.6 of the measured value (determined by taking the inverse log of 0.21).The mean absolute error and mean error for transmissivity estimated using the empirical approach are 0.073 and 0.00021 respectively. A mean absolute error of 0.073 indicates that, on average, the estimated value of transmissivity is within a factor of 1.18 of the measured value (determined by taking the inverse log of 0.073). The closeness of the mean error to zero indicates that the estimates may not have a systematic error towards overestimating or underestimating transmissivity. There for based on these parameters the empirical approach have better predictions than the analytical approach, even though, the estimated values of T using the analytical approach are within the acceptable range.

- Co Kriged and Kriged maps of transmissivity and hydraulic conductivity show the greatest values for the coarse deposits closer to the western marigin of the valley and decreasing tendency towards the eastern escarpment.
- Specific-capacity data are very useful for estimating transmissivity and should be used in water-resources investigations.
- These data allow the variability of transmissivity values to be better defined and allow better correlation to geology and better interpolation of transmissivity values.

The established relationships between borehole yield and transmissivity can also be used as a measure of aquifer productivity in areas where there is scarcity of transmissivity or specific capacity data. The transmissivity is related with borehole yield as T = 0.080Q - 11.81 where T (m^2/d) and Q (m^3/d) R^2 = 0.835, n = 50. Similar relations are obtained in Scotland by (Graham and others, 2009). The transmissivity is related with borehole yield as follows $T=0.13Q^{1.03}$ with (r^2 = 0.57 and n= 131) in power terms but it is directly proportional to discharge which is the same as above.

The correlation between transmissivity (T) and transverse resistance (R) of the unconsolidated sediments aquifer is related as T = 1.229R - 171.5, R^2 = 0.954, n = 24, a linear relationship with the range of values used. This relation can be used to extrapolate pumping test data to an area.

This relation has similar form to the relation developed by (Louis and others, 2010) in the alluvial plain area of Mornos river valley, central Greece

T= 0.22R-287.61 (R = 0.95)

A.Taheri Tizro (1), M. Salehzade (2) have also established a similar relation for alluvial deposits in kangavar basin, western Iran

$T = 2.1R + 768.7$, $R^2 = 0.82$

Therefore the geoelectric methods are an inexpensive way of characterizing an area quantitatively.

The transmissivity values estimated using the established relationship are compared with the measured transmissivity from pumping test and are found to be nearly similar with R^2 =0.95 between measured and estimated transmissivity values.

The established relationships can be applied in areas with similar geologic setting, but not in other geologic settings.

11.2 RECOMMENDATION

The measurement of specific capacity data at the time of drilling should be practiced in order to get an idea of the transmissivity of the area using the established relationships between specific capacity and transmissivity.

The geostatistical approach is a very important method for the interpolation of points with nearly similar values, so it is highly dependent on the distribution and spatial location of data sets, and it is highly recommended to apply this method with increased data volume. Because the quality of interpolated map is dependent on the size and distribution of the data set.

The difficulty of identifying geoelectric layers at different degrees of saturation levels, but similar resistivity response could be solved by applying a combination of methods in addition to VES for e.g. induced polarization.

REFERNCES

A.C. Ekwe[1], N.N. Onu[2] and K.M.Onuoha[1], 2006. Estimation of aquifer hydraulic Characteristics from electrical sounding data: the case of middle Imo River basin Aquifers, south- eastern Nigeria. http://www.spatialhydrology.com/journal/paper/fall2006/imo_river.pdf

Amare, M. 2007. Numerical Groundwater Flow Modeling of Mehoni Sub basin in the Raya Valley, Northern Ethiopia. M.Sc. Thesis, 2p

Anonymous, 2008. Geological investigation report on the raya basin (unpublished document.)

Anonymous, 2010. Pumping test raw data, geophysical data and lithological logs from WWDSE data base.

Anonymous, 1998. Raya Valley Agricultural Development Project (RVADP) REST (1998). Feasibility study report. Volume II, Water Resources. Annexes: Hydrology and Hydrogeology. Mekelle, Ethiopia

Anonymous, 2008. Raya valley pressurized irrigation project: Hydrogeology (phase-I) final Feasibility study. Volume II- 2008, water resources and irrigation annex-B, Water works design and supervision enterprise in association with concert Engineering and consulting enterprise.

Archie, G.E., 1942. The electrical resistivity log as an aid in determining some reservoir characteristics. Amer.Inst.Min.Met.Eng, Tech.Pub. 1422, Petroleum Technology.

A.Taheri Tizro (1), M. Salehzade (2), 2010. Estimation of Hydraulic Properties of Ground water by application of Geoelecterical Method– a case Study in West Iran. (1 & 2) Dept. of Water Engineering, College of Agriculture, Razi University, Kermanshah, Iran. http://www.geotunis.org/2009/file/ppt/pdf/Dr%20Tizro.pdf

Desse Nedaw, 2003. Aquifer characterization and hydro chemical investigation in the Raya Valley, Northern Ethiopia. PHD thesis, University of Natural Resources and Applied life sciences, Department of Applied Geology (Boku) Vienna. 53-60 p

Driscoll, F.G., 1986, Groundwater and wells: second edition, U.S. Filter/Johnson Screens, st,

E. Mace, R.., (2000), Estimating Transmissivity Using Specific-Capacity Data http://www.twdb.state.tx.us/gam/gam_documents/sc_report.pdf (cited onJanuary4, 2010)

Fetter, C.F., 2001. Applied Hydrogeology 4th edition, Prentice Hall Upper Saddle River, New Jersey, U.S.SA. pp 82, 88-90, 151, 154-155, 169

Graham et al (2009), Using transmissivity, specific capacity and borehole yield data to assess the productivity of Scottish aquifers; Quarterly Journal of Engineering Geology & Hydrogeology; v.42; p. 227-235 http://qjegh.geoscienceworld.org/cgi/content/abstract/42/2/227(cited on December 12, 2009)

Hagos, E. (2005). Hydrogeology of Mehoni sub-basin and Lake Ashenge catchment in the Raya Valley Northern Ethiopia. Addis Ababa University, Addis Ababa, Ethiopia, Unpublished M.Sc. thesis, 127p

Mace and others, 1999 Transmissivity, Hydraulic Conductivity, and Storativity of the Carrizo-Wilcox Aquifer in Texas (CW- Report) pp 1, 2, 19-21 http://www.twdb.state.tx.us/gam/czwx_s/cw_report.pdf

Niwas, S. and Singhal, D.C., 1981. Estimation of aquifer transmissivity from Dar Zarrouk parameters in porous media. Hydrology, **50**, 393-399.

Nonner, 2002 Principles of Groundwater exploration pp 215, 218-219

Salem, H.S. 1999. Determination of fluid transmissivity and electric transverse resistance for Shallow aquifers and deep reservoirs from surface and well log electric measurements. Hydro. Earth Sys. Science, **3**, 421-427.

Soupios[1] P.M. and others, Hydraulic Parameters from Surface Geophysical Methods:

Keritis Basin in Chania-Crete; (1) Technological Educational Institute of Crete, Department of Natural Resources and Environment, Laboratory of Geophysics & Seismology http://soupios.chania.teicrete.gr/papers/Pre8-Keritis.pdf (cited on January 4, 2010.)

Statistics and data analysis in geology, 2nd edition (John c. Davis) Kansas geological survey, pp87, 88

Tenalem Ayenew., & Tamiru Alemayehu., 2001, Principles of hydrogeology.

Tamiru Alemayehu., 2006, Groundwater Occurrence in Ethiopia.

William E. Kelly[a] (1977), Geoelectric Sounding for Estimating Aquifer Hydraulic Conductivity Vol. 15, No.6-Groundwater (https://info.ngwa.org/GWOL/pdf/772901056.PDF (cited on January 6, 2010)

Yang[1] and others (1997), Mapping of Groundwater with the Direct Current Resistivity Method in the Area between the Pachang-Chi and Tsengwen-Chi, Southern Taiwan, TAO, Vol. 8, No.3, 313-328 http://tao.cgu.org.tw/pdf/v83p313.pdf (cited on January 12, 2010)

Zekai Sen, 1995 applied hydrogeology for scientists and engineers pp241

APPENDICES

APPENDIX 1 Analysis results of pumping test and well information

No.	Well_Id	E	N	Q (m^3/d)	Measured drawdown Sw(m)	T (m^2/d) constant	K (m/day) constant	T (m^2/d) recovery	K (m/day) recovery	Well depth (m)	SWL (m)	Screen Length (m)	Alluvial thickness (m)
1	RPW-004	587866	1399382	518.40	42.34	10.5	0.14	10.30	0.132	260	72.56	77.4	30
2	RPW-005	577889	1409202	2030.40	7.36	401	11.10	400.00	11.1	128	59.95	36	114
3	RPW-006	577182	1408010	1209.60	24.63	251	0.60	258.00	0.614	148	46.5	42	142
4	RPW-008	559048	1366594	737.86	62.88	17.8	0.30	17.60	0.296	186	76.62	59.49	92
5	RPW-012	581052	1404035	2747.52	9.7	175	2.08	177.00	2.1	220	34.4	84	210
6	RPW-013	572677	1403437	1512.00	14.68	254	8.91	255.00	8.94	116	58.57	28.55	98
7	RPW-014	582104	1403603	4173.12	6.55	458	7.64	444.00	7.4	184	40.6	60	174
8	RPW-017	571732	1375106	4207.68	51.95	279	3.32	279.00	3.32	209	12.4	84	206
9	RPW-019	581768	1400964	2747.52	12.69	352	4.51	352.00	4.51	215	29.4	78	206
10	RPW-020	577596	1400661	2747.52	10.02	242	3.44	245.00	3.40	223	60	72	226
11	RPW-021	571906	1363793	5244.48	5.35	898	15.00	886.00	14.8	159	22.2	60	154
12	RPW-022	576837	1374986	432.00	37.16	12.1	0.29	15.20	0.365	146	39.22	41.61	18
13	RPW-023	568247	1400186	1133.57	35	12.2	0.41			111	34	30	76
14	RPW-024	574055	1399330	2419.20	4.16	525	11.00	522.00	11	140	38.34	47.6	128
15	RPW-025	574144	1368595	3568.32	12.17	448	4.98	448.00	4.98	267	18	90	256
16	RPW-026	570329	1389923	3412.80	3.98	777	25.90	775.00	25.8	108	26	30	104
17	RPW-028	578718	1398109	2419.20	3.45	672	8.13	671.00	8.12	226	33.58	82.66	218
18	RPW-030	573856	1396696	2073.60	8.42	305	4.98	306.00	5.00	176	45.5	61.15	164
19	RPW-031	566678	1378864	4795.20	2.95	1130	14.50	1130.00	14.4	220	20.01	78	206
20	RPW-032	576189	1395698	2764.80	17.85	129	2.19	128.00	2.17	182	31.27	58.74	178
21	RPW-033	575022	1395075	2611.87	14.32	351	6.80	350.00	6.77	162	33.2	51.67	140
22	RPW-034	576332	1394432	2002.75	11.6	234	3.03	236.00	3.06	224	36.2	77.06	214
23	RPW-035	566991	1377439	9457.34	31.68	305	4.24	309.00	4.29	203	7.3	72	200

24	RPW-036	574094	1392035	2702.59	3.5	1620	51.80	1630.00	26.6	160	39.75	61.45	134
25	RPW-037	574690	1390976	2592.00	9.56	309	5.27	308.00	5.24	160	33.54	58.72	154
26	RPW-038	574039	1389891	2185.92	19.92	108	1.66	108.00	1.65	182	39.2	65.33	176
27	RPW-040	569910	1391794	2747.52	16.05	101	2.01	105.00	2.11	143	40.09	50	138
28	RPW-042	572853	1372716	4495.39	15.34	356	5.44	356.00	5.45	184	13.9	65.42	170
29	RPW-043	572369	1384905	2747.52	29.39	152	1.94	153.00	1.96	192	51	78	250
30	RPW-044	569097	1378878	4371.84	23.38	164	2.49	165.00	2.49	209	-2	66	208
31	RPW-045	572436	1382113	2808.00	26.31	84.4	1.41	84.80	1.41	178	29.34	60	174
32	RPW-046	569905	1381800	2868.48	32.04	89.1	1.48	88.30	1.47	180	28.57	60	174
33	RPW-047	572052	1380755	2903.04	23.16	197	4.10	531.00	11.1	136	25.02	48	130
34	RPW-048	570343	1380681	1296.00	58.86	43.2	0.80	25.30	0.469	150	17.22	54	146
35	RPW-049	568921	1379801	4579.20	15.28	222	3.71	220.00	3.67	198	-2	60	182
36	RPW-050	571429	1379689	3818.88	10.59	308	5.13	309.00	5.15	166	18.17	60	160
37	RPW-051	568031	1379400	4622.40	18.7	187	2.60	186.00	2.58	200	8.28	72	192
38	RPW-052	570263	1378912	2903.04	39.86	111	2.65	111.00	2.64	136	9.92	42	130
39	RPW-053	568862	1377910	4795.20	17.47	155	2.35	150.00	2.28	218	-2	66	214
40	RPW-054	567333	1378232	10459.58	20.25	992	13.80	991.00	13.8	186	12.4	72	184
41	RPW-055	571864	1378166	4173.12	17.64	288	3.69	286.00	3.67	216	17.02	78	206
42	RPW-056	567995	1377085	9784.80	22.54	668	10.10	669.00	10.1	200	-2	66	198
43	RPW-057	569431	1376222	3136.32	20.48	213	3.55	215.00	3.58	142	8.8	60	136
44	RPW-058	571642	1376249	5624.64	16.68	292	4.05	291.00	4.04	186	11.95	72	180
45	RPW-059	565861	1379159	5019.84	5.26	1640	34.10	1640.00	34.2	174	24.25	48	162
46	RPW-060	566917	1374980	3196.80	3.98	1420	20.10			198	-2	70.7	184
47	RPW-061	567200	1375899	9457.34	40.5	190	3.95	191.00	3.98	156	-2	48	152
48	RPW-062	566450	1374975	4371.84	14.67	426	8.89	427.00	8.89	143	3.3	48	130
49	RPW-063	571462	1374198	2937.60	12.9	194	2.36	195.00	2.37	224	14.75	82.37	216
50	RPW-064	564467	1373141	3024.00	8.37	850	20.90	858.00	21.1	112	21.74	40.67	88
51	RPW-065	565658	1373049	4704.48	6.92	2480	51.90	2480.00	51.8	126		47.82	102
52	RPW-066	566444	1372391	3352.32	9.78	459	8.81	454.00	8.71	146	9.1	52.13	136
53	RPW-067	571726	1373354	2702.59	15.48	273	4.73	277.00	4.8	218	13.39	57.62	210
54	RPW-068	572613	1371922	3110.40	10.63	434	4.72	435.00	4.72	264	15.5	92.1	258

55	RPW-069	565204	1371005	9174.82	29.13	375	6.95	374.00	6.93	154	12.9	54	150
56	RPW-070	570481	1371229	1382.40	47.09	64.3	1.39	64.30	1.39	144	22.72	46.32	136
57	RPW-071	565705	1372178	4704.48	6.4	1100	16.70	1100.00	16.6	160	11.35	65.83	136
58	RPW-072	572671	1370616	2704.32	48.63	168	2.06	169.00	2.07	262	17.5	81.73	254
59	RPW-074	564898	1367281	4661.28	21.13	353	6.55	353.00	6.56	176	15.78	53.8	164
60	RPW-075	561215	1368924	4147.20	8.34	597	14.60	597.00	14.6	130	28.49	40.95	122
61	RPW-076	567162	1369865	3352.32	8	334	4.31	336.00	4.33	232	14.3	77.5	222
62	RPW-077	565483	1368490	3594.24	4.56	2060	49.00	2060.00	49.1	137	15.35	42	130
63	RPW-078	569076	1366877	2747.52	15.1	325	10.80	322.00	10.7	96	30.05	30	88
64	RPW-079	568008	1367866	3844.80	5.95	693	12.00	690.00	12	210	20.6	57.59	198
65	RPW-080	570393	1368715	1123.20	2.54	445	10.90	446.00	10.9	138	25.56	40.88	128
66	RPW-081	566566	1367059	3456.00	22.66	112	1.91	110.00	1.88	190	16.7	58.5	180
67	RPW-082	574045	1365777	3532.03	13.63	639	7.28	638.00	7.27	276	9.52	87.75	268
68	RPW-083	565271	1365661	4320.00	8.65	539	10.10	539.00	10.1	160	11.42	53.54	152
69	RPW-084	568850	1368728	2617.92	28.19	93.5	2.25	93.50	2.25	146	21.6	41.5	134
70	RPW-085	564906	1363929	9851.33	16.81	795	18.90	798.00	19	120	17.26	42	116
71	RPW-086	563445	1362750	8054.21	45.82	1930	41.40	1920.00	41.1	118	35.06	46.64	114
72	RPW-087	567591	1361714	3594.24	6.3	619	10.30	623.00	10.4	170	6.42	60	162
73	RPW-088	567019	1360930	4320.00	15.29	206	3.50	206.00	3.50	176	7.01	58.65	162
74	RPW-090	563934	1356825	10022.40	19.49	1230	19.10	1230.00	19.1	184	9	64.35	178
75	RPW-092	571968	1384297	2903.04	4.85	357	5.41	352.00	5.33	194	42.9	66	200
76	RPW-093	567588	1359766	3974.40	15.68	291	2.77	294.00	2.80	288	5.8	105.18	276
77	RPW-095	565153	1359042	3784.32	17.38	137	2.10	136.00	2.09	196	5.43	65	190
78	RPW-096	566902	1358605	3784.32	12.21	238	3.69	236.00	3.66	186	15.41	64.46	174
79	RPW-097	564016	1357876	3974.40	16.9	518	11.10	515.00	11	144	13.74	46.8	138
80	RPW-098	562933	1357904	3594.24	7.78	1160	25.00	1160.00	25.1	154	5.57	46.24	144
81	RPW-099	566904	1357791	9676.80	18.62	530	5.65	536.00	5.72	230	19.42	93.75	222
82	RPW-100	565838	1357528	9331.20	22.2	529	8.22	535.00	8.31	191	24.53	64.35	184
83	WF13/BH1	574502	1409298	2937.60	2.58	1540	32.20	1540.00	32.1	137.5	51.73	48	130
84	WF13/BH2	575754	1407602	3240.00	4.34	767	12.80	767.00	12.8	168	30.3	60	158
85	WF13/BH4	574837	1408721	2747.52	3.76	2400	50.00	2380.00	49.6	144	43.9	48	140

86	WF13/BH5	575406	1408290	3784.32	2.44	1800	42.90	1810.00	43.1	132	36.2	42	132
87	WF11/BH4	577896	1403786	3067.20	7.76	277	4.20	273.00	4.13	198	58.38	66	194
88	WF9/BH1	569813	1400983	3801.60	5.1	2680	49.70	2680.00	58.4	151	30.35	54	144
89	WF9/BH2	569708	1399528	3024.00	12.96	1200	22.60	1200.00	22.6	150	22.92	53	144
90	WF9/BH3	569798	1400023	2592.00	11.4	428	6.11	424.00	6.05	128	20.66	70	122
91	WF9/BH4	570553	1400160	3801.60	3.42	2400	30.80	2400.00	30.7	150	27.09	78	140
92	WF2/V9	565921	1376322	3801.60	8.75	805	19.20	817.00	19.5	78	2.15	42	43
93	WF4/BH1	567110	1381023	3412.80	7.08	546	10.20	552.00	10.2	172	40.71	54	172
94	WF4/BH2	565885	1378789	3974.40	3.38	1080	17.50	1070.00	17.3	139	20.4	62	138
95	WF4/BH3	564899	1378795	3715.20	6.34	1800	50.00	1800.00	49.9	132	45.53	36	128
96	WF0/BH1	562709	1370793	3024.00	5.12	689	28.70	689.00	23	98	17.75	24	86
97	WF0/BH2	562905	1370393	3456.00	3.15	5210	124.00	5220.00	121	88	10.37	42	82
98	WF0/BH3	563923	1369802	3456.00	16.01	233	5.55	233.00	5.55	80	12.15	42	70
99	WF0/BH4	562697	1368978	3456.00	14.5	223	4.30	220.00	4.08	106	10.31	52	90
100	WF0/BH5	561903	1369790	3456.00	5.34	810	16.90	1520.00	31.7	136	14.98	48	126
101	WF0/BH6	561399	1370777	3456.00	4.79	1980	47.30	1990.00	47.5	93	30.18	42	84
102	WFO/BH7	561796	1370780	3801.60	1.76	3890	92.60	3780.00	90.1	102	20.81	42	86
103	WF0/BH8	561409	1369799	3801.60	5.97	1820	37.90	1820.00	38	132	28.48	48	120
104	WF1/V1	562872	1371640	3024.00	16.36	273	7.81	274.00	7.61	78	17.03	35	68
105	WF1/V9	562713	1371855	3024.00	3.12	1610	53.50	1610.00	53.7	73	17.73	30	60
106	WF1/V10	562681	1371183	3024.00	4.64	972	32.40	976.00	32.5	102	17.22	30	92
107	WF5/BH1	563690	1366993	2592.00	14.56	210	57.60	207.00	5.76	96	15.88	36	64
108	WF5/BH2v8	564103	1368593	3024.00	6.06	611	14.60	611.00	14.6	108	24.77	42	102
109	WF5/BH3v3	563673	1367565	3024.00	6.15	504	14.00	508.00	14.1	84	18.8	36	78
110	WF5/BH4v5	563905	1367793	3024.00	16.15	155	3.22	150.00	3.13	101	20.52	48	94
111	WF6/BH3	563156	1366192	3024.00	6.43	584	19.50	586.00	19.5	96	24.47	30	92
112	WF6/BH4	563912	1364685	3456.00	2.95	1150	24.00	1150.00	24	122	27.51	48	114
113	WF7/BH1	564378	1363098	3801.60	1.65	2240	46.60	2240.00	48.7	137	27.79	48	130
114	WF7/BH2	563863	1364133	3240.00	2.51	1500	24.90	1500.00	23.4	162	30.47	60	148
115	WF Abergelle BH1	570017	1386373	3412.80	10.4	479	7.49	478.00	7.70	146	9.4	62	146
116	WF Kalibso BH1	571787	1401448	3067.20	11.01	213	3.74	210.00	3.68	146.5	39.13	56	138

117	WF GOBU BH1	564404	1358786	3343.68	3.07	1600	40.10	1610.00	40.3	79.5	8.13	40	80
118	WF Abergelle BH2	573832	1365003	2479.68	13.61	748	26.70	749.00	26.7	60	9.27	28	60
119	Galika Trading BH1	570245	1369978	2937.60	15.83	365	9.13	367.00	9.17	100	28.5	40	88
120	WF-SAV/BH1	576764	1390173	2592.00	8.2	386	6.89	386.00	6.89	183	31.3	56	172
121	WF-SAV/BH2	576732	1389596	2592.00	6.96	384	7.39	381.00	7.62	147	28.94	50	136
122	WF-SAV/BH3	575944	1389641	2747.52	5.02	519	6.49	518.00	6.56	173	37.7	79	161
123	WF-SAV/BH4	576495	1390581	2764.80	7.63	308	4.82	309.00	4.83	180	37.4	64	160
124	Friatna BH1	577594	1403257	2592.00	10.98	239	4.13	240.00	125	170	53.63	58	170
125	Tera BH1	571787	1401448	889.92	5.67	218	4.05	218.00	4.04	150	46.56	54	150
126	PZ1	581458	1402058	2903.04	12.71	275	2.87	275.00	2.87	240	32.82	96	222
127	PZ2	585168	1402537	172.80	5.95	25.5	0.85	25.50	0.851	90	46.85	30	84
128	PZ3	569257	1377425	3136.32	2.28	869	14.00	869.00	14.0	170	9.58	54	160
129	PZ4	565181	1379685	2730.24	5.07	1570	52.40	1570.00	52.4	90	30.75	30	76
130	PZ5	572491	1373604	2764.80	1.05	1230	21.50	1230.00	21.5	184	15.81	57	176
131	PZ7	574387	1361357	3006.72	14.42	326	3.97	335.00	4.09	311	8.93	84	310
132	PZ9	562943	1365069	2903.04	2.24	1030	26.80	1010.00	24.5	146	19.46	40	128
133	PBH1	571313	1415112	388.80	8.84	56.5	1.71	50.60	1.53	96	62.3	22	90
134	PBH3	587384	1411774	483.84	3.34	145	2.68	146.00	2.70	204	90.14	54	200
135	PBH7	568083	1385735	302.40	1.75	578	12.00	579.00	12.1	139	71.95	48	126
136	Dejena BH3	576046	1403659	2747.52	21.85	157	2.62	157.00	2.62	169	43.38	60	160

APPENDIX 2 EC data (µS/cm)

Well Id	E	N	EC	well Id	E	N	EC
RPW-005	577889	1409202	633.37	RPW-074	564898	1367281	851.52
RPW-006	577182	1408010	839.04	RPW-075	561215	1368924	648.00
RPW-008	559048	1366594	602.00	RPW-076	567162	1369865	627.00
RPW-012	581052	1404035	473.51	RPW-077	565483	1368490	1035.00
RPW-013	572677	1403437	918.00	RPW-078	569076	1366877	809.00
RPW-014	582104	1403603	454.01	RPW-079	568008	1367866	755.00
RPW-017	571732	1375106	415.78	RPW-080	570393	1368715	681.00
RPW-019	581768	1400964	462.12	RPW-081	566566	1367059	703.00
RPW-020	577596	1400661	546.39	RPW-082	574045	1365777	538.00
RPW-021	571906	1363793	989.02	RPW-083	565271	1365661	575.00
RPW-023	568247	1400186	600.00	RPW-084	568850	1368728	558.00
RPW-024	574055	1399330	920.00	RPW-085	564906	1363929	644.16
RPW-025	574144	1368595	695.93	RPW-087	567591	1361714	925.00
RPW-026	570329	1389923	508.76	RPW-088	567019	1360930	1740.00
RPW-028	578718	1398109	485.00	RPW-092	571968	1384297	623.77
RPW-030	573856	1396696	539.00	RPW-095	565153	1359042	636.00
RPW-031	566678	1378864	667.27	RPW-096	566902	1358605	783.00
RPW-032	576189	1395698	539.00	RPW-097	564016	1357876	484.00
RPW-033	575022	1395075	509.00	RPW-098	562933	1357904	646.00
RPW-034	576332	1394432	512.00	WF13/BH2	575754.1	1407602.4	453.00
RPW-035	566991	1377439	563.61	WF13/BH4	574836.8	1408721	604.00
RPW-036	574094	1392035	604.00	WF9/BH1	569813	1400983	521.00
RPW-037	574690	1390976	560.00	WF9/BH2	569708	1399528	308.00
RPW-038	574039	1389891	505.00	WF9/BH3	569798	1400023	543.00
RPW-040	569910	1391794	597.57	WF9/BH4	570553	1400160	542.00
RPW-042	572853	1372716	586.20	WF2/V9	565921.4	1376322.4	378.00
RPW-043	572369	1384905	755.26	WF4/BH2	565885.2	1378788.5	587.00
RPW-044	569097	1378878	415.78	WF0/BH1	562709.1	1370792.7	722.00
RPW-045	572436	1382113	683.41	WF0/BH2	562905	1370393	973.00
RPW-046	569905	1381800	551.22	WF0/BH4	562696.5	1368977.6	1475.00
RPW-047	572052	1380755	554.48	WF0/BH5	561902.6	1369790.4	708.00
RPW-048	570343	1380681	707.88	WF0/BH6	561399.4	1370776.7	683.00
RPW-049	568921	1379801	453.82	WFO/BH7	561795.7	1370779.5	433.00
RPW-050	571429	1379689	434.59	WF0/BH8	561408.5	1369799.3	620.00
RPW-051	568031	1379400	509.69	WF1/V9	562713.4	1371854.5	749.00
RPW-052	570263	1378912	607.30	WF1/V10	562680.6	1371182.6	642.00
RPW-053	568862	1377910	451.31	WF5/BH1	563690.3	1366992.6	901.00
RPW-054	567333	1378232	616.24	WF5/BH2v8	564103	1368592.9	1166.00

RPW-055	571864	1378166	474.88	WF5/BH3v3	563672.5	1367565.2	885.00
RPW-056	567995	1377085	456.56	WF5/BH4v5	563905	1367793	631.00
RPW-057	569431	1376222	691.64	WF6/BH3	563155.7	1366191.7	1172.00
RPW-058	571642	1376249	689.14	WF6/BH4	563912.4	1364684.5	747.00
RPW-059	565861	1379159	616.96	WF7/BH2	563863	1364132.9	552.00
RPW-060	566917	1374980	479.00	WF Abergelle BH1	570017	1386373	560.00
RPW-061	567200	1375899	442.64	PZ1	581458	1402058	467.00
RPW-062	566450	1374975	574.29	PZ2	585168	1402537	470.00
RPW-063	571462	1374198	674.00	PZ3	569257	1377425	1220.00
RPW-064	564467	1373141	664.00	PZ4	565181	1379685	458.00
RPW-066	566444	1372391	789.00	PZ5	572491	1373604	681.00
RPW-067	571726	1373354	645.00	PZ7	574387	1361357	955.00
RPW-068	572613	1371922	617.00	PZ9	562943	1365069	799.00
RPW-069	565204	1371005	924.71	PBH1	571313	1415112	946.00
RPW-070	570481	1371229	744.00	PBH3	587384	1411774	476.00
RPW-072	572671	1370616	640.00	PBH7	568083	1385735	1020.00

APPENDIX 3 Results of analysis using Analytic Approach

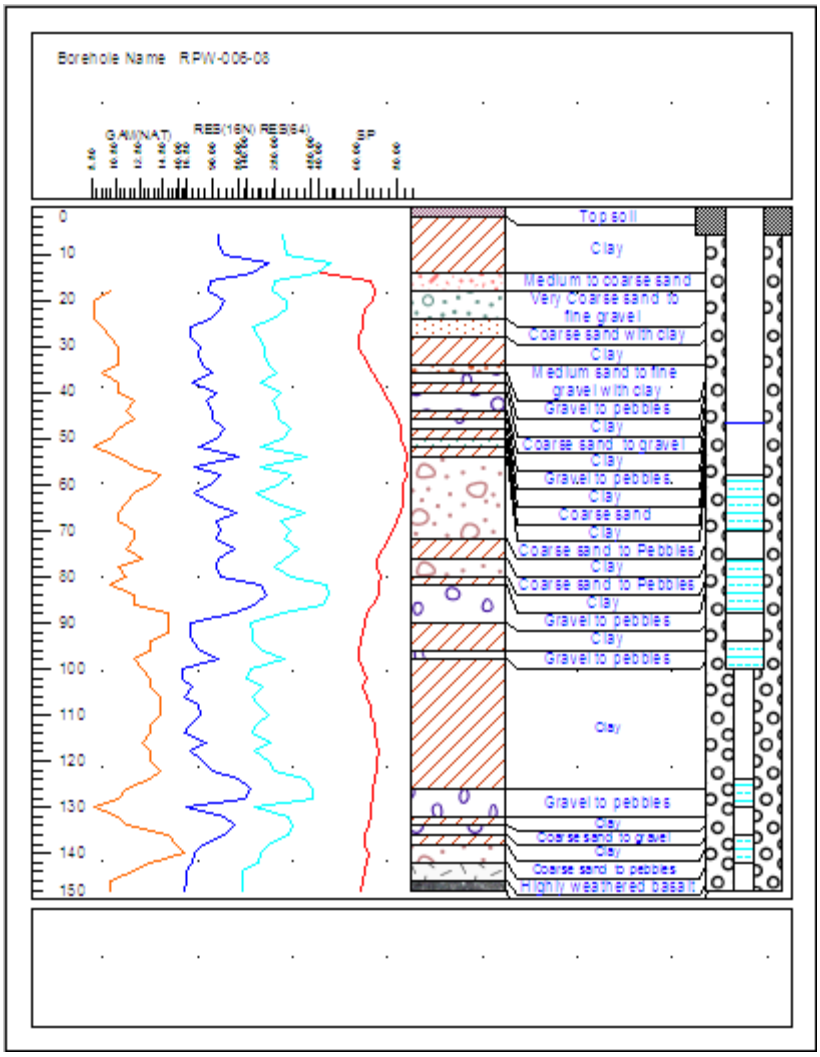
No.	Well_Id	E	N	T (m^2/d)(estimated)	T(m^2/d)measured
1	RPW-004	587866	1399382	15.27	10.5
2	RPW-005	577889	1409202	361.03	401
3	RPW-006	577182	1408010	62.73	251
4	RPW-008	559048	1366594	23.40	17.8
5	RPW-012	581052	1404035	408.85	175
6	RPW-013	572677	1403437	139.87	254
7	RPW-014	582104	1403603	989.26	458
8	RPW-017	571732	1375106	161.84	279
9	RPW-019	581768	1400964	307.61	352
10	RPW-020	577596	1400661	395.04	242
11	RPW-021	571906	1363793	2137.49	898
12	RPW-022	576837	1374986	13.42	12.1
13	RPW-023	568247	1400186	41.02	12.20
14	RPW-024	574055	1399330	874.62	525
15	RPW-025	574144	1368595	569.07	448
16	RPW-026	570329	1389923	1692.16	777
17	RPW-028	578718	1398109	1065.64	672
18	RPW-030	573856	1396696	352.57	305

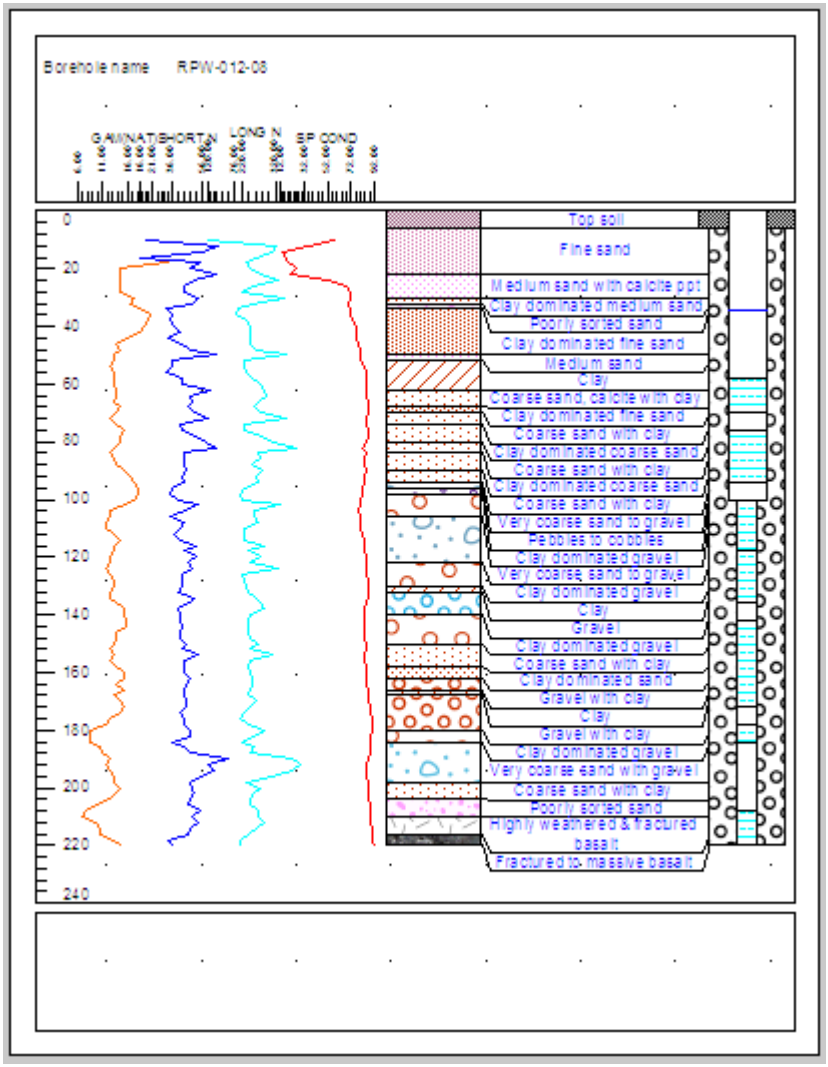
19	RPW-031	566678	1378864	2863.27	1130
20	RPW-032	576189	1395698	215.69	129
21	RPW-033	575022	1395075	256.50	351
22	RPW-034	576332	1394432	242.00	234
23	RPW-035	566991	1377439	626.37	305
24	RPW-036	574094	1392035	1179.72	1620
25	RPW-037	574690	1390976	345.77	309
26	RPW-038	574039	1389891	142.54	108
27	RPW-040	569910	1391794	239.82	101
28	RPW-042	572853	1372716	691.99	356
29	RPW-043	572369	1384905	126.19	152
30	RPW-044	569097	1378878	345.30	164
31	RPW-045	572436	1382113	145.26	84.4
32	RPW-046	569905	1381800	120.52	89.1
33	RPW-047	572052	1380755	172.31	197
34	RPW-048	570343	1380681	49.18	43.2
35	RPW-049	568921	1379801	1564.95	222
36	RPW-050	571429	1379689	769.79	308
37	RPW-051	568031	1379400	505.15	187
38	RPW-052	570263	1378912	96.77	111
39	RPW-053	568862	1377910	390.59	155
40	RPW-054	567333	1378232	1169.33	992
41	RPW-055	571864	1378166	356.37	288
42	RPW-056	567995	1377085	920.71	668
43	RPW-057	569431	1376222	430.53	213
44	RPW-058	571642	1376249	863.56	292
45	RPW-059	565861	1379159	2232.16	1640
46	RPW-060	566917	1374980	1234.98	1420
47	RPW-061	567200	1375899	393.71	190
48	RPW-062	566450	1374975	497.67	426
49	RPW-063	571462	1374198	324.51	194
50	RPW-064	564467	1373141	482.47	850
51	RPW-065	565658	1373049	1158.96	2480
52	RPW-066	566444	1372391	793.83	459
53	RPW-067	571726	1373354	244.88	273
54	RPW-068	572613	1371922	365.12	434
55	RPW-069	565204	1371005	664.69	375
56	RPW-070	570481	1371229	61.76	64.3
57	RPW-071	565705	1372178	1429.41	1100
58	RPW-072	572671	1370616	72.62	168
59	RPW-074	564898	1367281	541.08	353
60	RPW-075	561215	1368924	1179.47	597
61	RPW-076	567162	1369865	942.55	334

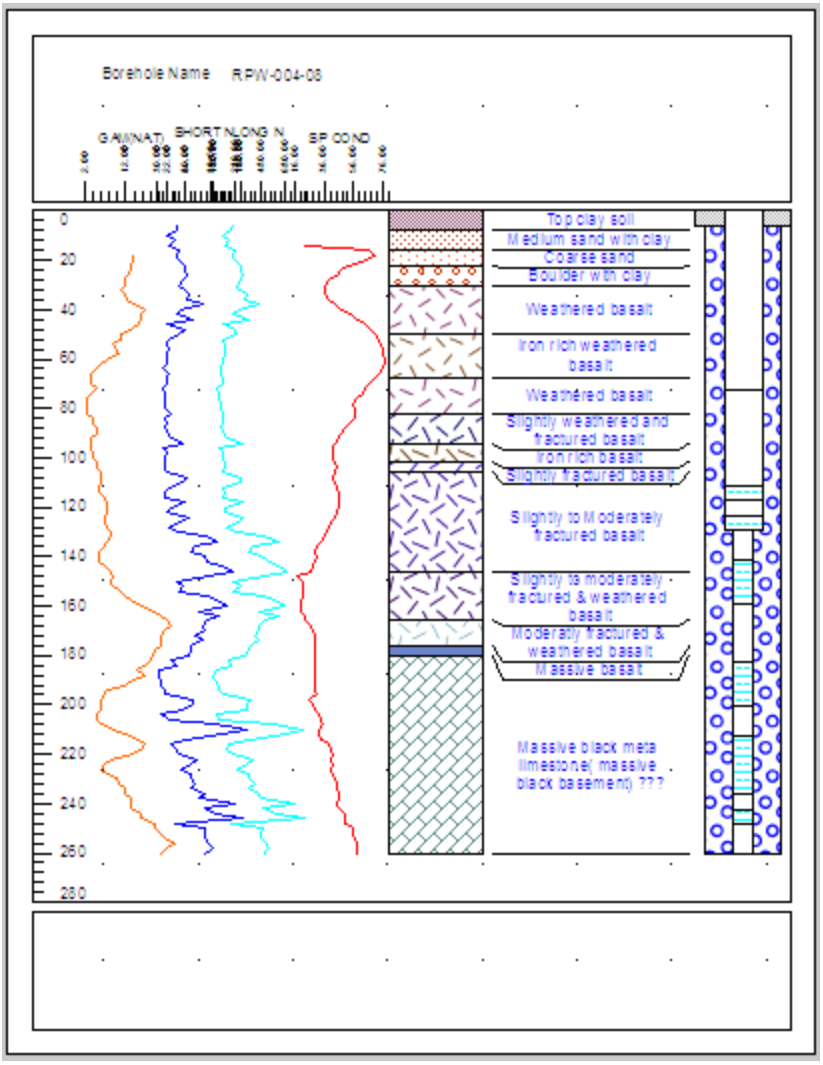
62	RPW-077	565483	1368490	2040.50	2060
63	RPW-078	569076	1366877	285.71	325
64	RPW-079	568008	1367866	1469.51	693
65	RPW-080	570393	1368715	543.41	445
66	RPW-081	566566	1367059	312.88	112
67	RPW-082	574045	1365777	477.86	639
68	RPW-083	565271	1365661	4427.87	539
69	RPW-084	568850	1368728	125.30	93.5
70	RPW-085	564906	1363929	1929.54	795
71	RPW-086	563445	1362750	283.95	1930
72	RPW-087	567591	1361714	1282.61	619
73	RPW-088	567019	1360930	594.87	206
74	RPW-090	563934	1356825	1293.12	1230
75	RPW-092	571968	1384297	901.68	357
76	RPW-093	567588	1359766	425.41	291
77	RPW-095	565153	1359042	359.33	137
78	RPW-096	569076	1366877	1034.48	238
79	RPW-097	564016	1357876	414.98	518
80	RPW-098	562933	1357904	806.14	1160
81	RPW-099	566904	1357791	1237.32	530
82	RPW-100	565838	1357528	744.83	529
83	WF13/BH1	574502	1409298	1531.25	1540
84	WF13/BH2	575754	1407602	1330.10	767
85	WF13/BH4	574837	1408721	938.63	2400
86	WF13/BH5	575406	1408290	5084.91	1800
87	WF11/BH4	577896	1403786	574.61	277
88	WF9/BH1	569813	1400983	1567.13	2680
89	WF9/BH2	569708	1399528	337.62	1200
90	WF9/BH3	569798	1400023	328.49	428
91	WF9/BH4	570553	1400160	15014.66	2400
92	WF2/V9	565921	1376322	1610.76	805
93	WF4/BH1	567110	1381023	1151.94	546
94	WF4/BH2	565885	1378789	2537.17	1080
95	WF4/BH3	564899	1378795	2347.49	1800
96	WF0/BH1	562709	1370793	808.11	689
97	WF0/BH2	562905	1370393	2448.53	5210
98	WF0/BH3	563923	1369802	571.06	233
99	WF0/BH4	562697	1368978	404.00	223
100	WF0/BH5	561903	1369790	1133.78	810
101	WF0/BH6	561399	1370777	1815.67	1980
102	WFO/BH7	561796	1370780	8932.14	3890
103	WF0/BH8	561409	1369799	1373.32	1820
104	WF1/V1	562872	1371640	283.28	273

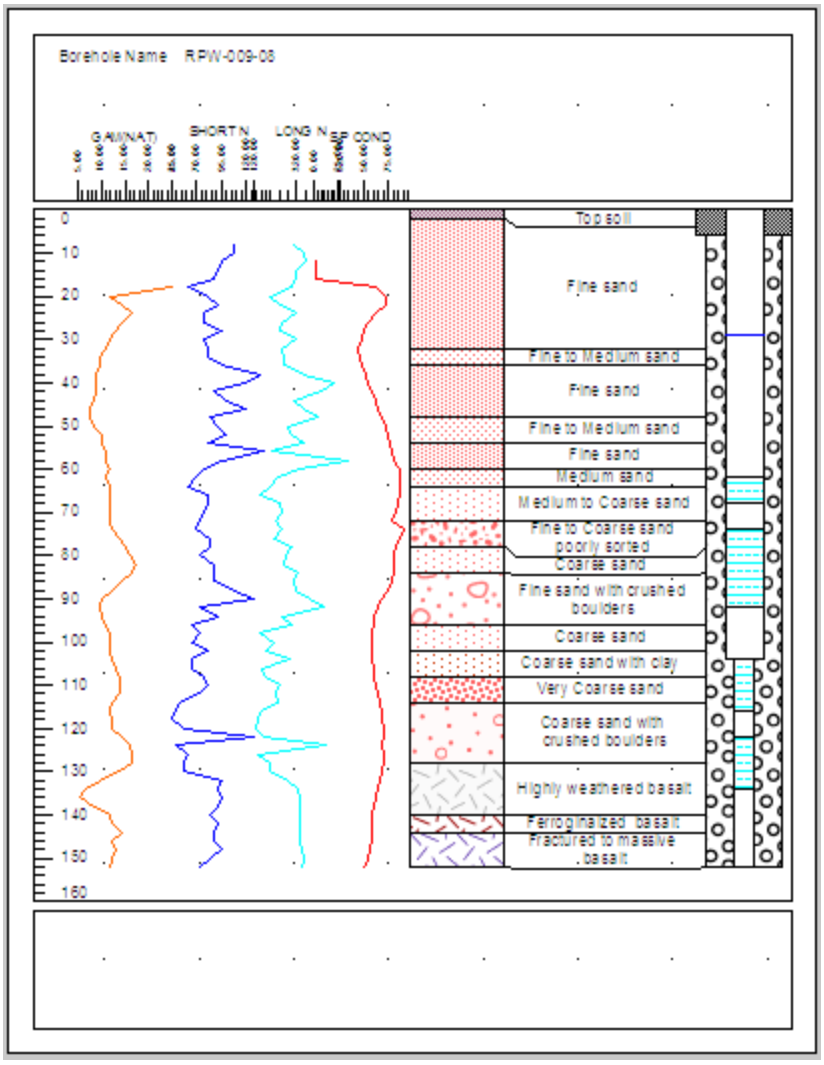
105	WF1/V9	562713	1371855	1326.32	1610
106	WF1/V10	562681	1371183	867.34	972
107	WF5/BH1	563690	1366993	252.05	210
108	WF5/BH2v8	564103	1368593	753.96	611
109	WF5/BH3v3	563673	1367565	723.86	504
110	WF5/BH4v5	563905	1367793	254.44	155
111	WF6/BH3	563156	1366192	690.58	584
112	WF6/BH4	563912	1364685	1585.12	1150
113	WF7/BH1	564378	1363098	18073.64	2240
114	WF7/BH2	563863	1364133	3597.89	1500
115	WF Abergelle BH1	570017	1386373	519.97	479
116	WF Kalibso BH1	571787	1401448	407.25	213
117	WF GOBU BH1	564404	1358786	2181.81	1600
118	WF Abergelle BH2	573832	1365003	282.61	748
119	Galika Trading BH1	570245	1369978	264.93	365
120	WF-SAV/BH1	576764	1390173	453.57	386
121	WF-SAV/BH2	576732	1389596	539.53	384
122	WF-SAV/BH3	575944	1389641	810.66	519
123	WF-SAV/BH4	576495	1390581	524.13	308
124	Friatna BH1	577594	1403257	341.81	239
125	Tera BH1	571787	1401448	221.85	218
126	PZ1	581458	1402058	330.08	275
127	PZ2	585168	1402537	36.90	25.5
128	PZ3	569257	1377425	1860.87	869
129	PZ4	565181	1379685	735.45	1570
130	PZ5	572491	1373604	4345.65	1230
131	PZ7	574387	1361357	299.73	326
132	PZ9	562943	1365069	1759.71	1030
133	PBH1	571313	1415112	57.66	56.5
134	PBH3	587384	1411774	203.78	145
135	PBH7	568083	1385735	201.96	578
136	Dejena BH3	576046	1403659	170.65	157

Appendix 4 sample boreholes for confined and unconfined aquifer




Borehole name RPW-012-08
GAMMA
SHORT N
LONG N
SP
COND
0
20
40
60
80
100
120
140
160
180
200
220
240
Top soil
Fine sand
Medium sand with calcite ppt
Clay dominated medium sand
Poorly sorted sand
Clay dominated fine sand
Medium sand
Clay
Coarse sand, calcite with clay
Clay dominated fine sand
Coarse sand with clay
Clay dominated coarse sand
Coarse sand with clay
Clay dominated coarse sand
Coarse sand with clay
Very coarse sand to gravel
Pebbles to cobbles
Clay dominated gravel
Very coarse sand to gravel
Clay dominated gravel
Clay
Gravel
Clay dominated gravel
Coarse sand with clay
Clay dominated sand
Gravel with clay
Clay
Gravel with clay
Clay dominated gravel
Very coarse sand with gravel
Coarse sand with clay
Poorly sorted sand
Highly weathered & fractured basalt
Fractured to massive basalt


Borehole Name RPW-004-08
GAMMA(AT)
SHORT NORM
LONG N
SP
COND
0
20
40
60
80
100
120
140
160
180
200
220
240
260
280
Top clay soil
Medium sand with clay
Coarse sand
Boulder with clay
Weathered basalt
Iron rich weathered basalt
Weathered basalt
Slightly weathered and fractured basalt
Iron rich basalt
Slightly fractured basalt
Slightly to Moderately fractured basalt
Slightly to moderately fractured & weathered basalt
Moderately fractured & weathered basalt
Massive basalt
Massive black meta limestone(massive black basement) ???


Borehole Name RPW-009-06
GAM(NAT)
SHORT N
LONG N
SP
COND
0
10
20
30
40
50
60
70
80
90
100
110
120
130
140
150
160
Top soil
Fine sand
Fine to Medium sand
Fine sand
Fine to Medium sand
Fine sand
Medium sand
Medium to Coarse sand
Fine to Coarse sand poorly sorted
Coarse sand
Fine sand with crushed boulders
Coarse sand
Coarse sand with clay
Very Coarse sand
Coarse sand with crushed boulders
Highly weathered basalt
Ferroginalized basalt
Fractured to massive basalt

Appendix 5 Final (calibrated) layer parameters

VES Station	Geoelectric cross Section	BH Id	ρ (Ωm)	Thickness (m) (electrical)	VES Station	Geoelectric cross Section	BH Id	ρ (Ωm)	Thickness (m) (electrical)
	WAJA					ALAMATA			
LV109(KA)		RPW-090			LV52(LM)		RPW-074	32.5	6
			18.5	5				10.1	6
			29	12				6.4	12
			24.1	12				5.3	30
			16.5	24	RV7(QR)		RPW-081	5.5	12
								4.9	18
RV3(KD)		RPW-093	6	6				11.6	6
			6.1	40.8	RV6(OP)		RPW-078	10.7	9
			6.1	17				10.9	6
			6	6				8	12
								11.1	12
LV72(M)		RPW-021	15	6					
			12	12	LV64(RS)		RPW-082	5.5	23
			8	6				5.6	18
			15	12				4	24
			13	17.8				8.7	12
			14	6				11.2	11
			13.9	6					
	MEHONI					KARA			
RV49(E)		RPW-007	10	18	RV48(H)		RPW-013	4.9	12
			12.8	6				9	18.1
			6	14	(L)		RPW-020	7	12

RV34(G)		RPW-012	8.9	12				9	12
			5.5	18				9.3	12
			9.3	6	RV33(K)		RPW-019	9	13
			6.5	6				8	18
RV35(I)		RPW-014	6	24				7	18
			8.3	20.4				12	6
			6.5	24					
			18.4	7.2					

VES Station	Geoelectric cross Section	BH Id	ρ (Ωm)	Thickness (m) (electrical)	VES Station	Geoelectric cross Section	BH Id	ρ (Ωm)	Thickness (m) (electrical)
	GERJALLE					HUJURA			
RPV5(T)		RPW-031	16.8	12	RV84(N)		RPW-023	12	6
			16	6				13	6
			13.4	6	RV27(P)		RPW-027	9.3	6
			13.5	6				8.8	18
			11.7	6				14.9	12
			9.8	12				34.7	17
			11	6				36.1	6
			13	12	RV75(Q)		RPW-028	7.6	18
			8.5	24				10.7	6
RV18(ZP)		RPW-054	18.9	6				6.9	17
			14.7	12				10.1	6
			12.2	12				3.7	30
			9.4	12				7.8	6
			10.4	6				7.9	6
			12.4	6				7	6
			11.7	12				6.2	6

RV19(ZS)		RPW-057	8.7	12		KUKUFTU			
			10.1	6	LV151(O)		RPW-026	17	12
			7.6	12				15	6
			9.7	6				18	18
RV50(ZY)		RPW-063	5	12				23	8
			10.4	6	RV63(X)		RPW-036	6	11.1
			3.5	17				17.5	6
			11.5	11				10	12
LV14(ZC)		RPW-042	2.8	12				14	6
			6.5	12				13	6
			8.8	12				14	6
			5.6	18				9.9	26.2
			9.1	6				19.5	5
			27.1	6				13.7	16
					RV23(V)		RPW-034	7	12

D E C L A R A T I O N

I hereby declare that the thesis entitled Aquifer Characterization of the “Raya Valley” based on Pumping Test and Geophysical Data Analysis, (Northern Ethiopia), has been carried out by me under the supervision of Prof. Tenalem Ayenew, Department of Earth Sciences, Addis Ababa University, Addis Ababa during the year 2010 as a part of Master of Science Program in Hydrogeology. I further declare that this work has not been submitted to any other University or Institution for the award of any Degree or Diploma.

AFEWORK HAILU GEBREEZGI

Signature: _____

Place: Addis Ababa

Date: July_____, 2010